ER intrabody mediated protein knockdown in zebrafish

Von der Fakultät für Lebenswissenschaften

der Technischen Universität Carolo-Wilhelmina zu Braunschweig

zur Erlangung des Grades

eines Doktors der Naturwissenschaften

(Dr. rer. nat.)

genehmigte

D i s s e r t a t i o n

von Giulio Russo

aus Napoli

1. Referent:	Prof. Dr. Stefan Dübel
2. Referent:	Prof. Dr. Reinhard Köster
3. Referent:	Prof. Dr. Roland Kontermann
eingereicht am:	17.12.2018
mündliche Prüfung (Disputation) am:	17.04.2019

Druckjahr 2019

Vorveröffentlichungen der Dissertation

Teilergebnisse aus dieser Arbeit wurden mit Genehmigung der Fakultät für Lebenswissenschaften, vertreten durch den Mentor der Arbeit, in folgenden Beiträgen vorab veröffentlicht:

Publikationen

Russo, G., Theisen, U., Fahr, W., Helmsing, S., Hust, M., Köster R.W., & Dübel, S. Sequence defined antibodies improve the detection of Cadherin 2 (N-Cadherin) during Zebrafish development. N. Biotechnol. 45, 98-112 (2018).

Russo, G., Meier, D., Helmsing, S., Wenzel, E., Oberle, F., Frenzel, A. & Hust, M. Parallelized antibody selection in microtiter plates. Phage display, Ed: Lim, T.S. and Hust, M. Methods Mol Biol. 1701: 273-284 (2018).

Russo, G., Lehne, F., Pose Mendez, S.M., Dübel, S., Köster R.W. & Sassen, W.A. Culture and Transfection of Zebrafish Primary Cells. JoVE 138, 1-9 (2018).

Beer, L.A., Tatge, H., Schneider, C., Ruschig, M., Hust, M., Barton, J., Thiemann, S., Fühner, V., **Russo G.** & Gerhard, R. The Binary Toxin CDT of Clostridium difficile as a Tool for Intracellular Delivery of Bacterial Glucosyltransferase Domains. Toxins 10(6), 225 (2018).

Sassen, W.A., Lehne, F., **Russo, G.**, Wargenau, S., Dübel, S. & Köster, R.W. Embryonic zebrafish primary cell culture for transfection and live cellular and subcellular imaging. Devel. Biol. 430, 18-31 (2017).

Führer, V., Heine, P.A., Zilkens, K., Meier, D., Roth, K.D.R., Moreira, G.M.S.G., Hust, M. & **Russo, G**. Epitope Mapping via Phage Display from single gene libraries. Human Monoclonal Antibodies, Ed: M. Steinitz. Methods Mol Biol. 1904: 353-375 (2019).

Namikawa, K., Dorigo, A., Zagrebelsky, M., **Russo, G.**, Kirmann, T., Fahr, W., Dübel, S., Korte, M. & Köster R.W. Modeling neurodegenerative Spinocerebellar Ataxia type 13 in zebrafish using a Purkinje neuron specific tunable co-expression system. The Journal of Neuroscience. 39, 3948-3969 (2019).

Tagungsbeiträge

Russo, G. Protein localization studies and targeted knockdown call for high specificity standards. Protein design and Engineering Conference, Frankfurt (2018).

Russo, G. Programming of and with antibodies. European Antibody Congress, Festival of Biologics, Basel (2018).

Posterbeiträge

Sassen, W.A., **Russo, G.**, Wargenau, S., Dübel, S. & Köster, R.W. Live cell imaging in zebrafish primary cell culture (2015).

Russo, G., Sassen, W.A., Lehne, F., Wargenau, S., Marschall A.L.J., Dübel, S. & Köster, R.W. Zebrafish primary cell culture: a versatile tool for cellular and molecular studies. AOZM and ZDMS conferences, Singapore (2016).

Russo, G., Theisen, U., Fahr, W., Helmsing, S., Hust, M., Köster R.W. & Dübel, S. Sequence defined antibodies improve the detection of Cadherin 2 (N-Cadherin) during Zebrafish development. PepTalk, San Diego (2018).

Table of Contents

List of abbreviations

°C	Degree Celsius
µg	Micrograms
µL	Microliters
A450	Absorption λ=450 nm
Ab	Antibody
APC	Allophycocyanin
BAC	Bacterial artificial chromosome
bp	Base pairs
BSA	Bovine serum albumin
Cdh2	Cadherin-2
CDR	Complementarity-determining regions
CMV	Cytomegalovirus
CNS	Central nervous system
CTR-	Negative control
Cy	Cyanine
DMSO	Dimethyl sulfoxide
DNA	Deoxyribonucleic acid
dNTPs	Deoxynucleotide triphosphates
dpf	Days post fertilization
ECD	Extracellular domain
EDTA	Eethylenediaminetetraacetic acid
ELISA	Enzyme-linked immunosorbent assay
ER	Endoplasmic reticulum
Fab	Fragment antigen binding
FACS	Fluorescence-activated cell sorting
Fc	Fragment crystallizable
FITC	Fluorescein isothiocyanate
Fig.	Figure

HC	Heavy chain
hpf	Hours post fertilization
Ig	Immunoglobulin
IgG	Immunoglobulin G (gamma (γ) heavy chain)
IHC	Immunohistochemistry
kb	Kilobases
kDa	Kilodalton
LC	Light chain
M	Molar
mA	Milliampere
mAb	Monoclonal antibody
MHB	Midbrain-hindbrain boundary
min	minutes
mM	Millimolar
MW	Molecular weight
ng	nanogram
nm	nanometer
pac	*parachute*
PBS	Phosphate buffered saline
PCR	Polymerase chain reaction
recAb	Recombinant antibody
RNA	Ribonucleic acid
rpm	Rounds per minute
RT	Room temperature
sec	Seconds
scFv	Single chain fragment variable
SDS	Sodium dodecyl sulfate
Tg	Transgenic
THN	Tegmental hindbrain nuclei neuron
U	Units

UAS	Upstream activating sequence
URL	Upper rhombic lip
UV	Ultraviolet
V_H	Heavy chain variable domain
V_L	Light chain variable domain
zCdh2	Zebrafish Cadherin-2

List of Figures

List of Tables

1. Introduction

1.1. The zebrafish model to study the gene function

The zebrafish (*Danio rerio, D. rerio*) constitutes a prominent model vertebrate to study gene function and model numerous human diseases (Ablain and Zon, 2013). Compared to rodent models, it shows particular advantages in personalized medicine (Baxendale et al., 2017) and High-throughput (HTP) studies (MacRae and Peterson, 2015).

The full annotation of the Tübingen strain zebrafish genome (Howe et al., 2013) unveiled that 70 % of the human genes have an orthologue in zebrafish; a percentage that raises to 82 % when considering only disease-associated genes (Howe et al., 2013). Not only individual genes, but several molecular processes and organ functions are conserved between fish and humans (Griffin et al., 2018). Beside its genetic and histological similarity to mammals, zebrafish offers a series of unique advantages, that makes it an amenable choice in studies that require high sample numbers or refined characterization of intracellular molecular dynamics. Compared to mammalian models, zebrafish are cheap to maintain, small in size, and characterized by a large number of progeny, therefore suitable for HTP screening and toxicology studies of small molecules and biologics. As 90 % of new drugs under clinical development fail to be approved by the FDA (in 83 % of the cases because of issues with efficacy or safety) (Hay et al., 2014), the zebrafish model may provide large datasets on these critical parameters quickly and directly in the *in vivo* context. Pharma companies leading the field of drug development decided to adopt this animal model "*..to study the effects of compounds on target organ toxicities*" prior clinical trials (technical note by Roche).

Additionally, zebrafish is unique among vertebrate animal models for the almost complete transparency of the embryo and the quick development outside the mothers body. These features permit to perform single cell resolution *in vivo* imaging starting from the very first developmental stages. Easy generation of transgenic lines with tissue- and cell- specific mutations further facilitate gene function studies with high spatial and temporal resolution. When using pigmentation mutants, as *Nacre, Casper* or *Crystal* (White et al., 2008; Antinucci et al., 2016), these advantages can be even partially maintained also in adult samples.

The advent of modern genome editing techniques, together with the external fertilization and development of the zebrafish, made this organism model extremely easy to be modified on the genetic level (Sassen and Köster, 2015). Originally, mutant fish lines were created to study the function of genes involved in embryonic development (see paragraph 1.1.1). Shortly afterwards scientists started to model human diseases in zebrafish for studying the molecular mechanisms that underline pathogenesis (Ceol et al., 2011; Berger and Currie, 2012). In 2015, a drug discovered in zebrafish entered the clinical trials (Cutler et al., 2013) and recently a new hope for epileptic patients resistant to available anti-epileptic drugs (AEDs) may arise from studies conducted in mutant fish modeling this disease (Griffin et al., 2017; Baraban et al., 2013).

The application of zebrafish in cancer biology deserves particular attention. From 2005 to nowadays, several zebrafish tumor lines have been generated and validated to model different human cancers (Amsterdam et al., 2004; Patton et al., 2005; Liu and Leach, 2011; Jung et al., 2013; Ju et al., 2015; Nguyen et al., 2016; Phelps et al., 2016; Anelli et al., 2017), but the main strength of zebrafish for cancer research remain the ease of generation of tumor xenograft models (Zhang et al., 2015; Moore and Langenau, 2016).

Furthermore in zebrafish, but not in mouse, it is possible to create patient-derived cancer cell xenografts for individualized prognosis and patient-tailored therapy (Marques et al., 2009; Welker et al., 2016; Mercatali et al., 2016; Au et al., 2016).

In conclusion, zebrafish is a reference animal model to unveil gene function and to allow for phenotype based screening of drugs on a fully integrated vertebrate organ systems (MacRae and Peterson, 2015; Rennekamp and Peterson, 2015; Wiley et al., 2017). Recently, the zebrafish model started to assume an additional pivotal role in personalized medicine thanks to its ease of manipulation (Baxendale al. 2017).

1.1.1. Zebrafish gene knockout technologies and limitations

Specific pathological human conditions can be reproduced or studied in organism models abolishing the expression of certain genes. When knocking out a gene *in vivo*, it is possible to infer its role from the effect produced by its absence at molecular, cellular, or systemic level. Different approaches have been developed over the time to inhibit gene expression and they go under two main categories: forward genetics and reverse genetics.

In forward genetic approaches, randomly mutagenized animals showing an abnormal phenotype are selected and the mutated genes identified. In reverse genetic approaches, known genes are disrupted and the consequent phenotype analyzed. Forward genetics approaches in zebrafish were initially based on the use of radiation as mutagenic agent (Walker and Streisinger, 1983), which was quickly replaced by the more efficacious chemical compound N-ethyl-N-nitrosourea (ENU) for large scale mutagenesis projects. Examples of successful large scale mutagenesis campaigns are the Tübingen and Boston screening projects (Haffter et al., 1996; van Eeden et al., 1996; Nusslein-Volhard,

2012), or the Zebrafish Mutation Project (Kettleborough et al., 2013). With these screening projects were introduced mutations in more than 12,000 genes, accounting for ca. 45 % of zebrafish protein-coding genes (Howe et al., 2013). Alternatively to chemical mutagenesis, insertional mutagenesis screen were used to generate large libraries of zebrafish mutants (Gaiano et al., 1996; Amsterdam et al., 1999; Golling et al., 2002; Amsterdam et al., 2004). Mutagenesis screening campaigns were aimed to discover developmental mutants. Indeed, with these approaches the first gene function (timewise) is the one to be revealed. This aspect, and the presence of post-embryonic lethal mutations, introduces a bias towards the discovery of mutations, which affect fish development. While ENU mutagenesis allows for quickly generating many mutants within very short time, the following work to map the mutations with positional cloning techniques is time consuming and laborious. The presence of genome duplication in *teleostei* fish, like zebrafish, further increased these difficulties, so that for several mutants could not be characterized (labeled as “ambiguous” location or unspecified function in ZFIN database). Differently from chemically mutated genes, those mutated via viral insertion are easy to clone, aspect which significantly speeds up the process of mutation identification.

Despite the enormous contribution of these large mutagenesis screens, the availability of a fully annotated zebrafish genome since 2010 (Howe et al., 2013), and the generation of new genome editing technologies opened the way to the gradual shift towards targeted mutagenesis approaches and the zebrafish era of reverse genetic. Targeted mutagenesis became available for the zebrafish community in 2008, when Xiangdong Meng and Yannick Doyon independently published (Meng et al., 2008; Doyon et al., 2008) the generation of the first heritable and targeted approach for gene knockout in zebrafish using

engineered zinc finger nucleases (ZFNs). ZFNs are fusions of a Cys_2His_2 zinc finger protein providing DNA binding to a FokI endonuclease providing cleavage activity. In the dimeric state, they introduce double-stranded breaks into the targeted gene sequence. The capability to introduce mutations is not intrinsic of the technique, but is based on the error-prone repair mechanism of the non-homologous end joining (NHEJ) pathway. The applicability of this technique is drastically limited by the laborious and expensive engineering of the ZFN to reach the desired target specificity, which remains context dependent and therefore unpredictable (Ramirez et al., 2008). Also, ZFNs cannot be applied universally due to the limited number of existing ZF modules (Sander et al., 2011). A system similar to ZFNs was introduced in 2012 by Bedell V. and colleagues (Bedell et al., 2012) based on the use of modular single nucleotide DNA-binding domains (DBDs). DBDs are derived from Transcription Activator-Like Effector (TALE) domains and when fused to FokI endonucleases form TALENs. TALENs DBDs are easier to design, not restricted to existing sequence specificities and not context dependent (Li, 2011). TALENs dimers need to recognize adjacent DNA sequences to introduce a double-stranded break in between, meaning that no monomer-mediated cleavage can occur, a condition that limits unwanted off-targeting. Up to date, TALENs based mutagenesis is still considered to provide very high specificity. Despite these techniques revolutionized the way to do reverse genetic in zebrafish, both are methylation sensitive and limited by the need of *de novo* probe design, synthesis, and *in vitro* specificity tests per each different gene target. Furthermore, the *in vitro* tests are not fully predictive of *in vivo* activity. These limitations were eliminated by the game-changing CRISPR/Cas9 based mutagenesis approach (Hwang et al., 2013; Li et al., 2016). The Cas9 DNA cleavage activity is RNA-directed, erasing the need for generating a DBD specific for each

target and limiting the *de novo* design to the *in silico* single guide RNA (sgRNA) design. The endonuclease Cas9 mRNA synthesized *in vitro* is co-injected with the sgRNA into the zebrafish embryo. Alternatively to the Cas9 mRNA, the purified protein can be directly co-injected with the sgRNA. This eliminates the lag introduced by the translation time required when injecting Cas9 mRNA. Also, direct GFP-fusion to Cas9 allows for direct screening of positively injected embryos. Cas9 cleaves double-stranded DNA introducing a double strand break (DSB) at a specific site. This DSB will be repaired by the host cellular Non-Homologous End Joining (NHEJ) repair mechanism, which introduces indels resulting in the target gene disruption. Alternatively, this technique can also be used to replace a gene or part of it, by homologous recombination, when co-injecting the new DNA strand in addition. In this way it is possible to knockout a gene introducing in its sequence a targeted mutation, or a deletion, this time using the Homology directed repair (HDR) mechanism. The fast and cheap design allows for testing in parallel different sgRNAs to mutate the same gene and afterwards verify that all the induced null mutant phenotypes are identical and not complementary. Many human diseases are associated to partial, and not complete, loss of protein activity. Also, it has to be noticed that ca. 30 % of genetic knockout are embryonically lethal in mouse (Dickerson et al., 2011) and that this technology does not permit to independently analyze different protein isoforms originating from the same gene. In these cases, gene knockout approaches are not applicable.

1.1.2. Zebrafish gene knockdown technologies and limitations

Together with gene knockout approaches, gene silencing (or gene knockdown) constitutes the most diffuse approach to study the function of a gene. Contrarily to gene knockout, where null mutations at DNA

level prevent the formation of the full-length gene transcript, in case of gene knockdown, mRNA translation is prevented in the cytosolic compartment by antisense morpholino-modified oligonucleotides (morpholinos) or double strand RNA (RNA interference; RNAi). These probes anneal to the target gene transcript, leading to translation repression and mRNA degradation. Their effect lasts for a few days because of short term degradation and it is suitable to study on the first function of a gene (timewise).

Morpholinos mediated knockdown in zebrafish was introduced in 2000 by Nasevicius and colleagues (Nasevicius and Ekker, 2000) and widely used until the scientific community realized the high risk of off-targeting associated to the use of antisense oligonucleotides (Place et al., 2017; Boer et al., 2016; Eve et al., 2017). One of the major cause of the off-targeting effects induced by morpholinos is the unspecific induction of p53-dependent apoptosis (Pickart et al., 2006; Robu et al., 2007; Gerety et al., 2011). Despite the fact that numerous appropriate controls can help to correctly interpret results generated with morpholinos (Bedell et al., 2011), the drawbacks of using this technology are not negligible.

RNA interference approaches do not induce the p53 pathway. Nevertheless, many cases reported that this approach is not highly specific for the intended target (Jackson et al., 2003; Jackson et al., 2004; Persengiev et al., 2004; Kulkarni et al., 2006; Ma et al., 2006; Echeverri et al., 2006; Dietzl et al., 2007; Seok et al., 2018). Beside unspecific targeting, RNAi has been shown to induce an unwanted interferon response, also dependent on the probe length (Bridge et al., 2003; Pebernard et al., 2004; Sledz et al., 2003). An other limitation when using RNAi, or morpholinos, is the absence of a straightforward and systematic specificity assessment.

The rescue of the induced phenotype via expressing an homologous gene from a different species or RNAi-resistant DNA (Kittler et al., 2005;

Langer et al., 2010; Sigoillot and Randall 2011) constitutes the only, even if valuable, option. Indirect prove of the knockdown specificity can be obtained comparing the knockdown phenotype to the phenotype generated via knockout of the same gene target.

This second, time consuming and laborious approach, is also risky since the effect of knockout and knockdown for the same gene are not necessarily overlapping (see paragraph 1.1.3).

Recently the CRISPR approach has been (Rousseauet al., 2018) adapted to introduce specific cleavage in RNA sequences (CRISPR interference, CRISPRi). So far this approach has been tested only *in vitro*, and it showed to have reduced off-target effects, but also showed a strong clonal effect.

1.1.3. Controversial mutant phenotypes

Over the past years, the zebrafish community encountered increasing difficulties in recapitulating mutant phenotypes with morpholino induced phenotypes (Kok et al., 2015; Novodvorsky et al., 2015). Accordingly, a comparison of published morpholino induced phenotypes with mutant phenotypes from the Zebrafish Mutation Project data (Kettleborough et al., 2013) indicated that circa 80 % of morphant phenotypes are not observed in mutant embryos (Kok et al., 2015). What was supposed to be an approach to certify mutant phenotype specificity became argument of concern in respect of both, gene knockout as well as gene knockdown technologies.

This discrepancy may be explained considering the off-targeting effects induced by antisense oligonucleotides, RNAi and CRISPRi. A systematic comparison (Stojic et al., 2018) of these three techniques proved the induced phenotype was different in the three cases, as different were the off-target genes expressed. On the other side, very often knockout mutants do not show any overt phenotype because of genetic

compensation (Rossi et al., 2015), or incomplete loss of function (Anderson et al., 2017). Anderson and colleagues proved how alternative splicing and splice sites, ribosomal frameshifting, or nonsense readthrough in zebrafish, can lead to genotypically null mutants with wild type phenotype, even for mutations introduced in essential genes. Similar findings emerged also when looking at the human genome of healthy subjects (Sulem et al., 2015; Chen et al., 2016; Narasimhan et al., 2016; Jagannathan et al., 2016). Understanding the underlying compensatory mechanisms is a new and ongoing field of research and does not yet allow one to completely explain or avoid these phenomena (El-Brolosy and Stainier 2017), which are consequently very hard to detect (especially when involving nonsense readthrough).

Gene silencing and gene knockout induced phenotypes may not reflect each other and they may be biased by unspecificity in the case of gene silencing or cryptic compensatory mechanisms in the case of gene knockouts. This aspects can compromise the functional analysis of certain genes. Being aware that gene silencing and gene knockout cannot be systematically used to crosscheck a certain phenotype, an alternative approach is needed. This alternative should be highly specific and avoid the limitations of classic gene knockdown and knockout approaches. Recently emerging methods to directly interfere with the target protein activity would provide such an alternative.

1.2. Intrabody technology

Immunoglobulins (Ig) are molecules produced by the plasma cells during the activation of the humoral immune system in response to pathogen invasion and cancer, or during allergic reactions and autoimmune diseases. Because of their direct (e.g. by neutralizing) and indirect (via an effector function) activity of target inhibition, these molecules are

characterized by an intrinsic very high affinity and specificity towards their target, allowing to bind to one particular antigen molecule within highly concentrated and diverse mixtures of biomolecules, like in the blood plasma. Like other plasma proteins, antibodies are produced through the secretory pathway. ER oxidizing milieu, and ER resident chaperones have been proved to be necessary for correct antibody folding (Feige et al., 2010). In addition, correct folding of the antigen-contacting Ig heavy chain variable domains (VH) and light chain variable domains (VL) depends on the formation of intrachain disulfide bonds. VH and VL can be connected by a flexible linker (Huston JS et al., 1988) to generate a single chain fragment variable antibody fragment (scFv). The scFv constitutes the smallest IgG-derived antibody format that maintains the original antibody high specificity to its target. When intracellularly expressed, an scFv can be designated as an intrabody, and can interfere with the function of it's target protein. Intrabodies can be produced in different cellular compartments: in the endoplasmic reticulum (ER) where the secretory pathway starts (ER intrabody), or in the cytosol (intracellular antibodies, ICAbs). In addition to the significantly different groups of antigens that can be targeted in the two cases (plasma/membrane versus cytoplasmic proteins), other intrinsic properties differentiate these two intrabody applications, impacting their individual benefits and ease of use.

ICAbs typically are scFv fragments expressed into the cytosol, thus their effect on the target protein relies on some direct inhibition of target function provided by the mere binding.

Without such inhibitory effect, ICAbs, even when highly specific and binding with high affinity, can only be used to “label” a protein. Common targets of ICAbs are cytosolic and nuclear proteins. The cytosolic compartment is characterized by the presence of reducing biochemical conditions, lacking necessary chaperones and not allowing disulfide

bridges to form, so only very few IgGs can fold correctly in this cellular compartment (Biocca et al., 1995; Wörn and Plückthun, 2001). Consequently, expression of scFv antibodies in the cytosol, as such, often results in the production of unfolded insoluble antibodies aggregates, or soluble but non-functional scFv with short half life (Cattaneo and Biocca, 1999). Also, antibody solubility during production in bacterial cells (often used for antibody selection) is not predictive of correct folding in mammalian cells, thus limiting the chances to preselect stable ICAbs in bacteria (Guglielmi et al., 2011). Partial solution to the natural absence of antibody folding in the cytosol is offered by the following two alternatives: the adoption of extremely sophisticated screening techniques designed *ad hoc* for ICAbs selection in the scFv format (Biocca et al., 1994; Visintin et al., 1999, 2002), or the generation of libraries for antibody selection in a different format than scFv. These formats include: single domain antibodies, mainly Camelid and shark antibodies (Philibert et al., 2007; Dong et al., 2010; Tremblay et al., 2010; Saerens et al., 2005), cysteine-free scFv's (Seo et al., 2009), or antibody-like or completely different scaffolds naturally lacking disulfide bonds (like fibronectin VIII or DARPINs) (Amstutz et al., 2005; Kohl et al., 2005; Gross et al., 2016). Independently from individual benefits and drawbacks, no one of the systems developed to improve functionality after expression in the cytosol solves the need for selecting not only highly specific and affine antibodies, but in addition those capable of neutralizing the antigen activity upon binding.

In contrast, an ER intrabody is an scFv fused to the KDEL ER-retention signal and reduces the protein target levels in their final destination (membranes or plasma) via physically retaining it in the ER compartment. The retention is mediated by the binding of the KDEL to the ER lumen protein-retaining receptors (KDEL receptor) (Figure 1). The retention prevents the antigenic target from reaching its active

compartment. This way, antigen neutralization upon binding is not required to mediated ER intrabody protein knockdown. As ER intrabodies are made in the native compartment of their production, they are expected to fold correctly. Consequently, no laborious and time consuming screening techniques are required to generate ER intrabodies. The fusions in frame to a selected scFv of the KDEL peptide sequence (C-terminal) and of the SP (N-terminal) are the minimal and only change necessary to constitute an ER intrabody. Circa 39 % of the human proteome is destined to the secretory pathway (Uhlén et al., 2015) and can be therefore subjected to ER intrabody targeting. Most common targets are proteins displayed on the cell surface, secreted proteins, glycosyltransferases Golgi-resident, and other endomembrane system proteins. Significantly, therapeutically relevant targets form a large fraction among proteins of the secretory pathway (Kuhlmann et al., 2018).

In contrast to all methods to analyze gene function by inactivation described above, the ER intrabody approach consists in knocking down a target at protein level, offering the unique possibility to finely discriminate among different isoforms of a protein. Acting at protein level, it is not influenced by genetic compensatory mechanism which affect the efficiency of DNA or RNA based approaches. Nevertheless, it should be considered the exponentially higher number of antigen proteins to be addressed with intrabodies compared to DNA methods which target only two alleles in the genome. ER intrabodies provide an alternative to classic nucleotide based knockdown and knockout methods, crucial when the latter fail to reciprocally recapitulate their induced phenotype. The absence of need for target inhibition upon binding allows for using the ER intrabody for target knockdown in a selective subcellular compartment. Best example of this approach, is the the functional knockdown of Sec61a in the endosomal compartment without affecting

its natural activity in the ER compartment (Zehner et al., 2016).

Intrabody application has also been proposed for therapeutic applications, for these diseases characterized by gene expression upregulation, which includes infectious diseases and cancer therapy (Kontermann, 2004; Marschall and Dübel, 2016). Recently, it has been demonstrated to be applicable in vivo, by knocking down the VCAM1 expression levels in transgenic mice (Marschall et al., 2014).

1.2.1. ER intrabody mechanism of action

The high level of compartmentalization inside of eukaryotic cells requires complex vesicular systems for the specific trafficking of certain lipids and proteins from one compartment to the other. In the secretory pathway, proteins expressed in the ER reach the Golgi apparatus in COPII-coated vesicle (anterograde transport). In the Golgi, proteins are further sorted for secretion, surface display, retention in the Golgi, or retrieval to the ER compartment. Export from the ER is partially regulated and only properly folded proteins can be targeted to the cis-Golgi and from there to the Golgi apparatus. In the latter compartment, ER resident proteins are recognized for the presence of a tetrapeptide motif, KDEL (Lys-Asp-Glu-Leu) and retrotransported to the ER into COPI-coated vesicle (retrograde transport). In humans, the receptors that mediate KDEL binding and provide retrotransport to the ER are ERD21, ERD22, and ERD23. All three proteins share the same function and show only slight substrate differences (Raykhel et al., 2007), so they are commonly referred to as KDEL receptors. They are all homologous of the yeast Erd2, which specifically recognizes the HDEL sequence of yeast ER-resident proteins (Semenza et al., 1990). The KDEL receptors interact simultaneously with the cargo (KDEL) and COPI vesicle components (Majoul et al., 2001). The KDEL binding is pH dependent, providing binding in the Golgi and inside the COPI-coated vesicle, but

the release in the ER lumen, since the pH in the cis-Golgi is lower (pH 6.7) than in the ER lumen (pH 7.2) (Scheel and Pelham, 1996). The KDEL receptor retrotransport system can be found in all eukaryotes and plants and is highly conserved. Among vertebrates in particular, the degree of sequence similarity for the KDEL receptor is extremely high. Between human and mouse KDEL receptor 2, the amino acid sequence identity is 98,6 %; and for human and zebrafish 91,5 %.

As ER intrabodies are KDEL-fused scFv antibodies, they undergo the same pathway of all the ER resident proteins. Due to the high affinity binding to their target, they force their antigen to the same locations: even when an ER intrabody-antigen complex escapes the ER, it is duly retrotransported to this compartment (Figure 1). Here, it may be degraded by the proteasome-dependent or proteasome-independent ER-associated protein degradation (ERAD) system (Schmitz et al., 2004; Meusser et al., 2005; Donoso et al., 2005). This ER retention mechanism is very powerful as the KDEL receptor is capable of retaining ca. a tenfold molar excess of protein substrate (Pelham, 1996).

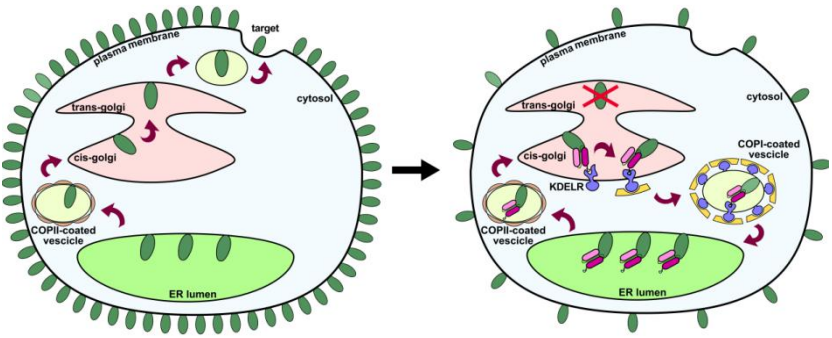

Fig. 1: ER intrabody mediated knockdown schematic illustration.

Upon expression into the secretory pathway the ER intrabody binds the antigen target inside the lumen of the ER. From this compartment the two molecules are

transported into COPII-coated vesicle to the cis-golgi. Here, due to slight pH acidification, the KDEL receptor (KDELR) binds the KDEL sequence of the ER intrabody. Upon binding, KDELRs multimerize and induce the formation of COPI-coated vesicles containing the ER intrabody - antigen complex as well.
The vesicles are retro-transported to the ER where the lower pH induces the release of the KDEL-fused protein from the KDELR. Hence, the antigen target is retained between the ER lumen and the cis-golgi without reaching its final destination.

1.2.2. ER intrabody generation

The most convenient format of an ER intrabody comprises of a polypeptide chain where an scFv fragment in fused N-terminally to a signal peptide (SP) and C-terminally to the KDEL sequence. To fuse the scFv gene in frame with the SP and the KDEL DNA sequences, it is sufficient a single cloning step inserting the scFv gene into a ER intrabody mammalian expression vector. Therefore the main effort for the generation of an ER intrabody is to provide DNA sequences encoding for a VH and VL antibody pair specific to the desired target. This information can be extracted from available hybridoma clones, but this requires careful analysis for correct function in the not infrequent cases where more than one specificity is secreted by one hybridoma cell (Bradbury et al., 2018).
These problems are avoided by using sequence defined antibodies from the start, typically generated by *in vitro* display techniques (Breitling et al., 1991; Bradbury et al., 2011; Hust et al., 2011) to select recombinant monoclonal antibodies directly in the scFv format from antibody gene libraries, through a highly customizable selection method. An antibody gene library can be generated from any animal species, including human, without any need for immunization (universal non-immune

library) (Glanville et al., 2009; Schofield et al., 2007; de Wildt et al., 2000; Hust et al., 2011; Kügler et al., 2015), but it can also be patient derived or follow animal immunization (immune library) (Trott et al., 2014; Chan et al.,1996). Alternatively the library can be of synthetic or semi-synthetic origin (Tiller et al., 2013; Hoet et al., 2005). The most widely used *in vitro* technology for antibody selection is antibody phage display (Breitling et al., 1991), and the antibody selection process is named panning. The panning procedure can be designed to reduce unwanted cross-reactivities, to obtain cross species specific antibodies, target post-translational modification or conformation specific antibodies (Frenzel et al., 2017). With this approach it is possible to generate highly specific recombinant monoclonal scFv antibodies ready to be cloned and expressed as ER intrabodies (Zhang et al., 2012). Nowadays, phage display for antibody selection is one standard for therapeutic human antibody generation, and is progressively replacing animal immunization and hybridoma technology in the generation of research antibodies as well (Gray et al., 2016). In many cases, scFv genes for ER intrabody generation is already available thanks to international research efforts, like the “Affinomics” EU project (www.affinomics.org), which provided antibodies to hundreds of different targets. The increasing availability of recombinant monoclonal antibody sequences (Colwill et al., 2011; Schofield et al., 2007; Sidhu 2012; Mersmann et al., 2010; Hust et al., 2011) will drastically reduce the effort for ER intrabody generation in the future. So, even if RNAi based knockdown approaches remain easier and faster in respect of the reagent generation, ER intrabody today constitute a practicable alternative, providing the advantages of a different mechanism of action directly at the protein level.

1.3. Cadherin-2 (Cdh2)

Cadherins constitute a superfamily of calcium-dependent adhesion molecules required for the formation of adherens junctions, cell polarization, and hetero/homophilic interactions between juxtaposed cells (Takeichi, 1991; Zhu and Luo, 2004), conducting a pivotal role in morphogenesis and tissue repair (Gumbiner et al., 2005). Cadherin-2 (N-cadherin; Cdh2), is a type I transmembrane glycoprotein belonging to the subfamily of *classical* cadherins. It is the first cadherin discovered in the vertebrate nervous system (Hatta and Takeichi, 1986; Miyatani et al., 1989; Redies, 2000; Yagi and Takeichi, 2000), and its function is highly conserved among vertebrates.

Cdh2 domain structure is composed of a N-terminal propeptide, required to avoid intracellular aggregation, an extracellular region, a transmembrane single-pass domain, and an intracellular domain which directly interacts with the cell cytoskeleton, mainly via ß-catenin binding. The extracellular domain is in turn composed by five extracellular immunoglobulin (Ig)-like domains (Cdh2-ECDs) with calcium binding pockets interspersed at the interface between consecutive EC-domains (Tepass et al., 2000).

1.3.1. Cdh2 expression pattern and physiologic function

Indicating a crucial role in development morphogenesis, Cdh2 is almost ubiquitously expressed throughout the early developmental stages of vertebrates. In the adult, its expression is restricted to specific neuronal populations in the central nervous system (CNS), and the myocardium (Redies et al., 1993; Redies and Takeichi, 1993). Neurodevelopmental processes depending on Cdh2 activity include: migration of newly synthesized neurons, axonal growth, target identification, formation of synaptic contacts, and generally tissue architecture formation and tissue homeostasis (Suzuki and Takeichi, 2008). Mice, or zebrafish, lacking

Cdh2 activity, which results in loss of cell-cell adhesivity, show compromised neural tube formation (Lele et al., 2002; Radice et al., 1997). This primary neurulation effects induced by the absence of c*dh2* expression, in turn result in impaired neuronal migration (Kawauchi et al., 2010; Shikanai et al., 2011; Taniguchi et al., 2006; Luccardini et al., 2013; Rieger et al., 2009). The role of Cdh2 in the cardiac muscle is essential for cardiomyocyte mechanical coupling and differentiation (Ferreira-Cornwell et al., 2002; Bagatto et al., 2006; Luo et al., 2001). A role of Cdh2 in promoting cell motility has been observed in several tumors, resulting in increased cancer invasion and metastatic behavior. This mechanism affects also tissues that do not normally express this molecule, and is part of a process named Epithelial–mesenchymal transition (EMT) where tumor cells are subjected to class switch from Cadherin-1 to Cadherin-2 (Hsu et al., 1996; Li and Herlyn, 2000; Hirohashi, 1998; Perl et al., 1998; Nieman et al., 1999; Suyama et al., 2002; Islam et al., 1996). The role of Cdh2 in tumor progression allows for using this antigen as prognostic factor and potential biomarker for the prediction of metastases.

1.3.2. Zebrafish Cdh2 knockout and knockdown phenotype

ENU-generated Cdh2 defective zebrafish mutants show loss of neuroepithelium pseudostratification which translates in cells delamination and aggregation, demonstrating the crucial role of Cdh2 to guarantee the neural tube integrity and correct morphogenesis (Lele et al., 2002). This role of Cdh2 was already documented in chicken (Gänzler-Odenthal and Redies, 1998) and mouse (Kostetskii et al., 2001) embryos. For all of these models, the loss of neural tube integrity can be attributed to the loss of Cdh2 mediated cell adhesivity. Cdh2 seems also to have a relevant role in the regulation of neuronal proliferation, as its ablation during midsegmentation leads to hyperproliferation in the alar

regions of the neural tube (Gänzler-Odenthal and Redies, 1998; Lele et al., 2002), an effect which may rely on the Cdh2 mediated distribution of ß-catenin, its intracellular partner.

In zebrafish, loss of Cdh2 further impairs neurulation, axonogenesis, and pathfinding, convergence of alar plate, and in general restriction of neuron motility within the neural tube, with consequent loss of regionalization (Lele et al., 2002). The phenotypical effects found in *pac*R2.10 Cdh2 zebrafish mutants were fully recapitulated by two different Cdh2 morpholinos induced phenotypes (Lele et al., 2002). The particular possibility to phenocopy the *pac*R2.10 mutant phenotype with knockdown approaches offers the possibility to test the ER intrabody mediated knockdown system to reproduce already described effects and validate this technology in zebrafish for the first time.

1.4 Aim of the study

Consequently, this study aims to demonstrate for the first time the ER intrabody knockdown technology can be successfully used in zebrafish to interfere in cell culture and *in vivo* with the activity of Cadherin 2 during CNS development. This includes the initial generation of recombinant cadherin variants as antigens, the generation of recombinant (sequence defined) antibodies against these antigens by phage display, their characterization and finally their application as intrabodies in zebrafish cell culture (*in vitro*) and in the whole organism (*in vivo*).

2. Materials and Methods

2.1 Materials

2.1.1 Equipment

The technical equipment used in this study is listed in table 2.1.

Table 2.1: Technical equipment

Equipment	Name	Supplier
Analytical balance	Model 1205MP E 1200 S Analytic A 120 S EMB 220-1	Sartorius (Göttingen, DE) Sartorius (Göttingen, DE) Sartorius (Göttingen, DE) Kern (Balingen, DE)
Blotting device	Trans-Blot Turbo Transfer	Bio-Rad (München, DE)
Centrifuge	Eppendorf 5810R Eppendorf 5804R Eppendorf 5415D Multifuge 3 S-R	Eppendorf (Hamburg, DE) Eppendorf (Hamburg, DE) Heraeus (Hanau, DE)
Confocal laser scanning microscope	SP8	Leica microsystems (Wetzlar, DE)
ELISA-Washer	Columbus Pro Columbus Plus Hydrospeed	Tecan (Crailsheim, DE) Tecan (Crailsheim, DE) Tecan (Crailsheim, DE)
ELISA-Reader	SUNRISE Epoch	Tecan (Crailsheim, DE) BioTek (Bad Friedrichshall, DE)
Electroporation device	Gene Pulser Xcell + CE module	BioRad (München, DE)
Epifluorescent	DM5500B	Leica microsystems

Equipment	Name	Supplier
microscope		(Wetzlar, DE)
Flow cytometer	SH-800 cell sorter CytoFLEX	Sony (San Jose, CA, USA) Beckman Coulter (Brea, CA, USA)
Gel documentation	Chemicoc MP Imaging System	Bio-Rad (München, DE)
Gel electrophoresis chamber	PerfectBlue Mini S PerfectBlue Mini ExM Mini-Protean 3 Cell	Peqlab (Erlangen, DE) Peqlab (Erlangen, DE) Bio-Rad (München, DE)
Incubator for bacterial cells	Incubator BE400	Memmert (Schwabach, DE)
Incubator for mammalian cells	Heraeus	HeraCell (Langenselbold, DE)
Incubator for zebrafish cells	Incubator I	Memmert (Schwabach, DE)
Incubator for zebrafish embryos	B6120	Heraeus Instruments (Hanau, DE)
Incubator shaker for bacterial cells	Multitron standard Certomat BS-1 VorTemp 56	Infors HT (Einsbach, DE) Satorius (Göttingen, DE) Labnet (Austin, USA)
Incubator shaker for mammalian cells	Minitron	Infors HT (Einsbach, DE)
Laminar flow bench for bacteria	LaminAir HLB 2472 MSC Advantage	Thermo Scientific (Waltham, USA)
Laminar flow bench for mammalian cells	HeraSafe	Heraeus Instruments (Hanau, DE)
Laminar flow bench for	Vertical laminar flow	Bio Base, Wolfenbüttel,

Equipment	Name	Supplier
zebrafish cells	bench	DE
Light microscope	TELAVAL 31 TS100	Zeiss, Oberkochen, DE Nikon, Dűsseldorf, DE
Microinjector	Femtojet Express	Eppendorf (Hamburg, DE)
Microplate shaker	VorTemp™ 56	Labnet-Corning (New York, USA)
Needle puller	P-87	Sutter Instrument (Novato, CA, USA)
pH meter	CG810	Schott (Mainz, DE)
Pipette	Research Pipetman Proline Plus	Eppendorf (Hamburg, DE) Gilson (Middelton, USA) Satorius (Göttingen, DE)
Pipette Controller	Accu-Jet pro	Brand (Wertheim, DE)
Power supply	EPS 301/601	Amersham plc, GE Healthcare, Freiburg, DE)
Sonicator	Bioruptor® Pico	Diagenode (Denville, USA)
Spectrophotometer	Nano Drop ND1.000	Peqlab (Erlangen, DE)
Stereo microscope	M205FA	Leica microsystems (Wetzlar, DE)
Thermocycler	DNAEngine S1000 Thermal Cycler	Bio-Rad (München, DE) Bio-Rad (München, DE)
Thermomixer	Thermomixer comfort Thermomixer compact	Eppendorf (Hamburg, DE) Eppendorf (Hamburg, DE)
Ultrapure water device	Arium 611	Sartorius (Göttingen, DE)
Vertical tube rotator	model LD-79	Labinco B.V. (Breda, Netherlands)
Vortex	Vortex-Genie 1	Scientific Industries (New

Equipment	Name	Supplier
		York, USA)
Water bath	Water bath GFL	Laborbedarf (Braunschweig, DE)

2.1.2 Consumables

All consumables used in this study is listed in table 2.2.

Table 2.2: Consumables

Application	Consumables	Supplier
General	Multiply-µStrip Pro 8-strip	Sarstedt (Nürmbrecht, DE)
	Parafilm	American National Can (Chicago, USA)
	Pasteur pipettes (3 mL)	Hartenstein (Würzburg, DE)
	Petri dish 10 cm	Greiner Bio-One (Frickenhausen, DE)
	Pipette tips 10 µL; 200 µL; 1000 µL; 5000 µL	Sarstedt (Nürmbrecht, DE) Biohit/Satorius (Göttingen, DE)
	Pipette filter tips 10 µL; 200 µL; 1000 µL	Sarstedt (Nürmbrecht, DE), NerbePlus (Winsen, DE)
	Polypropylene centrifugation tubes (15 mL, 50 mL)	Corning (New York, USA)
	Polystyrene lid	Greiner Bio-One (Frickenhausen, DE)
	Reaction tube 1.5 mL; 2 mL	Sarstedt (Nürmbrecht, DE)
	Sterile syringe needle 26g	TERUMO (Eschborn, DE)
	Syringe Inject 1 mL, 2 mL 5 mL,	B. Braun (Melsungen, DE)

Application	Consumables	Supplier
	20 mL	
Bacterial culture	Air-o-Seal hydrophobic Gas permeable seal	4titude (Dorking, UK)
	Disposable Cuvettes 1.5 mL half-micro	Brand (Wertheim, DE)
	Disposable spatula (L-shape)	VWR (Darmstadt, DE)
	Inoculation loops	Sarstedt (Nürmbrecht, DE)
	Microtiter-polypropylene plate 96 well, U-shape	Greiner Bio-One (Frickenhausen, DE)
	Screw Cap Micro Tube (2 mL)	Sarstedt (Nürmbrecht, DE)
Cell culture	BD Falcon Cell Strainer (40 µm)	FALCON/BD Bioscience (Heidelberg, DE)
	Cryo tube vials (2 mL)	Nunc/ Thermo Scientific
	EasyStrainer (40 µm)	Greiner Bio-One (Solingen, DE)
	Electroporation Cuvettes (0.4 cm)	Kisker (Steinfurt, DE)
	Glass coverslips	Heinz Herenz Medizinalbedarf GmbH (Hamburg, DE)
	Neubauer chamber	Henneberg-Sander GmbH (Giessen, DE)
	Petri dishes 10 cm	Sarstedt (Nürmbrecht, DE)
	Polycarbonate Erlenmeyer Flask graduated	Corning (New York, USA)
	Polystyrene TC plate 12/24/96x wells	SPL Life Sciences (Pocheon, KOR)
	Serological pipettes (2, 5, 10, 25 mL)	Corning (New York, USA)
	TC plate 96 well V shape with lid	Greiner Bio-One (Frickenhausen, DE)

Application	Consumables	Supplier
	Ultra-Low attachment 6-well plates	CELLSTAR/Greiner Bio-one (Frickenhausen, DE)
ELISA	Polystyrene assay plate 96x Well (high binding)	Corning (New York, USA)
Flow Cytometry	Deepwell plates, Protein LoBind, 96 wells	Eppendorf (Hamburg, DE)
	Filter CellTrics 50 µm	Sysmex (Norderstedt, DE)
	Polystyrene lid	Greiner Bio-One (Frickenhausen, DE)
Protein A purification system	Uniplate PP (10 mL) Unifilter (10 mL) Melt blown PP (10 µm) MabSelect SuRe Protein A affinity matrix	Whatman/GE Healthcare (Freiburg, DE)
	Zeba™ Spin Desalting Columns 89892	Thermo Scientific, DE
Western blot	Blotting paper (550 g/m2)	Sartorius (Göttingen, DE)
	PVDF membrane	Bio-Rad (München, DE)
	Whatman filter paper	Whatman/GE Healthcare (Freiburg, DE)

2.1.3 Chemicals

All chemicals used were purchased from Carl Roth, Sigma-Aldrich, Merck, AppliChem, Roche, and SERVA GmbH (all located in DE).

2.1.4 Buffers and solutions

All buffers and solutions used in this study are listed in tables 2.3 and 2.4.

Buffer and solutions were prepared with ultrapure water or as indicated in the table.

Table 2.3: Buffers and solutions prepared in house

Application	Buffer/ Solution	Recipe
General	Glycerine	80 % (v/v) Glycerine
	PBS	137 mM NaCl; 1.76 mM KH_2PO_4 • 2 H_2O
	PBS-T	0.05 % (v/v) Tween20 in PBS
DNA electrophoresis	Agarose gel	1 % (w/v) Agarose in TAE
	Ethidium bromide solution	0.01 % (w/v) Ethidium bromide
	TAE buffer	40 mM Tris; 20 mM Acetate; 2 mM EDTA
Coomassie staining	Coomassie®-Destaining	10 % (v/v) Acetic acid
	Coomassie®-Staining	10 % (v/v) Acetic acid, 0.05 % (w/v) Coomassie® Brilliant Blue R250
ELISA	ELISA stop solution	1 N H_2SO_4
	PBST ELISA-Washer	0.05 % (v/v) Tween20 in PBS
	M-PBST (Blocking)	2 % (w/v) Milk powder in PBS; 0.05 % Tween20
	TMB solution A	30 mM Potassium citrate; 1 % (w/v) Citric acid (pH 4.1)
	TMB solution B	10 mM Tetramethylbenzidine; 10 % (v/v) Acetone; 90 % (v/v) Ethanol; 80 mM H_2O_2 (30 %)
	TMB solution	20 parts TMB-A; 1 part TMB-B
SDS-PAGE	APS-solution	10 % (w/v) Ammonium persulfate in H_2O

Application	Buffer/ Solution	Recipe
	Laemmli buffer (5x)	500 g/L Glycerine; 100 g/L SDS; 250 mL β-Mercaptoethanol; 200 mL 1.5 M Tris-HCl (pH 6.8); 0.5 g/L Bromphenol Blue
	SDS solution	10 % (w/v) SDS
	SDS-PAGE buffer	25 mM Tris; 192 mM Glycine; 0.1 % (w/v) SDS solution
	Acrylamide mix	30 % (w/v) Acrylamide, 0.8 % (w/v) Bisacrylamide
Western blot and Immunostaining	AP substrate buffer	100 mM Tris; 0.5 mM $MgCl_2$ (pH 9.5)
	BCIP solution	1.5 % (w/v) BCIP in 100 % (v/v) Dimethylformamide
	Blotting buffer	25 mM Tris; 192 mM Glycine (pH 8.3)
	MPBS (Blocking)	2 % (w/v) Milk powder in PBS-T
	NBT solution	3 % (w/v) NBT in 70 % (v/v) Dimethylformamide
Flow Cytometry	FACS buffer	0.5 % BSA, 5 mM EDTA in 1x PBS
Whole mount immunostaining	Fixation and permeabilization	4 % PFA, 0.1 % Triton X-100 in PBS
	Washing	0.1 % Triton X-100 in PBS
	Antigen retrieval	Ultrapure acetone (Panreac AppliChem, Darmstadt, DE)
	Blocking	5 % goat normal serum, 1 % BSA, 1 % Triton X-100, DMSO in PBS
	Staining solution	1 % BSA, 1 % Triton X-100 and 1 % DMSO
Protein A purification	Washing[1]	PBS
	Washing[2]	100 mM sodium citrate buffer pH 5.0
	Elution	100 mM sodium citrate buffer pH 3.0

Application	Buffer/ Solution	Recipe
	Neutralization solution	1 M tris-HCl pH 9.0
Zebrafish embryo solution	Danieau 30 %	5.8 mM sodium chloride, 0.07 mM potassium chloride, 0.04 mM magnesium sulfate, 0.06 mM calcium nitrate, 5 mM HEPES (2-[4-(2-hydroxyethyl)piperazin-1-yl]ethanesulfonic acid), pH 7.2

Table 2.4: Commercial solutions and buffers

Application	Buffer/ Solution	Supplier
DNA cloning	5x Phusion® HF Buffer	New England Biolabs (Frankfurt a. M., DE)
	6x loading dye	Fermentas, (St. Leon-Rot, DE)
	CutSmart buffer/NEBuffer endonuclease specific	New England Biolabs (Frankfurt a. M., DE)
	GeneRuler™ 1kb Plus DNA Ladder	Fermentas, St. Leon-Rot, DE
	GoTag®Flexi Buffer	Promega (Mannheim, DE)
	Magnesium Chloride Solution	Promega (Mannheim, DE)
	T4 DNA Ligase Reaction Buffer	New England Biolabs (Frankfurt a. M., DE)
Protein markers	Precision Plus Protein™ Standards unstained	Bio-Rad (München, DE)
	Precision Plus Protein™ All Blue Prestained Protein Standards	Bio-Rad (München, DE)

Application	Buffer/ Solution	Supplier
DNA/RNA microinjection	Red phenol	Sigma (Steinheim, DE)
	HPLC-grade water (RNase-Free)	Carl Roth GmbH (Karsruhe, DE)
Zebrafish embryo treatment	Propylthiouracil (PTU)	Sigma (Steinheim, DE)
	Tricaine	Sigma (Steinheim, DE)
Immunostaining	SuperSignal West Pico Plus Chemiluminescent Substrate	Thermo Scientific, DE
	Paraformaldehyde	Merck (Darmstadt, DE)
	Triton X-100	Bio-Rad (Münich, DE)
	Acetone ultrapure	Panreac AppliChem (Darmstadt, DE)
	goat normal serum	Vector labs/BIOZOL (Eching, DE)
	Dimethyl sulfoxide (DMSO)	Carl Roth GmbH (Karsruhe, DE)

2.1.5 Media, supplements, and solutions

Media, supplements, and solutions for the cultivation of Prokaryotic or Eukaryotic cells used in this study are listed respectively in tables 2.5 and 2.6. Media for bacterial culture without supplements were autoclaved for 20 min at 121 °C and 1 bar.

Table 2.5: Media and supplements for E.coli culture

	Medium/ supplement	Recipe
Media	SOC	2 % (w/v) Tryptone; 0.5 % (w/v) Yeast extract;

	Medium/ supplement	Recipe
		0.05 % (w/v) NaCl (pH 7.0); 20 mM Mg^{2+} solution (1 M $MgCl_2$, 1 M $MgSO_4$); 20 mM Glucose
	LB	1 % (w/v) Tryptone; 0.5 % (w/v) Yeast extract; 1 % (w/v) NaCl
	2xYT	1.6 % (w/v) Tryptone; 1 % (w/v) Yeast extract; 0.5 % (w/v) NaCl (pH 7.0)
	2xYT-GA	2xYT medium; 100 mM D-Glucose; 100 µg/mL Ampicillin
	2xYT-GA-Agar	2xYT medium; 1.5 % (w/v) Agar; 100 mM D-Glucose; 100 µg/mL Ampicillin
Supplements	Ampicillin solution	100 mg/mL Stock solution
	Glucose solution	2 M Glucose Stock solution
	IPTG solution	1 M Isopropyl-β-D-thiogalactopyranosid Stock solution
	Tetracycline solution	10 mg/mL Stock solution

Table 2.6: Media and supplements for Eukaryotic cell culture

	Product	Supplier	Catalog number
Media	DMEM	gibco® (Life Technologies, Darmstadt, DE)	11965092
	Free Style™ F17 Expression medium		A13835-01
	Leibovitz's L-15 medium		11415049

	Product	Supplier	Catalog number
Solutions	Collagenase (Type 2)	Thermo Scientific (Waltham, USA)	17101015
	Bambanker freezing medium	NIPPON Genetics (Düren, DE)	BB01
	Opti-MEM™	gibco® (Life Technologies, Darmstadt, DE)	31985062
	PBS (Dulbecco's Phosphate Buffered Saline)		14190-169
	Polyethylenimine (PEI) MAX, 40 KDa	Polysciences, Warrington, USA).	24765-1
	Poly-L-lysine	Biochrom (Berlin, DE)	L 7240
	Trypsin/EDTA	Biochrom (Berlin, DE)	L2153
Supplements	Penicillin/streptomycin	Biochrom (Berlin, DE)	A2212
	L-Glutamine	Biochrom (Berlin, DE)	K0283
	Fetal bovine serum (FBS)	Biochrom (Berlin, DE)	S0615
	DMSO	Carl Roth (Karsruhe, DE)	A994.2
	Pluronic-F68	PAN^{TM} BIOTECH (Aidenbach, DE)	P08-02100
	TNFα	gibco® (Life Technologies, Darmstadt, DE)	PHC3015
	Tryptone N1 (casein peptone)	Organotechnie (La Courneuve, France)	19553

2.1.6 Bacterial strains and bacteriophages

The bacterial strains used in this study are listed in table 2.7.

Table 2.7: Bacterial strains and bacteriophages

Cell line	Note	References
E. coli XL1-Blue MRF`	_(mcrA)183 _(mcrCB-hsdSMR-mrr)173 endA1 supE44 thi-1 recA1 gyrA96 relA1 lac [F_ proAB lacIqZ_M15 Tn10 (Tetr)]	Stratagene (LA Jolla, USA)
E. coli TG1	K-12 supE thi-1 _(lac-proAB) _(mcrB-hsdSM)5, (rK-mK-) F' [traD36 proAB+ lacIq lacZ_M15]	GE Healthcare (Freiburg, DE)
Hyperphage M13K07ΔgIII	-	Rondot et al., 2001
M13K07	-	Vieira and Messing, 1987

2.1.7 Eukaryotic cell lines

The cell lines used in this study are listed in table 2.8.

Table 2.8: Eukaryotic cell lines

Cell line	Note	References
HEK293 (human)	Adherent, epithelial, tumorigenic	ATCC (CRL-1573)
Expi293F™ Cells (human)	Derived from HEK293-6E cells, optimized for growth in higher densities in suspension.	Thermo Fisher Scientific Inc. (Waltham, USA)
PAC2 cells (zebrafish)	Spontaneously immortalized. Fibroblast.	CVCL_5853

2.1.8 Zebrafish lines

Zebrafish lines used in this study are listed in table 2.9.

Table 2.9: Zebrafish lines

Fish line	Genotype	References
AB	Wild-type	Streisinger, 1981; (ZIRC)
Brass	*Brs*$^{+}$	Postlethwait et al., 1994
parachute (*pac*) cdh2 mutant	*cdh2 r2.10* heterozygote	Lele et al., 2002
zf516 Tg (Cdh2-sfGFP-TagRFP)	TgBAC(cdh2:cdh2-sfGFP-TagRFP, crybb1:ECFP) inserted on a cdh2 *parachute* genetic background (*pac*, allele *tm101b*)	Revenu et al., 2014; Jiang et al., 1996
Tg(atoh1a:KalTA4)	*atoh1a:KalTA4* construct genome integrated on wild-type background	Distel et al., 2010
Tg(4xUAS:GFP)	*4xUAS:GFP* construct genome integrated on wild-type background	Distel et al., 2010

2.1.9 Expression vectors

Expression vectors used in this study are listed in table 2.10.

Table 2.10: Expression vectors

Plasmid	Description	Reference
pCSE2.6-(scFv)hIgG1-Fc	scFv-hFc antibody production in HEK293-6E cells	Beer et al., 2018
pCSE2.6-(antigen)mIgG2a-Fc-Xp	Cadherin 2 ECD and ECD-domains production as mouse Fc-fusion in	Miethe et al., 2015

Plasmid	Description	Reference
	HEK293-6E cells	
pHAL30 (Phagemid)	Antibody Phage-Display and soluble scFv production in *E. coli*	Kügler et al., 2015
Tol1 donor vector	Transposon-donor plasmid containing the cassette for genome integration	Provided by A. Koga Lab
Tol2 donor vector	Transposon-donor plasmid containing the cassette for genome integration	Provided by K. Kawakami Lab
pKJ-Tol2 transposase(A25) (internal database #3816))	Vector for Tol2 transposase mRNA *in vitro* synthesis	Provided by K. Namikawa
pCMV-mp75NTR-YFP	Mouse p75-YFP eukaryotic expression vector	Zhang et al., 2012
pCMV-scFv α-phOx-KDEL	Eukaryotic expression of ER intrabody to PhOx	Zhang et al., 2012
pCMV-scFv α-p75-KDEL	Eukaryotic expression of SH325-G7 ER intrabody to mouse p75	Zhang et al., 2012

2.1.10 Enzymes

All enzymes and related buffers used in this study are listed in table 2.11.

Table 2.11: Enzymes

Product	Supplier	Catalog number
Calf Intestinal alkaline Phosphatase	New England Biolabs (Frankfurt a. M., DE)	M0290
Collagenase (Type 2)	Thermo Scientific, DE	17101015
GoTaq® DNA-Polymerase	Promega (Mannheim, DE)	M300
Phusion DNA-Polymerase	New England Biolabs (Frankfurt a. M., DE)	M0530
Restriction endonucleases		-
T4 DNA Ligase	Promega (Mannheim, DE)	M180A
Trypsin	Sigma-Aldrich (Taufkirchen, DE)	-
Trypsin/EDTA	Biochrom	L2153

2.1.11 Commercial antibodies

Commercial antibodies used in this study are listed in table 2.12.

Table 2.12: Commercial antibodies

Antibody	Conjugation	Catalog No/ Clone name	Supplier/ Origin
Rabbit α- zebrafish Cdh2	-	GTX125885	GeneTex (BIOZOL, Eching, DE)
Mouse α-p75 NGF Receptor (muse, rat) (monoclonal)	-	ab61425	Abcam (Berlin, DE)
Mouse α-c-Myc	-	9E10	Produced in house

(monoclonal)			
goat α-mouse IgG (Fc)	HRP	A0168	Sigma-Aldrich (Hamburg, DE)
goat α-hIgG (Fc)	AP	109-055-098	Dianova (Hamburg, DE)
goat α-hIgG (Fc)	HRP	A0170	Sigma-Aldrich (Hamburg, DE)
goat α-human IgG (Fc)	FITC	109-095-098	Dianova (Hamburg, DE)
goat α-human IgG (Fc)	FITC	F9512	Sigma-Aldrich (Hamburg, DE)
goat α-human IgG (Fc)	APC	109-135-098	Dianova (Hamburg, DE)
rat anti-human IgG (Fc) (monoclonal)	APC	M1310G05	Biolegend/BIOZOL (Eching, DE)
goat anti-rabbit IgG (H + L)	Cy3	111-136-144	Dianova (Hamburg, DE)
goat α-mouse IgG (Fc)	FITC	F5897	Sigma-Aldrich (Hamburg, DE)
goat α-mouse IgG (Fc)	APC	115-136-072	Jackson ImmunoResearch (Ely, UK)

2.1.12 Commercial kits

Commercial kits used in this study are listed in table 2.13.

Table 2.13: Commercial kits

Kit	Description	Supplier
NucleoBond®PC500 Xtra Midi	Preparation of plasmid DNA	Macherey-Nagel (Düren, DE)
NucleoSpin® Plasmid easy pure	Preparation of plasmid DNA	Macherey-Nagel (Düren, DE)
NucleoSpin® Gel and PCR clean-up	Clean up of DNA-fragments	Macherey-Nagel (Düren, DE)

2.1.13 Bioinformatics software

Bioinformatics software used in this study are listed in table 2.14.

Table 2.14: Bioinformatics software

Software	Reference	Purpose
Image Lab Software	Bio-Rad	ChemiDoc MP images processing
VBase2	Mollova et al., 2010	Analysis of antibody sequences
ImageJ	Schneider et al., 2012	
Leica Las X	Leica microsystems	
PyMol v1.3	The PyMOL Molecular Graphics System, Schrödinger, LLC.	Molecular visualization
SH-800 software	https://www.sonybiotechnology.com/us/instruments/sh800s-cell-sorter/software/	Flow cytometry analysis and data visualization
CytExpert 1.2 software	https://www.beckman.com/coulter-flow-cytometers/cytoflex/cytexpert	
Weasel	http://www.frankbattye.com.au/Weasel/?utm_source=Chromocyte&utm_medium=Educate	
Mendeley	https://www.mendeley.com	Reference management
SWISS-MODEL	Arnold et al., 2006	Protein structure homology modelling
NCBI	http://www.ncbi.uhm.nih.gov	Literature, Protein- and Gene-sequences
LibreOffice Suite	https://de.libreoffice.org	Text and Data

WPS Suite	https://www.wps.com/	Text and Data
Inkscape 0.91	https://inkscape.org/	Figures editor
Geneious 4.8.5	https://www.geneious.com	*In silico* cloning, sequence analysis
GraphPad Prism 6	Prism version 6.00 for Windows, GraphPad Software, La Jolla California USA, www.graphpad.com	scFv-hFc antibody EC50 values calculation from titration ELISA results

2.1.14 Oligonucleotide primers

Oligonucleotide primers used in this study are listed in table 2.15.

Table 2.15: Oligonucleotide primers list

Primer ID	Primer name	Seq 5' → 3'
2563	zCdh2-ECD1_BssHII_f	ATATGCGCGCACTCCATGTGGGTCATTCCTCCTG
3035	zCdh2-ECD1_NotI_r	ATGTGCGGCCGCGAACTCTGGCCGGTTGTC
3036	zCdh2-ECD2_BssHIII_f	ATATGCGCGCACTCCACACACCAGATCTGGAATGG
2561	zCdh2-ECD2_NotI_r	TAATGCGGCCGCGAACTCGGGAGCG
3037	zCdh2 148-207_NotI_r	TAATGCGGCCGCAGAGAGAAGTCCTGAAATGG
3038	zCdh2 195-273_BssHII_f	ATATGCGCGCACTCCGGCCTGTTTATCATCGACC
3039	zCdh2 195-273_NotI_r	TAATGCGGCCGCTACGAATGTTCCTGGTTTGG
3040	zCdh2	ATATGCGCGCACTCCGTGGATGAGGGTGC

	263-324_BssHII_f	CAAAC
3041	zCdh2 263-324_NotI_r	TAATGCGGCCGCCAGGCCTGCAGCTACTG
3042	zCdh2 315-369_BssHII_f	ATATGCGCGCACTCCGGCAAAATCATCACA GTAGC
2562	zCdh2 propeptide_BssHII_f	ATATGCGCGCACTCCATGCCATGTCAGCCT G
2560	zCdh2-ECD5_NotI_r	TAATGCGGCCGCGATGCGCTCCATGTC
2815	zCdh2_PvuII_f	AGCTCAGCTGAGTCTGAAGATTAG
2817	zCdh2_XbaI_r	ATCATCTAGATTTATTTATCCCGTCTCTTCAT CC
3757	hCdh2-BssHII_f	ATTAGCGCGCACTCCTCTGGTGAAATCGCA TTATGC
3758	hCdh2-NotI_r	TAATGCGGCCGCAATCCTGTCCACATCTGT GC
3211	Linker-mClover_NotI_f	ATTAGCGGCCGCGGATCCACCGGTCGCCA CCGTGAGCAAGGGCGAGG
3212	mClover_XbaI_r	ATCATCTAGATTTACTTGTACAGCTCGTCCA TGC
2849	tagRFP-T_EcoRV_f	ATTAGATATCGCAAACATGGTGTCTAAGGG CGAAG
2850	tagRFP-T_XbaI_r	ATGGTCTAGATTACTTGTACAGCTCGTCCA TGC
2701	mCMV CpG-free-PacI_f	GCCGTTAATTAAGAGTCAATGGGAAAAACC CAT
2702	mCMV CpG-free-SbfI_r	ATTACCTGCAGGCACCCCTATTGACCTTAT GTATG
2703	xEF1a-PacI_f	CGCGTTAATTAACAGGGGGATCATCTAATC AAG
2704	xEF1a-SbfI_r	ATATCCTGCAGGGCATGCCTGAGAATTTCA G

2831	xEF1a_NheI_for	ATATGCTAGCAGGATCATCTAATCAAGCACA AATAAGG
2832	xEF1a_BamHI_rev	TCATGGATCCAGAGAATTTCAGAATGTAAT GATACCTTTG
2851	Intrab.cassette_EcoRI_f	AGATGAATTCGCAAACATGCACAAGG
2852	Intrab.cassette_XhoI_r	GCATCTCGAGTTTATAGTTCGTCCTTTAGAT CTTCTTCTG

2.2 Methods

2.2.1 Molecular biology techniques

2.2.1.1 DNA amplification via PCR

2.2.1.1.1 DNA polymerases

In this study we used two different polymerases based on the purpose of the experiment experiment. GoTaq DNA polymerase (Promega) was used in Colony-PCR reactions to determine insert length after cloning. Phusion® High-Fidelity DNA Polymerase (NEB, Thermo Scientific) was used for the amplification of coding or non-coding DNA to be used as insert in the generation of new plasmid.

2.2.1.1.2 Colony-PCR

Colony-PCR was used to confirm the presence of the correct insert after cloning into the desired vector backbone. Indirectly, it constituted a method to validate the success of the cloning experiments. The primer pair used for each Colony-PCR was based on the destination vector used. This allowed to generate an amplicon also in the absence of a correctly ligated insert. Colony-PCR reaction mix was prepared as shown in table 2.16, while the temperature profile of the reaction in table 2.17.

Table 2.16: Colony-PCR reaction mix

Component	Volume (µL)	Final Concentration
Material from single bacterial colony	/	
5x GoTaq Flexi Buffer (green)	2	1 X
MgCl2 [25 mM]	0,8	2 mM
dNTPs mix [10 mM]	0,5	0.5 mM
Primer F [10 µM	0,5	0.5 µM
Primer R [10 µM]	0,5	0.5 µM
GoTaq-Polymerase [5 U/µL]	0,05	0,025 U/µL
dH2O	5.65	
	10 µL	

Table 2.17: Colony-PCR reaction temperature profile

Step	Temperature (°C)	Time (min:s)	Cycles
Bacterial cell lysis and DNA denaturation	95	2:00	1x
DNA denaturation	94	0:30	29x
Annealing	Depending on primer pair & DNA polymerase in use	0:30	
Elongation	72	1 min/Kb	
Final elongation	72	5:00	1x
Conservation	16	∞	

2.2.1.1.3 High-Fidelity polymerase DNA amplification

The DNAEngine, or the S1000 Thermal Cycler, Bio-Rad thermocyclers were used for the amplification of the DNA fragment of interest.

Primers were designed to add specific restriction site ends for direct cloning into the destination vector. The different DNA templates and primer pairs used for the generation of the antigen vectors are shown in table 2.18. PCR reaction mix was prepared as shown in table 2.19, while the temperature profile of the reaction in table 2.20.

Table 2.18: Oligonucleotide primers and vectors for antigen cloning

Final vector	Primer pair	Destination vector	PCR template	Cloning
pCSE2.6-zCdh2-ECD 1-2-hIgG1Fc	# 2561 # 2563	pCSE2.6-hIgG1 Fc-XP	Zebrafish brain cDNA	BssHII - NotI
pCSE2.6-zCdh2-ECD 1-5-mIgG2aFc	# 2560 # 2562	pCSE2.6-mIgG 2aFc-XP	Zebrafish brain cDNA	BssHII - NotI
pCSE2.6-zCdh2-ECD 1-2-mIgG2aFc	# 2561 # 2563	pCSE2.6-mIgG 2aFc-XP	Zebrafish brain cDNA	BssHII - NotI
pCSE2.6-zCdh2-ECD 1-mIgG2aFc	# 3035 # 2563	pCSE2.6-mIgG 2aFc-XP	Zebrafish brain cDNA	BssHII - NotI
pCSE2.6-zCdh2-ECD 2-mIgG2aFc	# 2561 # 3036	pCSE2.6-mIgG 2aFc-XP	Zebrafish brain cDNA	BssHII - NotI
pCSE2.6-zCdh2-ECD -148-207-mIgG2aFc	# 2563 # 3037	pCSE2.6-mIgG 2aFc-XP	Zebrafish brain cDNA	BssHII - NotI
pCSE2.6-zCdh2-ECD -195-273-mIgG2aFc	# 3038 # 3039	pCSE2.6-mIgG 2aFc-XP	Zebrafish brain cDNA	BssHII - NotI
pCSE2.6-zCdh2-ECD -263-324-mIgG2aFc	# 3040 # 3041	pCSE2.6-mIgG 2aFc-XP	Zebrafish brain cDNA	BssHII - NotI
pCSE2.6-zCdh2-ECD -315-369-mIgG2aFc	# 2561 # 3042	pCSE2.6-mIgG 2aFc-XP	Zebrafish brain cDNA	BssHII - NotI
pCSE2.6-hCdh2-ECD 1-5-mIgG2aFc	# 3757 # 3759	pCSE2.6-mIgG 2aFc-XP	HEK293 cDNA	BssHII - NotI
pCSE2.6-zCdh2-ECD	# 3211	pCSE2.6-zCdh	pCS2-mClov	NotI - XbaI

-TM-mClover	# 3212	2-LSSmKate2 (GiR094-1)	er	
pCSE2.6-zCdh2-truncated (aa 147-738)	# 2815 # 2817	pCSE2.6-zCdh2-ECD1-5-hIgG1Fc (GiR054-1)	zCdh2 whole length gene	PvuII - XbaI

Table 2.19: High-Fidelity polymerase reaction mix

Component	Volume (µL)	Final Concentration
Template DNA (pDNA/cDNA)	1 - 3	0.02 - 0.2 ng/µL
5x Phusion HF Buffer	10	1 X
dNTPs mix [10 mM]	1	0.2 mM
Primer F [10 µM]	2,5	0.5 µM
Primer R [10 µM]	2,5	0.5 µM
Phusion DNA Polymerase [2 U/µL]	0,75	0,03 U/µL
dH2O	30.25 - 32.25	
	50 µL	

Table 2.20: High-Fidelity polymerase PCR temperature profile

Step	Temperature (°C)	Time (min:s)	Cycles
Initial DNA denaturation	98	2:00	1x
DNA denaturation	98	0:10	28x (9x + 19x in twp-steps PCR)
Annealing	Depending on primer pair & DNA polymerase in use	0:30	
Elongation	72	1 min/Kb	
Final elongation	72	5:00	1x
Conservation	16	∞	

2.2.1.2 Agarose gel electrophoresis

Gels of 1 % (w/v) agarose in TAE buffer were used for analytic separation of DNA. DNA fragment of different length were separated electrophoretically applying a current of 120-130 V and 400 A for 20-35 min. For the UV visualization of DNA after the run, ethidium bromide was added to the gel prior agar polymerization to a final concentration of 100 ng/mL. DNA samples were mixed with 6x loading dye (MBI Fermentas, DE) before gel loading. GeneRuler 1 Kb DNA Ladder Mix (MBI Fermentas, DE) was used as a marker. DNA detection under UV light (λ = 312 nm) was done using the ChemiDoc™ MP Imaging System (Bio-Rad, München, DE).

2.2.1.3 Linear DNA purification

PCR products or DNA after endonuclease digestion were purified directly or after gel extraction via NucleoSpin Gel and PCR Clean-Up (Macherey-Nagel).

2.2.1.4 DNA quantification

Assessment of dsDNA concentration and purity after any DNA preparation was assessed by measuring the absorbance at 260 nm and 280 nm with the use of a spectrophotometer (NanoDrop 1000, Peqlab, DE). A ratio of A260nm/A280nm comprised between 1.84 and 1.94 was considered as sufficiently pure for cell transfection or injection into zebrafish embryo.

2.2.1.5 Restriction endonucleases digestion of DNA

Restriction enzyme digestion of PCR products, as well as destination vectors, or insert present in pDNA were performed in a volume of 50 µL for 1-2 h using NEB enzymes accordingly to the manufacturer protocol. When available, the high fidelity (HF) version of the endonuclease was

used. Restriction enzymes were always heat inactivated for 20 min at the temperature indicated by the manufacturer, at 65 °C where heat inactivation was not recommended.

2.2.1.6 Linearized vector backbone Dephosphorylation

Linearized vector DNA was dephosphorylated adding directly into the endonuclease reaction 10U of calf intestinal alkaline phosphatase (CIP) (NEB, USA) for 1 h.

2.2.1.7 DNA ligation

Insert and vector, in the molar ratio of 3.5:1, were ligated overnight at 16 °C or 1 h at RT with 1U T4 DNA Ligase (Promega, DE). For the ligation reaction, 50 ng of destination vector DNA were used in a final volume of 10 µL together with the insert. An additional ligation reaction containing the destination vector alone was included in any experiment as control.

2.2.1.8 Cloning validation and DNA sequencing

Identification of clones containing the newly generated expression vector was made via Colony-PCR first and afterwards confirmed via sequencing. In the cases the Colony-PCR could not be used to discriminate between newly generated plasmid and negative control plasmid, specific restriction digestions or direct sequencing were used to verify cloning exactness. All DNA sequences were obtained from Seqlab Sequence Laboratories Gmbh (Göttingen, DE).

2.2.1.9 Preparation of plasmid DNA

E. coli cells were isolated from the culture media via centrifugation and used for plasmid DNA extraction using the NucleoSpin Plasmid kits (Macherey & Nagel, DE) according to the manufacturer protocol.

Plasmid DNA was always eluted with sterile ultrapure water.

2.2.1.10 Generation of scFv-hFc antibody construct

Selected genes of scFv antibodies to zCdh2-ECD1-2 were cloned into the pCSE2.6-hIgG1-Fc-XP (Beer et al., 2018) mammalian expression vector for production of bivalent scFv-hFc antibodies. NcoI - NotI cloning allowed direct fusion in frame to the N-terminal signal peptide gene and the C-terminal human Fc gene.

2.2.1.11 Generation of new enhancer/promoter expression cassettes

Different enhancer/promoter combinations had to be tested for the generation of a new CpG-free and bidirectional vectors suitable to drive widespread gene expression in zebrafish *in vivo* as well as in eukaryotic cell lines. In every construct the promoter element, Super Core Promoter 2 (SCP2), was kept constant, while the enhancer elements were exchanged. To allow later characterization of each enhancer/promoter combination, a fluorescent reporter gene was cloned per each side of the bidirectional expression cassette. The expression cassette was subcloned into the Tol2 donor vector (transposon-donor plasmid) to allow its transposon mediated genome integration in zebrafish, resulting in the following architecture:

Tol2 IR - pA - tagRFP-T ← SCP2 - Enhancer/s - spacer - Enhancer/s - SCP2 → mClover - pA - Tol2 IR. The following enhancers were cloned and tested alone or in combination: hCMV, mCMV, xEF1a, SV40. Finally, SV40 and hCMV were discarded as resulting constructs did not meet selection criteria. Two enhancer/promoter combinations were kept, GiR077 (Figure 22) and GiR085-1 (Figure 17). The SCP2 CpG-free sequence (Juven-Gershon et al., 2006), as well as the SV40 and Xenopuse EF1a enhancer sequences, were generated via gene

synthesis. Mouse and human CMV CpG-free enhancer sequences are derived from pCpG-free-LacZ plasmids (Invivogen, Toulouse, France). Fluorescent reporter protein genes were obtained from in-house expression vectors. Oligonucleotide primers designed for DNA amplification of the described genetic elements are shown in Table 2.15.

2.2.1.12 Generation of ER intrabody knockdown vectors

The ER intrabody expression cassette was generated via gene synthesis and is constituted by the following elements in order from 5' to 3': zebrafish Kozak sequence - *C.elegans* signal peptide - NcoI-NotI restriction site (for in frame scFv gene cloning) - HA-tag - Myc-tag - KDEL peptide coding sequence - STOP codon. The cassette was cloned on the right arm of GiR085-1 Tol2 vector (Figure 17) instead of the fluorescent reporter mClover. Oligonucleotide primers designed for DNA amplification of the ER intrabody expression cassette are shown in Table 2.15.

2.2.2 Microbiological methods

2.2.2.1 Preparation of *E. coli* culture

E. coli cells transformed with pDNA after ligation or derived from phage infection were plated onto 2x YT-A agar plates and incubated ON at 37 °C. Single colonies were used to inoculate liquid 2x YT-A culture containing or not 100 mM glucose, based on the vector (pHAL30 vector with glucose; any eukaryotic expression vectors without glucose). Cultures were incubated at 37 °C, overnight, shaking at 250 rpm and used for glycerol stock preparation and plasmid DNA extraction.

2.2.2.2 Glycerol stocks

Bacteria clones of interest were stored in the form of glycerol stock at

-80 °C. For the 20 % (w/v) glycerol stock preparation, 1 mL freshly cultured *E. coli* cells were mixed with 333 µL of 80 % (w/v) glycerol in cryogenic tubes (screw cap) and stored at -80 °C.

2.2.2.3 *E. coli* transformation and plating

Per each reaction, 20 µL of chemically competent *E. coli* cells were thawed on ice. Afterwards, a maximum amount of 100 ng DNA from the ligation were added to the bacteria and gently mixed prior 20 min incubation on ice. Mixed DNA and bacteria were then incubated 60 sec at 42°, followed by 2 min on ice, before adding 1 mL SOC medium pre-warmed at 37 °C. At this point cells were incubated 1 h at 37 °C and 650 rpm in a Thermomixer. After 1 h cells were pelleted for 30 sec at 16,100 xg and resuspended in 100 µL of their own supernatant before plating on 2x YT-AG agar plates. Plates were incubated 16 h at 37 °C.

2.2.3 Selection of human recombinant antibodies

For the selection of human antibodies to the zebrafish Cdh2 extracellular domain, the first two extracellular domains of the molecule fused to human Fc were used as antigen (zCdh2-ECD1-2-hFc). The antibody selection (panning) was performed in 96 well microtiter plates (High Binding Costar/Corning, New York, USA) on immobilized antigen as previously shown (Russo et al., 2018, Methods Mol Biol.). Antibodies binding to the target were selected from 1×10^{11} phage particles of Hyperphage (Rondot et al., 2001; Soltes et al., 2007) packaged human naïve antibody gene libraries HAL9/10 (Kügler et al., 2015). Ninety-two mAb producing clones were randomly picked after three rounds of panning. The 92 different soluble scFv antibodies produced were tested in ELISA for presence of binding against the zCdh2-ECD1-2-hFc and absence of binding to an unrelated hFc-fused protein. Antibody selection here described has been performed by Saskia Helmsing.

2.2.4 Biochemical methods

2.2.4.1 Affinity purification of Fc-fused proteins

One week after transfection, HEK293-6E supernatant was collected after centrifugation (500 xg, 10 min) and used for Protein A affinity chromatography on 24-well binding plates. These are made by three components assembled together: a 10 mL Uniplate PP, a 10 mL Unifilter, 10 µm melt blown PP, and a MabSelect SuRe Protein A affinity matrix (GE 7701-5110; GE 7700-9917; GE 17-5438-01; Whatman, Munich, DE). After loading the sample onto the matrix, the matrix was washed first with phosphate-buffered saline (PBS), then with 100 mM sodium citrate buffer pH 5.0. Elution was performed in 1.5-2 mL of 100 mM sodium citrate buffer pH 3.0. Fractions were neutralized by adding 1 M tris-HCl pH 9.0. Buffer was exchanged to PBS using the Zeba™ Spin Desalting column according to the manufactured protocol. Purified antibodies integrity and purity was assessed in coomassie staining after SDS-PAGE. Antibody solution was stored at -20 °C in 50-100 µL aliquots or used directly. In the second case, antibodies were stored at 4 °C for few months.

2.2.4.2 Determination of protein concentration

Purified protein concentration was assessed by measuring the absorbance at 280 nm with the use of a spectrophotometer (NanoDrop 1000, Peqlab, DE). Measured concentration was adjusted based on the calculated molecular weight and molar extinction coefficient (Geneious 4.8.5 bioinformatics tool).

2.2.4.3 SDS-PAGE

Protein samples were separated according to their electrophoretic mobility in Sodium dodecyl sulfate polyacrylamide gel electrophoresis

(SDS-PAGE). For a better resolution of high molecular weight proteins 10 % polyacrylamide gels were used, otherwise 12 % was preferred. Gel composition is shown in Table 2.21.

Samples were mixed with Laemmli's sample buffer containing ß-Mercaptoethanol and incubated at 96 °C. Purified protein samples were boiled for for 10 min, while cell lysate for 30 min. Samples were directly used after preparation. HEK293 cell lysate, of untransfected cells or cells transfected with the vector expressing zCdh2-ECD-mFc, was prepared for 30 min at 95 °C with Laemmli SDS sample buffer containing β-Mercaptoethanol (ß-ME) (reducing conditions) and loaded onto a 10 % SDS polyacrylamide gel. Sample concentration was approximately 80,000 cells per lane. Cell lysate sample was centrifuged 5 min at maximum speed before gel loading.

Purified protein samples were prepared also in SDS sample buffer containing β-Mercaptoethanol (ß-ME), but boiled for only 10 min at 95 °C and loaded onto the gel at a concentration of 0.5 µg per lane.

Precision Plus protein standard (Bio-Rad, DE) was loaded onto the gel as marker. Electrophoretic run was performed at 300 V, 20 mA per one gel.

Table 2.21: Polyacrylamide gel preparation mix

Component	Stacking gel (4 %)	Running gel (10 %)	Running gel (12 %)
30 % Acrylamide mix	0.26 mL	1.3 mL	1.6 mL
1.5 M Tris-HCl (pH 8.8)	/	1.0 mL	1.0 mL
1 M Tris-HCl (pH 6.8)	0.20 mL	/	/
10 % (w/v) SDS	15 µL	40 µL	40 µL
10 % (w/v) APS	15 µL	40 µL	40 µL
TEMED	2 µL	2 µL	2 µL
dH2O	1.0 mL	1.6 mL	1.3 mL

2.2.4.4 Coomassie blue staining

Every protein sample after affinity chromatography purification was analyzed for purity, integrity, and degradation using Sodium dodecyl sulfate polyacrylamide gel electrophoresis (SDS-PAGE) and Coomassie blue (Carl Roth GmbH, Karsruhe, DE) staining. Proteins on SDS-gels were stained with Coomassie staining solution and de-stained in destaining solution until protein bands were clearly distinguishable from the background.

2.2.5 Cell culture methods

Cell manipulation described in this section was performed in sterile conditions under a laminar flow clean bench using sterile consumables and reagents.

2.2.5.1 HEK293 adherent cells culture

Human embryonic kidney 293 (HEK293) adherent cell line was cultured in DMEM medium supplemented with 8 % FCS, 4.5 g/L glucose, and 100 µg/mL penicillin/streptomycin. Cells were maintained in 10 cm petri dish at 37 °C, 5 % CO_2, 96 % humidity. Cells at 80 - 90 % confluency were washed with PBS and then detached with 1 mL trypsin/EDTA solution. Trypsin was inhibited with 4 mL medium containing supplements. Cells were seeded at a confluent state of ~10 % into new plates containing 10 mL of pre-warmed fresh medium. Cell passage was repeated every 2-3 days depending on the rate of cell division.

2.2.5.2 HEK293 adherent cells transfection

Each ER intrabody knockdown vector encoding for a specific scFv-KDEL to zCdh2 and tagRFP-T was cotransfected together with pCSE2.6-zCdh2-ECD-TM-mClover or pCSE2.6-zCdh2-truncated (aa 147-738) antigen vector in a 10:1 ratio. This particular DNA ratio was the

result of optimization tests and depends on the different strength of the enhancer/promoter used. The simian CMV IE94 enhancer/promoter of the pCS2+ vector drives a much stronger expression than the mCMV-xEF1a CpG-free enhancers combined to the SCP2 (ER intrabody bidirectional vector). Per each transfection reaction 150 µL Opti-MEM transfection medium were added into one well (DNA well) of a 48x well plate, while 125 µL Opti-MEM transfection medium were added into a different well of the same plate (PEI well).

A total of 1820 ng of ER intrabody vector + 180 ng antigen vector were added into the DNA well, while 8µL of PEI 25KDa were added into the PEI well. The two wells were fused after some minutes and the DNA-PEI solution thoroughly resuspended ten times. After 25 min incubation, DNA-PEI complexes were added onto 70 % confluent cells in a 6x well plate in 2 mL medium.

2.2.5.3 Fc-fusion protein production in HEK293-6E

Suspension HEK293-EBNA1-6E (HEK293-6E) cells were cultured in F17 medium (Invitrogen, Life Technologies) supplemented with 7.5 mM L-glutamine, 0.1 % Pluronic-F68. Cells for transfection were maintained by Doris Meier.

For transfection, mammalian expression vector (5 µg) and PEI (25 µg) were thoroughly mixed in 500 µL transfection medium and incubated at RT. After 20 min incubation, the DNA-PEI mix was added to 5 mL HEK293-6E culture at the density of $1.5x10^6$ cells/mL and incubated at 37 °C, 5 % CO_2, and 190 rpm (50 mm orbital). After 48 h, 5 mL of cell culture medium containing 0.5 % Tryptone N1 were added to the culture and the incubation prolonged for other 120 h. The presence in the mammalian expression vector used for transfection of a N-terminal signal peptide, in frame with the gene of interest, allows for antigen or antibody secretion into the cell supernatant.

2.2.5.4 Zebrafish PAC2 cell culture conditions

Zebrafish fibroblast cells are non-directly-immortalized cells obtained from embryonic zebrafish. Hence, the growth rate of these cells is particularly low compared to standard immortalized cell lines. Also, these cells are particularly sensitive to low levels of confluency and were always kept at a confluency higher than 30 %. PAC2 cells were cultured in Leibovitz's L-15 medium supplemented with 10 % FCS and 100 µg/mL penicillin/streptomycin. Cells were maintained in 10 cm petri dish at 28 °C without CO_2. Cells at ~90 % confluency were washed with PBS and then detached with 1.5 mL trypsin/EDTA solution. Incubation time required for the dissociation may vary, but it was never inferior to 10 min. Trypsin was inhibited with 4 mL medium containing supplements. Cells were seeded at a confluent state of ~30 % into new plates containing 10 mL of pre-warmed fresh medium. Cell passage was repeated every 5-7 days depending on the rate of cell division.

2.2.5.5 Transfection of zebrafish cells via electroporation

For electroporation, zebrafish cells were pelleted by centrifugation, resuspended in sterile 1x PBS, and diluted to a final concentration of 10^6 cells in 350 µL. Afterwards, 350 µL cell solution was mixed with 20 µg DNA and the solution adjusted to 400 µL adding sterile ultrapure water. Mix has been gently resuspended bu pipetting up-and-down for at least 20 sec, before being transferred into a 0.4 cm gap electroporation cuvette. Samples were electroporated using the Gene Pulser XcellTM Electroporation System (BIO-RAD) using the parameters shown in Table 2.22. If necessary, because of limiting DNA or cells availability, the electroporation reaction mix has been scaled down to a maximum of $0.5x10^6$ cells plus 10 µg DNA in a volume of 100 µL. For electroporation of multiple constructs, same overall amount of DNA was used, but equally split by the number of the constructs used.

Table 2.22: DNA Electroporation - Exponential decay protocol

	PAC2 cells	Primary cells
Voltage (V)	250 V	280 V
Capacitance (µF)	950 µF	950 µF
Resistance (ohm)	PBS R < 30 ohm	PBS R < 30 ohm
Cuvette	4 mm	4 mm
Buffer	PBS	PBS

2.2.5.6 Zebrafish PAC2 cells preparation for FACS analysis

PAC2 cells after electroporation were directly seeded into Ultra-Low attachment 6-well plates (CELLSTAR 657185, Greiner Bio-one, Frickenhausen, DE) at a concentration of 1×10^6 cells/well in 2 mL Leibovitz's L-15 Medium supplemented with 10 % FCS and 1 % Pen./Strep. Cells were incubated at 28 °C w/o CO_2 before immunostaining and flow cytometry analysis. The use of Ultra-Low attachment plates allowed to mechanically detach the cells without any need of enzymatic dissociation. Most of the proteases used for cell detachment or tissue dissociation (including trypsin and collagenase) impair the display of Cdh2.

2.2.5.7 Zebrafish embryonic primary cell preparation for FACS analysis

Single cell suspension from 3 dpf zebrafish Wt, *parachute*, and *zf516 Tg* larvae (obtained as described in paragraph 2.2.6.5) was seeded into Ultra-Low attachment 6-well plates (CELLSTAR 657185, Greiner Bio-one, Frickenhausen, DE) in Leibovitz's L-15 Medium supplemented with 10 % FCS and 1 % Pen./Strep. at a concentration of 1-2 × 10^6/mL. Cells were incubated at 28 °C w/o CO_2 until immunostaining and flow cytometry analysis. The use of Ultra-Low attachment plates allowed to detach the cells without any need of enzymatic dissociation.

2.2.5.8 Zebrafish embryonic primary cell culture for confocal imaging

Primary embryonic zebrafish cells were obtained and cultured as previously described (Sassen et al., 2017; Russo et al., 2018, JoVE). Single cell suspension after electroporation was seeded directly on poly-L-lysine-coated glass bottom dish for confocal microscopy. A total of $0.5x10^6$ electroporated cells per dish were seeded in 500 µL. After 1 h incubation, 6 mL of complete medium was added and the cells incubated at 28 °C without CO_2. Half of the medium volume was daily replaced with fresh medium. At 48 h in culture cells were imaged at the confocal laser scanning microscope SP8 (Leica microsystems, Wetzlar, DE).

2.2.5.9 Zebrafish embryonic primary cell culture for TNFα treatment

Embryonic primary zebrafish cells (obtained as described in paragraph 2.2.6.5) were seeded at a density of $0.1x10^6$ cells/well onto poly-L-lysine-coated 96-well plate and incubated ON in L-15 medium supplemented with 10 % FCS and 100 µg/mL penicillin/streptomycin. The morning after, medium was completely replaced with starvation medium containing only 1 % FCS. Eight hours post starvation, TNFα was added to a final concentration of 30 ng/mL. As the reagent has been diluted 1:3,300 in starvation medium, as control it has been used starvation medium only. After 12 h, the expression level of mClover fluorescent reporter was assessed with an epifluorescent microscope, as well as quantified via flow cytometry.

2.2.5.10 Fluorescence imaging of living cells

Leica inverted epifluorescent microscope DM5500B equipped with temperature control chamber system was used for documentation. Acquisition parameters were kept constant between samples for

comparison. Alternatively, Leica SP8 confocal laser scanning microscope was used for high resolution image acquisition.

2.2.5.11 Cells freezing and thawing

For long-term storage, HEK293 cells were resuspended in complete growth medium supplemented with 5 % (v/v) DMSO and transferred into cryovials with screw cap. After gradual freezing at -80 °C in apposite freezing containers, cells were transferred in liquid nitrogen. PAC2 zebrafish fibroblast cells were stored at -80 °C in Bambanker freezing medium (NIPPON Genetics). All eukaryotic cell lines were thawed quickly via immersion in 37 °C water bath. Right after thawing, cells were resuspended in 10 mL complete medium to dilute the DMSO. After centrifugation, cells were resuspended into fresh pre-warmed medium and seeded on tissue culture plates.

2.2.6 Zebrafish husbandry and embryos manipulation

All experiments and fish maintenance were performed in accordance to the European animal welfare standards and German legislation.

2.2.6.1 Zebrafish husbandry

Raising, spawning, and maintaining of zebrafish were performed as described previously (Westerfield, 2000). After spawning, Zebrafish embryos were maintained at 28 °C in 10 cm Petri dishes containing Danieau 30 % solution (5.8 mM sodium chloride, 0.07 mM potassium chloride, 0.04 mM magnesium sulfate, 0.06 mM calcium nitrate, 5 mM HEPES (2-[4-(2-hydroxyethyl)piperazin-1-yl]ethanesulfonic acid), pH 7.2). Danio solution was replaced daily. Only the Zebrafish embryos used for whole mount immunostaining experiments were maintained in 30 % Danieau solution supplemented with 0.003 % Propylthiouracil (PTU) (Sigma, Steinheim, DE). PTU was added starting from 1 dpf.

Zebrafish larvae designated to generate a new transgenic line were raised to adulthood.

2.2.6.2 Zebrafish embryos microinjection

After spawning, fertilized eggs were collected and directly used for nucleic acid microinjection. For DNA construct evaluation, expression vector DNA was injected into zebrafish embryos at the single cell stage. For zebrafish transgenic line generation, DNA vector containing an expression cassette flanked by Tol2 inverted repeats sequences was co-injected with Tol2 transposase mRNA into each zygote. Mix preparation for injection is shown in Table 2.23. The Eppendorf Femtojet Express Microinjector device was used for injection. Estimated volume injected per cell: 2 nL.

Table 2.23: Zebrafish egg microinjection reaction mix

	DNA injection	RNA/DNA injection	Final concentration
Tol2 transposase mRNA	/	0.5 - 2 µL	25 ng/µL
Transposon-donor plasmid	0.5 - 2 µL	0.5 - 2 µL	25 ng/µL
Red phenol	1 µL	1 µL	10 %
HPLC-grade water (RNase-Free)	7 - 8.5 µL	5 - 8 µL	
	10 µL	10 µL	

2.2.6.3 Zebrafish larvae spinal cord injury

Three days post-fertilization (3 dpf) zebrafish larvae were anesthetized in 0.05 % tricaine (Sigma, Steinheim, DE) Danio 30 % solution for 10 min before wounding. Larvae were also kept in tricaine containing

solution for the duration of the experiment. With a sterile syringe needle (TERUMO 26g), a small transverse incision was applied to the dorsal side of the fish at the high of the urogenital opening, aiming to cut the spinal cord without cutting off the notochord and the dorsal aorta underneath. Afterwards, larvae were transferred into Danieau 30 % solution without anesthetic and incubated at 28 °C.

2.2.6.4 Fluorescence imaging of living zebrafish larvae

Zebrafish larvae between 2 and 5 dpf were anesthetized in 0.05 % tricaine (Sigma, Steinheim, DE) Danio 30 % solution for 10 min prior image acquisition. Leica epifluorescent stereo microscope (Leica M205FA) was used for documentation. Acquisition parameters were kept constant between samples for comparison. It should be noted that cdh2r210pac mutants and tm101b pac mutants have fully comparable phenotypes (Lele et al., 2002).

2.2.6.5 Embryonic zebrafish dissociation

Three days post-fertilization (3 dpf) zebrafish larvae were anesthetized in 0.05 % tricaine (Sigma, Steinheim, DE) for 10 min prior dissociation. Dissociation into homogeneous cell suspension was done as previously described with minor modifications (Sassen et al., 2017; Russo et al., 2018, JoVE). A minimum of 100 embryos were used per each dissociation. Anesthetized 3 dpf embryos were transferred into a 6 cm cell culture dish using a sterile Pasteur pipette. Embryos were concentrated in a volume of few mL (max 2 mL).

Under a laminar flow clean bench embryos were de-yolked via up-and-down pipetting through a 200 µL-pipette tip opening. De-yolked embryos were pipetted into a sterile cell strainer placed in 70 % (v/v) ethanol. After embryos complete immersion in ethanol for 5 sec, the cell strainer containing embryos was transferred into a dish filled with

Leibovitz's L-15 medium supplemented with 10 % FCS and 100 µg/mL penicillin/streptomycin. Embryos were completely submerged in medium to remove ethanol traces. All the embryos contained in the cell strainer were than collected and transferred in a 1.5 mL sterile reaction tubes and incubated in 1 mL solution of 4 mg/mL Collagenase Type II in Leibovitz's L-15 medium supplemented with 10 % FCS and 100 µg/mL penicillin/streptomycin. Dissociation reaction was incubated on a vertical tube rotator with 30 revolutions per min for 45 min at RT. Dissociation was promoted via up-and-down pipetting through progressively smaller pipette tip opening (down to 10 µL tips). Generation of an almost completely homogeneous single cell suspension was assessed with the use of a microscope. Cell suspension was then filtrated through a 40 µm-net sterile cell strainer prior cultivation. Cells were counted and used for different applications. The cell yield varied between 0.55×10^5 and 1.3×10^5 cells per 3 dpf larva. Variation can be attributed to the different fish line growth speed, number of larvae used per each dissociation reaction, and dissociation time.

2.2.7 Immunological methods

2.2.7.1 Blotting and staining of HEK293 cell lysate

Cell lysate of HEK293 cells transiently transfected with zCdh2-ECD-mFc was used in this experiment. Sample was transferred from SDS gels onto polyvinylidene fluoride (PVDF) membranes via semi-dry Western blot using the Trans-Blot Turbo device (Bio-Rad, DE). Transfer was performed under the following parameters: 0.4 A and 20 V for 30 min. After protein transfer, PVDF membrane was blocked overnight at 4 °C in blocking buffer (MPBST). Individually, each scFv-hFc antibody to zCdh2 was loaded onto pre-cut blot lanes. Antibody was used at a concentration of 500 ng/mL in MPBST. After 1.5 h incubation, membrane

was washed 3 times with PBST for 5 min each. Afterwards, goat anti-human IgG (Fc-specific) alkaline phosphatase (AP)-conjugated secondary antibody (Dianova 109-055-098, Hamburg, DE; 1:10,000) was incubated for 1 h in MPBST. After washing three times with PBST for 5 min each, the membrane was incubated in substrate buffer (100 mM Tris-HCl, 0.5 mM MgCl2, pH 9.5) for 5 min. Visualization was done via incubation with substrate buffer with 1 % (v/v) 5-Brom-4-chlor-3-indolylphosphat (BCIP) and 1 % (v/v) nitro-blue tetrazolium (NBT) (both from Applichem, Darmstadt, DE).

2.2.7.2 Titration ELISA

For scFv-Fc bivalent antibody binding characterization in ELISA, a microtiter plate (High Binding Costar/Corning, New York, USA) was coated overnight with 1 µg/mL (100 ng/well) antigen in PBS at 4 °C. Zebrafish and human Cdh2-ECD-mFc antigens were used in this experiment. An unrelated mIgG2a-Fc fused antigen was used as negative control. Coated wells were blocked with MPBST (2 % Milkpowder in PBS, 0.1 % Tween 20) for 1 h at RT, and then washed three times with PBST (PBS, 0.05 % Tween 20). Soluble scFv-hFc antibodies were diluted in 100 µL MPBST at a final concentration ranging between 0.08 pM and 90.9 nM (for a total of 11 concentration intervals differing by a factor of 4). Antibody solution was incubated for 1.5 h at room temperature (RT) in the antigen-coated wells. After washing three times with PBST, bound scFv-hFc antibody was detected with a goat anti human IgG (Fc-specific) horseradish peroxidase (HRP) -conjugated secondary antibody (Sigma-A0170; 1:70,000). TMB (3,3′,5,5′-tetramethylbenzidine) was used as HRP substrate for visualization. The staining reaction was stopped by adding 100 µL 1 N sulphuric acid. The absorbance at 450 nm and scattered light at 620 nm were measured using a SUNRISE microtiter plate reader (Tecan,

Crailsheim, DE) and the 620 nm values were subtracted to calculate the ELISA signal.

2.2.7.3 Domain mapping ELISA

ELISA assay was used to identify the single zCdh2 domains and domain fragments recognized by the scFv-hFc antibodies. A microtiter plate (High Binding Costar/Corning, New York, USA) was coated overnight at 4 °C with the mIgG2a-Fc fused recombinant zCdh2 antigens (Figure 2) and unrelated mIgG2a-Fc fused antigen (CTR-) at a concentration of 2 µg/mL (200 ng/well) in PBS. Coated wells were blocked with MPBST for 1 h at RT. After washing three times with PBST, scFv-hFc antibodies diluted in 100 µL MPBST were incubated in the antigen-coated wells for 1.5 h at RT. The wells were then washed three times with PBST. Bound scFv-hFc antibody was detected with a goat anti human IgG (Fc-specific) HRP-conjugated secondary antibody (Sigma-A0170; 1:70,000). The visualization was performed as in 2.2.7.2.

2.2.7.4 Epitope mapping on PepSpot membrane

A PepSpot membrane covering the entire zCdh2-ECD1 by 29 peptides was generated (JPT Peptide Technologies GmbH, Berlin, DE) to refine the epitope of antibodies directed to this zCdh2 domain (aa 148-254). Each peptide had a length of 15 aa. Peptide overlap was consisting of 11 aa, hence the offset was 4 aa. The PepSpot membrane was stained accordingly to the manufacturer's instructions. The membrane was activated with methanol before washing with tris-buffered saline (TBS) supplemented with 0.05 % Tween20 (TBST), and blocked with 2 % (w/v) skim milk powder in TBST (MTBST). Primary scFv-hFc antibody to zCdh2 was diluted in MTBST to a final concentration of 1 µg/mL and incubated on the membrane overnight at 4 °C or 3 h at RT. Afterwards, the membrane was washed three times with TBST for 5 min each,

before incubation with goat anti human IgG (Fc-specific) HRP-conjugated secondary antibody (Sigma-A0170; 1:70,000) for 2 h at RT. Afterwards the membrane was washed 3x with TBST before incubation with substrate solution (SuperSignal West Pico Plus Chemiluminescent Substrate, Thermo Scientific, DE). ChemiDoc™ MP Imaging System (Bio-Rad, München, DE) was used for image acquisition.

2.2.7.5 Immunostaining of zebrafish or human cells

Independently from the source, cell for flow cytometry were always detached from the respective culture plate with non-enzymatic methods, mechanically, to preserve the integrity of surface antigens. A total of 4–5x10^5 cells/sample were aliquoted into FACS plates (Eppendorf Deepwell plates, Protein LoBind, 96 wells, Hamburg, DE). Cells were pelleted by centrifugation (350 ×g, 5 min) at 4 °C. Supernatant was removed without disturbing the pellet. Cells were resuspended in ice-cold FACS-buffer (0.5 % BSA, 5 mM EDTA in PBS). Each centrifugation step was performed at 4 °C, while every incubation on ice. Primary antibody was diluted in FACS-buffer at the concentration specified for every experiment and incubated on ice for 1 h. Afterwards, cells were washed twice with FACS-buffer. Appropriate fluorescently coupled secondary antibody were incubated 30 min on ice in the dark (see table 2.12). Cells were washed twice, than filtered through CellTrics 50 µm filters (Sysmex, Norderstedt, DE). Flow cytometry analysis measurements were done with an SH-800 cell sorter (Sony, San Jose, CA, USA) and a CytoFLEX device (Beckman Coulter, Brea, CA, USA). A 488 nm laser was used to excite GFP or FITC. Emission was detected with a 525 ± 25 nm optical filter or a 525 ± 40 nm filter, respectively when using the SH-800 cell sorter or the CytoFLEX device (FITC-channel). The use of the SH-800 cell sorter (Sony, San Jose, CA, USA) was

possible thanks to the support of the instrument responsible person, Fahr Wieland.

APC-coupled antibody was detected in the range 665 ± 30 nm (SH-800 cell sorter) or 660 ± 20 nm (CytoFLEX device) for excitation with a 638 nm laser. Per each sample 10^5 events were analyzed. Forward scatter (FSC) vs backward scatter (BSC) dot plot served to gate alive cells, categorized as larger and less granular in average compared to dead cells. FSC signal height (FSC-H) plotted against FSC area (FSC-A) allowed to distinguish between single cells and doublets. Cdh2-GFP cells (*zf516vTg* line derived) were mostly found as doublets despite the presence of 5 mM EDTA in solution and the cell filtration step. This information was used to adjust the gating in order to enrich the Cdh2-positive cell population. For all the flow cytometry experiments on cell lines alive single cells were used for analysis.

2.2.7.6.1 Whole mount zebrafish immunofluorescent staining

GFP-positive *zf516 Tg*, and zCdh2 pac mutants larvae at 3 dpf were incubated 10 min in 0.05 % tricaine solution (Sigma, Steinheim, DE). After anesthesia, larvae were fixed and permeabilized in a 4 % paraformaldehyde (Merck, Darmstadt, DE) solution containing 0.1 % Triton X-100 (Bio-Rad, Münich, DE) in PBS for 3 h at 4 °C. Sample was rotated during all incubation and washing steps, with the exception of the acetone antigen retrieval one. Fixed tissue was rinsed for 10 min with PBS plus 0.1 % Triton X-100. Subsequent incubation for 15 min at −20 °C in ultrapure acetone served for antigen retrieval. Samples were then washed twice for 10 min in PBS supplemented with 1 % BSA, 1 % Triton X-100 and 1 % DMSO. Samples were blocked with 5 % goat normal serum (Vector labs/BIOZOL, Eching, DE) and 1 % BSA in PBS plus 1 % Triton X-100 and 1 % Dimethyl sulfoxide (DMSO), 1 h at RT. Afterwards, primary antibody solution was incubated overnight at 4 °C in

PBS plus 1 % BSA, 0.1 % Triton X-100 and 1 % DMSO. Rabbit polyclonal antibody GTX125885 α-zCdh2 was diluted 1:100 or 1:500 (8 µg/mL or 1.6 µg/mL respectively). ScFv-hFc antibodies were diluted to a final concentration of 10 µg/mL. After primary antibody incubation, samples were washed four times for 10 min each with PBS containing 0.1 % Triton X-100. Secondary antibody solution prepared in PBS plus 1 % BSA, 0.1 % Triton X-100, and 1 % DMSO was incubated 3 h at RT. Depending on the primary antibody, goat α-rabbit IgG (H + L-specific) Cy3-conjugated (Dianova 111-136-144, Hamburg, DE; 1:100) or rat α-human IgG (Fc-specific) APC-conjugated (Biolegend/BIOZOL M1310G05, Eching, DE; 1:100) secondary antibody were used. Afterwards, washing step was repeated as previously described. The two different fish lines were stained in the same reaction tube by each antibody to respect best comparison criteria. Morphological and fluorescent properties of the two lines allow for discriminating them after the staining during the imaging. GFP-positive *zf516 Tg* and zCdh2 pac mutants larvae after immunostaining were mounted in 1.2 % ultra-low melting agarose. A confocal laser scanning microscope Leica SP8 (Leica microsystems, Wetzlar, DE) was used for image acquisition with the help of Dr. Theisen Ulrike. GFP and APC were excited by a Argon laser (488 nm) and a 633 nm HeNe laser respectively. Multiple z-Stacks spanning the whole tissue of interest were acquired. Image analysis was performed as described in the related paragraph of Bioinformatics methods (2.2.8.4).

2.2.8 Bioinformatics methods

2.2.8.1 In silico cloning

Using the bioinformatics software Geneious 4.8.5, every DNA cloning experiment was simulated *in silico* prior wet lab execution. Newly

generated vectors were sequenced and related results used to verify the exactness of the cloning based on the *in silico* design. Oligonucleotide primers were also designed using this bioinformatics platform. Primer annealing temperature, risk of dimer formation, 3'-extension, and presence of hairpins were verified using the online tool Promix, from the CRIBI Genomics Group University of Padua.

2.2.8.2 Bioinformatics analysis of the antibody sequences

VBASE2 Fab Analysis Tool (Mollova et al., 2010) was used for the scFv antibody sequence analysis to identify heavy and light chain variable region subfamilies.

2.2.8.3 Protein sequence characterization

Estimated protein molecular weight was obtained with the bioinformatics software Geneious 4.8.5, which was also used to calculate their molar extinction coefficient.

2.2.8.3 Sequence and structure analysis of zCdh2 mapped epitopes

SWISS-MODEL online platform (Arnold et al., 2006; Guex et al., 2009; Kiefer et al., 2009; Biasini et al., 2014) was used to model the the zCdh2-ECD (Uniprot: Q90275, aa 148-711) on the base of the crystal structure of the murine Cdh2-ECD (pdb 3Q2W) (Harrison et al., 2011). Amino acid similarity between the two extracellular domain is 75.4 %, 80.4 % when considering only domain 1. The epitopes of antibody SH1352-B11 and SH1352-C6, discovered on PepSpot membrane analysis, have been represented on the model of zCdh2-ECD1 using the software for protein structure analysis PyMol v1.3.

2.2.8.4 Zebrafish whole mount images processing

Leica Application Suite X (Las X) software or the Grid/Collection

stitching plugin of ImageJ (Schneider et al., 2012) were used to stitch frames composing the whole mount. Las X, ImageJ, and Adobe Photoshop were used for images processing. Images from larvae stained by the same antibody in an individual reaction tube were processed using identical parameters for optimum comparison conditions.

2.2.8.5 Flow Cytometry data analysis and plots generation

Display of flow cytometry data and respective analysis was performed using SH-800 software (Sony, San Jose, CA, USA), CytExpert 1.2 software (Beckman Coulter, Brea, CA, USA), or Weasel v3.3.

2.2.8.6 scFv-hFc antibody EC50 value determination

Apparent scFv-hFc antibody affinity was estimated by ELISA-based determination of the EC50 value. In the titration ELISA experiment (Figure 4), EC50 is defined as the concentration of antibody where half of the maximum signal is reached. The maximum signal is reached when antibody binding to the antigen is in saturation. Therefore, EC50 could be calculated only when the titration curve spanned from antibody concentration values that corresponded to absence of binding, to concentration values that corresponded to saturation of the binding towards the antigen. These EC50 values were calculated using the equation for 4 parameter logistic (4PL) symmetrical sigmoid curve fit (Sigmoidal, 4PL, X is log(concentration)) available from the interpolation analysis tool of the bioinformatics software GraphPad Prism 6.

3. Results

3.1. Generation and characterization of antibodies to zCdh2

3.1.1. Production of recombinant zCdh2-ECD antigens

For antibody selection and for subsequent epitope mapping, recombinant versions of zebrafish Cdh2 were produced. DNA encoding the zebrafish Cdh2 extracellular domain was amplified via PCR from zebrafish AB strain cDNA. To generate Fc-fused antigens for antibody selection and epitope determination, eight variants including the whole zCdh2 extracellular domain (zCdh2-ECD), as well as seven truncated recombinant variants of the same molecule, were cloned into pCSE2.6-mIgG2a-Fc-XP mammalian expression vectors (Miethe et al., 2015; Froude et al., 2017) (Figure 2). One recombinant variant (zCdh2-ECD1-2) was cloned as well into the pCSE2.6-hIgG1-Fc-XP vector (encoding for a human Fc part) to generate the antigen suitable for antibody selection (Figure 2). HEK293-6E cells and Protein A affinity chromatography purification allowed the production of the recombinant Fc-fusion proteins. SDS-PAGE analysis and Coomassie blue staining confirmed the purity of the antigen preparation (Figure 3) and the expected relative molecular mass of the antigens (Table 3.1).

Table 3.1: Yields, molecular mass, and N-glycosylation of the Fc-fused zCdh2-ECD domains and domain fragments

Zebrafish Cdh2 domains and recombinant fragments	Conc. (mg/mL)	mg/L (protein/culture volume)	Predicted molecular mass (kDa)	N-glycosyl. sites
zCdh2-ECD (aa 148-702)-mIgG2a-Fc	0.23	34.5	101.1	2
zCdh2-ECD1-2 (aa 148-369)-mIgG2a-Fc	0.34	51.0	50.3	1
zCdh2-ECD1-2 (aa 148-369)-hIgG1-Fc	0.55	82.5	50.5	1
zCdh2-ECD1 (aa 148-254)-mIgG2a-Fc	0.53	79.5	37.8	0
Cdh2-ECD2 (aa 255-369)-mIgG2a-Fc	0.22	33.0	38.1	1
zCdh2-ECD-aa 148-207-mIgG2a-Fc	0.58	87.0	32.2	0
zCdh2-ECD-aa 195-273-mIgG2a-Fc	0.13	20.2	34.4	0
zCdh2-ECD-aa 263-324-mIgG2a-Fc	0.52	78.0	32.2	0
zCdh2-ECD-aa 315-369-mIgG2a-Fc	0.05	7.5	31.5	1

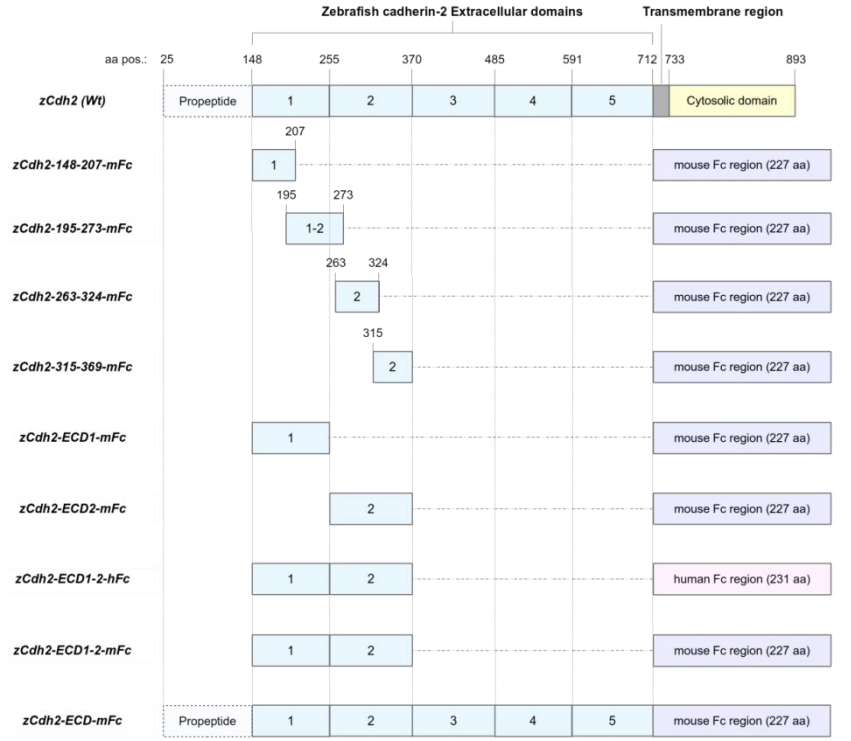

Fig. 2: zCdh2-ECD derived antigens fused to human/mouse Fc-part.

Zebrafish Cdh2 extracellular region and single domain fragments were generated as mouse or human Fc-fusion antigens. Amino acid numbering according to Uniprot Q90275.

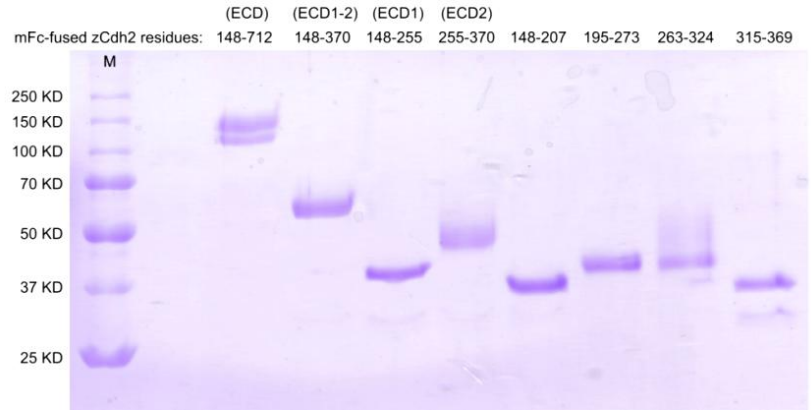

Fig. 3: Mouse Fc-fusion Cdh2-ECD derived antigens purity evaluation.
Coomassie stained 12 % SDS-PAGE-gel chromatography of purified mouse IgG2aFc-fused zCdh2-ECD and derived fragments. Purified zCdh2 derived antigens are assumed to appear as single or double band dependent on the glycosylation state of the molecule. N-glycosylation is expected at residues: 260, 312, 389, 442, 559, 609, 638, and 679; as such it will be more visible for some antigens than others. M, marker.

3.1.2. Generation of human scFv antibodies to zCdh2

The naive human antibody gene libraries HAL9 and HAL10 were used as starting material for the generation of recombinant scFv antibody fragments to zCdh2-ECD1-2 via phage display. zCdh2-ECD1-2-hFc recombinant protein immobilized on microtiter plates was used as antigen for antibody selection, while an unrelated hFc-fused antigen was used for negative selection, by means of library preincubation and competition, in each round of antibody selection (panning round).
After three panning rounds, 92 *E. coli* clones were randomly picked and cultivated to produce soluble scFv fragments. Their cultivation supernatants were individually tested in screening ELISA for binding to immobilized zCdh2-ECD1-2-hFc or the unrelated hFc-fused antigen.

Out of 92 tested scFv's, 21 bound to the zCdh2-ECD1-2-hFc but not to the negative control antigen. The DNA encoding each selected scFv clone was isolated and treated with the restriction enzyme BstNI. Twelve different restriction patters were identified and the corresponding scFv DNA sequence of one clone representative for each pattern was determined. The sequencing result confirmed the selection of 11 unique human mAb sequences. Analysis of these 11 scFv sequences using the VBASE2 Fab Analysis Tool (Mollova et al., 2010) showed their high genetic diversity in respect of their heavy and light chain variable region subfamilies origin (Table 3.2).

Table 3.2: recAb heavy chain (VH) and light chain (VL) variable region subfamilies.

Gene segments: V (variable region), D (diversity region), J (joint region)

Antibody clone	VH - V	VH - D	VH - J	VL - V	VL - J
SH1352-A3	IGHV3-33*01	IGHD2-21*02	IGHJ4*02	IGLV3-19*01	IGLJ3*02
SH1352-B11	IGHV3-33*01	IGHD6-13*01inv	IGHJ4*02	IGLV6-57*01	IGLJ3*02
SH1352-C6	IGHV5-51*01	IGHD1-26*01inv	IGHJ4*02	IGLV3-19*01	IGLJ3*01
SH1352-D7	IGHV3-33*01	IGHD1-1*01inv	IGHJ6*02	IGLV1-47*01	IGLJ3*02
SH1352-E1	IGHV3-33*01	IGHD6-19*01	IGHJ4*02	IGLV6-57*01	IGLJ3*02
SH1352-E11	IGHV1-46*03	unclear	IGHJ4*02	IGLV1-47*02	IGLJ3*01
SH1352-F4	IGHV1-18*01	IGHD2-21*02inv	IGHJ5*02	IGLV2-14*01	IGLJ3*01
SH1352-F6	IGHV3-33*01	IGHD1-26*01	IGHJ4*03	IGLV1-47*02	IGLJ3*02
SH1352-F9	IGHV1-2*02	IGHD2-15*01	IGHJ1*01	IGLV2-8*01	IGLJ1*01
SH1352-G9	IGHV1-8*01	IGHD5-5*01	IGHJ4*02	IGLV3-19*01	IGLJ3*01
SH1352-G12	IGHV5-a*03	IGHD5-18*01	IGHJ4*02	IGLV1-44*01	IGLJ3*02

3.1.3. Production of bivalent human antibodies (scFv-hFc)

DNA encoding each unique scFv antibody was subcloned into the mammalian expression vector pCSE2.6-hIgG1-Fc-XP to produce mAbs in the scFv-Fc format by addition of the human IgG1-Fc moiety. HEK293-6E cells were transfected with the scFv-hFc antibody expression vectors for transient antibody production. After about one week, Protein A affinity chromatography purification of cultivation supernatant yielded highly purified scFv-hFc antibodies with yields ranging between 12 mg/L and 124.8 mg/L (Table 3.3). ScFv-hFc antibody purity was confirmed by SDS-PAGE under reducing conditions and Coomassie blue staining (data not shown).

Table 3.3: Yields of scFv-hFc antibodies

Antibody clone	Concentration (mg/mL)	mg/L (protein/culture volume)
SH1352-A3-hIgG-Fc	0.26	30.0
SH1352-B11-hIgG-Fc	0.10	15.0
SH1352-C6-hIgG-Fc	0.08	12.0
SH1352-D7-hIgG-Fc	0.38	57.0
SH1352-E1-hIgG-Fc	0.10	15.0
SH1352-E11-hIgG-Fc	1.56	124.8
SH1352-F4-hIgG-Fc	0.27	40.5
SH1352-F6-hIgG-Fc	0.27	40.5
SH1352-F9-hIgG-Fc	0.13	19.5
SH1352-G9-hIgG-Fc	0.73	109.5
SH1352-G12-hIgG-Fc	0.29	43.5

3.1.4. scFv-hFc antibody binding to recombinant zCdh2-ECD

Titration-ELISA on coated antigen zCdh2-ECD-mFc was used to determine the binding of the purified scFv-hFc antibodies to the whole

zCdh2 extracellular domain. The apparent EC-50 obtained in this assay, despite it does not allow for determining absolute antibody affinity, it permits to generate an affinity-based ranking of the tested antibodies. The scFv-hFc antibodies were tested in a concentration series ranging from 0.08 pM to 90.9 nM (Figure 4). All the antibodies originally generated against the zCdh2-ECD1-2 bound to the recombinant antigen zCdh2-ECD-mFc. Antibody SH1352-C6-Fc showed the strongest binding in ELISA, while SH1352-G12-Fc showed the weakest binding, as shown by the apparent antibody affinity estimated by ELISA-based determination of the EC50 values (Table 3.4). No one of the tested antibodies showed reactivity to the unrelated mFc-fused antigen used as CTR-.

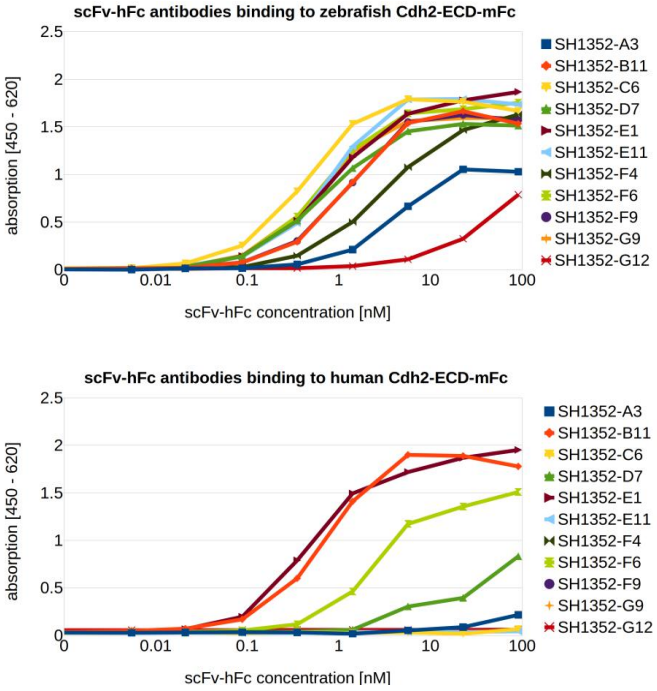

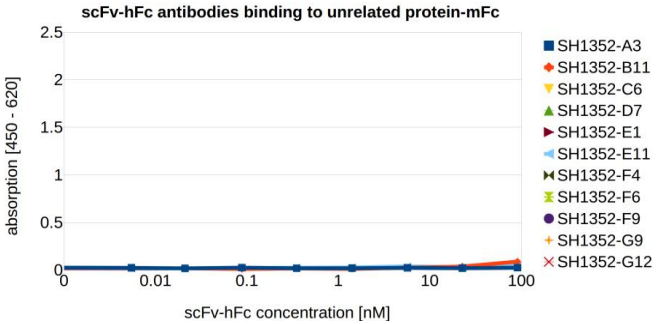

Fig. 4: scFv-hFc mAbs binding to zCdh2-ECD coated Ag in ELISA.

Titration ELISA to evaluate the binding of scFv-hFc α-zCdh2-ECD mAbs to the recombinant antigens zCdh2-ECD-mFc or hCdh2-ECD-mFc. An unrelated mFc-fusion protein was used as negative control. 100 ng antigen per well were immobilized and incubated with 0.08 pM to 90.9 nM scFv-hFc mAbs.

Table 3.4: scFv-hFc mAbs apparent affinity expressed as ELISA-based EC50 values

Antibody clone	EC50 [nM] on zCdh2-ECD	EC50 [nM] on hCdh2-ECD
SH1352-A3-hIgG-Fc	3.90	-
SH1352-B11-hIgG-Fc	1.12	0.62
SH1352-C6-hIgG-Fc	0.37	-
SH1352-D7-hIgG-Fc	0.67	Not quantifiable
SH1352-E1-hIgG-Fc	0.85	0.49
SH1352-E11-hIgG-Fc	0.70	-
SH1352-F4-hIgG-Fc	3.25	-
SH1352-F6-hIgG-Fc	0.64	2.45
SH1352-F9-hIgG-Fc	1.12	-
SH1352-G9-hIgG-Fc	0.56	-
SH1352-G12-hIgG-Fc	Not quantifiable	-

3.1.5. ScFv-hFc antibodies bind to zebrafish primary cells

Whether the new monoclonal human scFv-hFc antibodies can bind to native fish Cdh2 was assessed by flow cytometry analysis of living zebrafish primary cells derived from 3 dpf larvae. To unequivocally assess antibody specificity, three different zebrafish lines were used in the experiment: Wt, Cdh2-GFP-RFP (line *zf516 Tg (TgBAC (cdh2:cdh2-sfGFP-TagRFP, crybb1:ECFP))*), and Cdh2 loss of function *parachute* (*pac*) mutant (*pac*R2.10 mutant) (Lele et al., 2002; Revenu et al., 2014). In the *zf516 Tg* line, Cdh2-positive cells express the construct zCdh2-GFP-RFP, while eCFP is expressed in the lens to enable easy screens of transgene expressing carriers during early stages of development when the zCdh2-GFP-RFP is not yet detectable. In contrast to other *pac* mutants, *pac*R2.10 originates from a 'G' to 'A' mutation in the splicing donor cite (GT) of an intron at position +48 of the Cdh2 coding sequence. The consequent incorrect splicing does not allow the formation of correct transcripts with resulting absence of even partial protein product translation (Lele et al., 2002). In this *parachute* line, no Cdh2 is expressed, so that any binding detected on this line has to be considered unspecific.

In this assay only the GFP fluorescence was specifically acquired to identify Cdh2-positive cells, as no yellow-green laser for RFP excitation was used, neither filters for the detection of eventual RFP emission. Thanks to the GFP reporter expression in the Cdh2-GFP-RFP *zf516 Tg* line, back-gating of the Cdh2-positive cells in the FSC-A - FSC-H plot allowed to enrich the Cdh2-positive cells for a better visualization of the antibody staining. An antibody has been classified as specific and non-cross-reactive when meeting the following two conditions: absence of staining on the *pac* embryo-derived cells and positive staining of the GFP positive cells (*zf516 Tg* line). The scFv-hFc antibodies were tested at the concentration of 10 µg/mL.

Of the 11 antibodies tested (Figure 5), 8 showed reactivity in this assay, while SH1352-E1, -E11, and -G12 did not stain any cell from any of the used samples. Of the 8 reactive antibodies 6 could be classified as fully specific to the target accordingly to the above mentioned parameters: SH1352-A3, -B11, -D7, -F4, -F9, and -G9. The binding profile of the 2 antibodies which showed cross-reactivity was different. SH1352-F6, in addition to the binding of Cdh2-GFP cells, showed a minimal cross-reactivity to a small Cdh2-negative cell population, observable in null-mutant derived cells.

On the contrary, SH1352-C6 unwanted cross-reactivity was more pronounced and clearly identified as presence of staining in *pac* mutant derived cells, as well as staining of GFP-negative cells from the *zf516 Tg* sample (Cdh2-GFP line). Flow cytometric analysis was then used to compare the specificity profile of the commercial antibody to zCdh2-ECD (GTX125885) with that of scFv-hFc SH1352-G9. GTX125885 was used in several previous studies to map the expression of Cdh2 (Tuttle et al., 2014; Xing et al., 2015; Han et al., 2016; Mochizuki et al., 2017; Gays et al., 2017; Powell et al., 2018) and was the only α-zCdh2 antibody commercially available at the time. Even at very high concentration (up to 50 µg/mL), no reactivity of SH1352-G9 was found on homozygous *pac* mutant cells. On the contrary GTX125885 stained 45 % of cells known not to express Cdh2 (Figure 6). GTX125885 stained also 57 % of the Wt and 65 % of the *zf516 Tg* line derived cells, where only ~30 % are GFP-positive. GTX125885 as well as our highly specific scFv-hFc antibodies SH1352-B11, -D7, -F4 and -G9, could not stain a low percentage of Cdh2-GFP-RFP cells from *zf516 Tg* larvae.

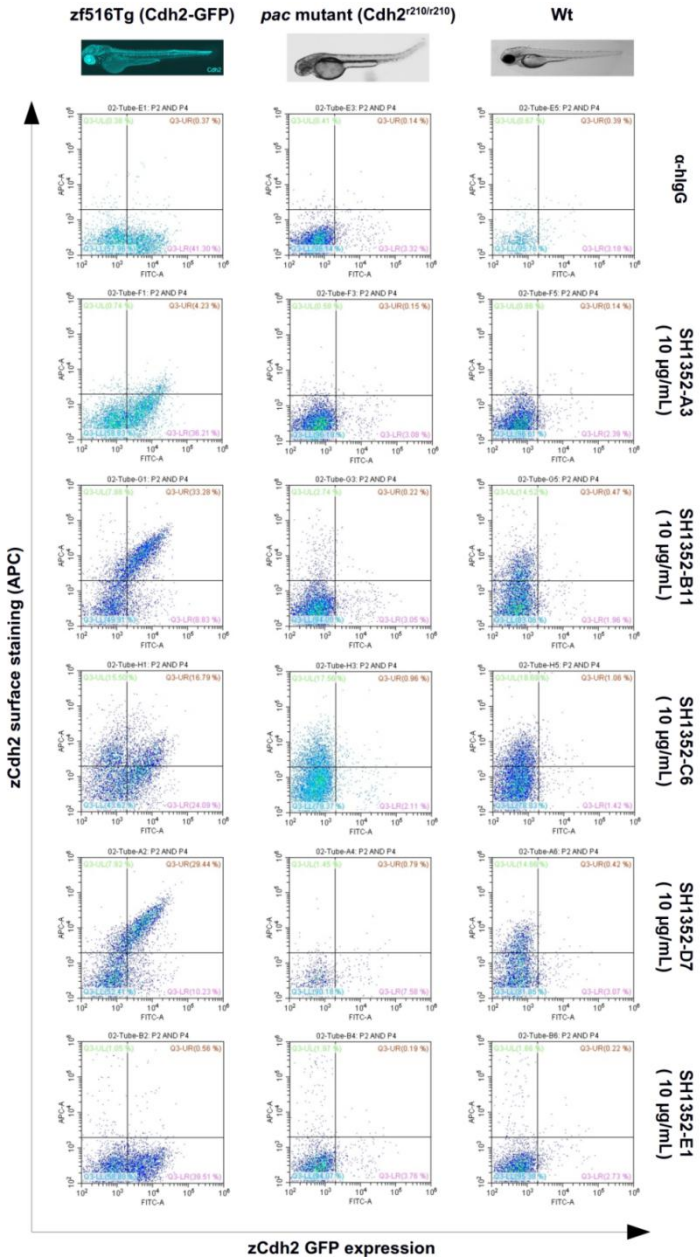
zf516Tg (Cdh2-GFP)
pac mutant (Cdh2r210/r210)
Wt
α-hIgG
SH1352-A3 (10 µg/mL)
SH1352-B11 (10 µg/mL)
SH1352-C6 (10 µg/mL)
SH1352-D7 (10 µg/mL)
SH1352-E1 (10 µg/mL)
zCdh2 surface staining (APC)
zCdh2 GFP expression
APC-A
FITC-A

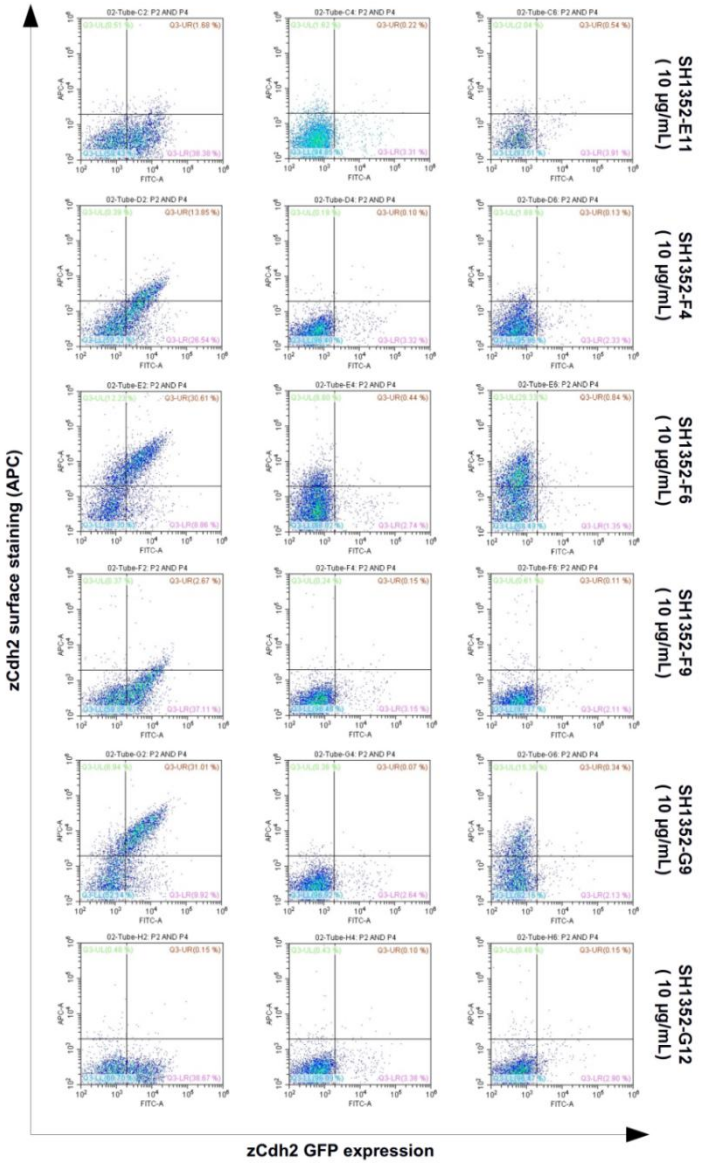
zCdh2 surface staining (APC)
zCdh2 GFP expression
SH1352-E11 (10 µg/mL)
SH1352-F4 (10 µg/mL)
SH1352-F6 (10 µg/mL)
SH1352-F9 (10 µg/mL)
SH1352-G9 (10 µg/mL)
SH1352-G12 (10 µg/mL)

Fig. 5: scFv-hFc specificity assessment in flow cytometry.

Antibody binding to endogenous zCdh2 on zebrafish primary cells was evaluated by immunofluorescent staining and flow cytometry analysis. Living zebrafish primary cells were derived from three different fish lines at 3 dpf: *zf516Tg* (zCdh2-GFP fusion) in the left panels, zCdh2 homozygous *pac* mutant in the middle panels, and Wt in the right panels. y-axis: antibody staining (APC-channel), x-axis GFP signal from zCdh2-GFP fusions. All monoclonal antibodies were used at 10 µg/mL. α-hIgG: secondary antibody control.

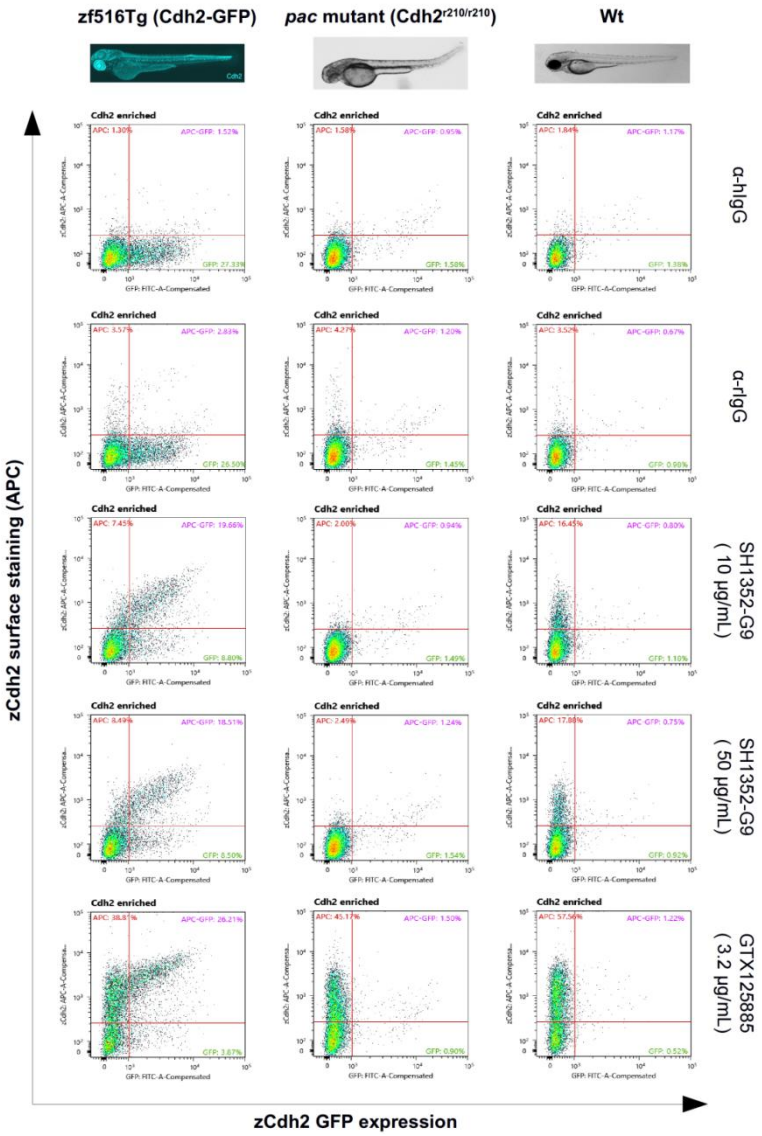

Fig. 6: GTX125885 Ab and SH1352-G9 mAb binding comparison in FACS. Binding to endogenous zCdh2 on zebrafish primary cells was evaluated by

immunofluorescent staining and flow cytometry analysis. Living primary cells were derived from three different fish lines at 3 dpf as described in figure 5. α-rIgG: secondary antibody control for GTX125885. α-hIgG: secondary antibody control for SH1352-G9. Note the concentration differences between GTX125885 and SH1352-G9.

3.1.6. ScFv-hFc antibodies identify Cdh2 in zebrafish whole mounts

The scFv-hFc antibodies specifically recognizing zCdh2 on zebrafish primary cells (SH1352-B11, -D7, -F4, -G9) were used for whole mount immunofluorescent staining of 3 days old larvae after fixation. Direct comparison of the antibody staining with the zCdh2 expression pattern was achieved using the *zf516 Tg* larvae, which express zCdh2-GFP-RFP under the control of the original zCdh2 promoter (note: only GFP fluorescence was acquired). To assess antibody specificity, *pac* mutant larvae (zCdh2 null mutant) were included in the experiment as well. For a more appropriate comparison of the results, *pac* mutant and *zf516 Tg* larvae were stained in the same reaction tube by each antibody. The different larvae origin was easily discriminated by their different morphology, and by the presence/absence of GFP fluorescence. All the images acquired were processed equally, and APC-conjugated secondary antibody was used for detection. APC emission range (emission max at 660 nm) allowed us to avoid signal spillover from the GFP-RFP channels (emission max respectively at 510 nm and 588 nm). After the staining, images were recorded from whole larvae, or specific tissues and fish body parts, always in lateral view, via confocal microscopy.

SH1352-G9 antibody staining fully overlapped with the expression pattern of the zCdh2-GFP-RFP in *zf516 Tg* larvae (Figure 7C and 8C) and did not show any reactivity on *pac* mutant larvae (Figure 7D and 8D).

The absence of antibody staining in the lens is explained by the fact that the lens do not express zCdh2-GFP-RFP, but the eCFP lens-marker (*crybb1*:ECFP). The low eCFP excitation by the 488 nm laser is considered to be compensated by the high protein density in lens fiber cells and by the fact eCFP has bimodal emission and excitation spectra.

SH1352-B11 and SH1352-F4 scFv-hFc antibodies also specifically recognized the antigen in whole mount immunofluorescent staining (Figure 9), but signal intensity was lower than the one of SH1352-G9 staining. SH1352-D7 antibody staining failed to fully recapitulate the endogenous zCdh2 expression pattern in this particular IHC assay (Figure 9).

SH1352-G9 and GTX125885 specificity profiles were further compared in this IHC assay, recapitulating the results obtained by comparing the activity of these two antibodies in flow cytometry on primary cells. While SH1352-G9 did not bind to the homozygous *pac* mutant larvae, GTX125885 stained several tissues despite the complete absence of Cdh2 expression in the *parachute* line (Figures 7B and 8B).

Consequently it bound to structures which did not match the zCdh2 fluorescence pattern in the *zf516 Tg* fish line (Figures 7A and 8A). Interestingly, despite its polyclonal nature and its tendency to bind ectopically, GTX125885 failed to stain the spinal cord, where Cdh2-GFP is highly expressed. It therefore elicited both false positive and false negative reactivity. On the contrary, SH1352-G9 correctly bound to this structure.

The secondary antibody control sample showed none of the unspecific staining observed with GTX125885, thus unspecific staining results cannot be attributed to the secondary antibody used in this assay (Figure 10).

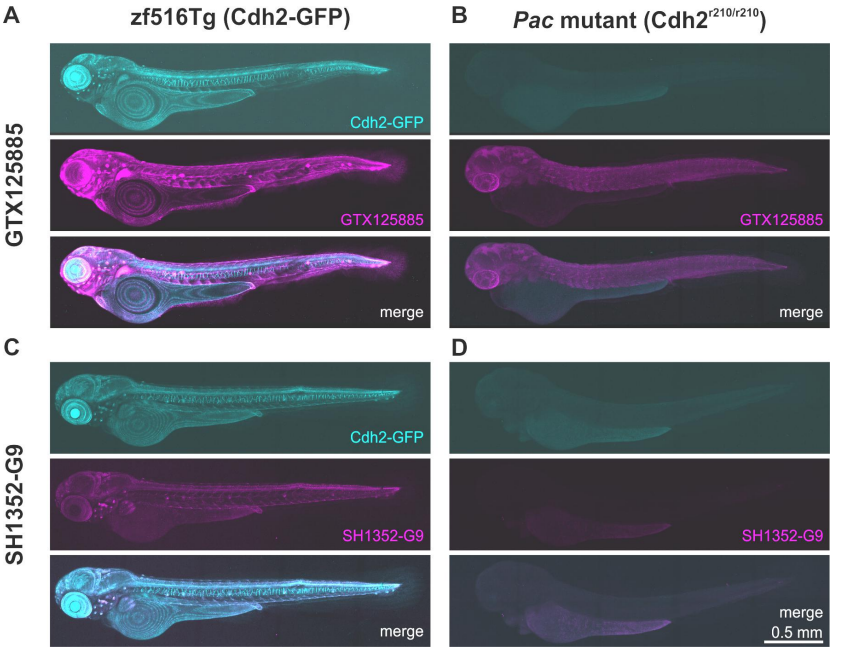

Fig. 7: GTX125885 Ab and SH1352-G9 mAb binding comparison in whole mount IHC.

Confocal images from *zf516 Tg* (Cdh2-GFP) or *Pac* mutant (not expressing Cdh2) 3 dpf larvae stained respectively with A, B) GTX125885 antibody (1.6 µg/mL) or C, D) SH1352-G9 scFv-hFc (10 µg/mL). Cyan = GFP channel (zCdh2-GFP fusion protein expression); Magenta = antibody staining.

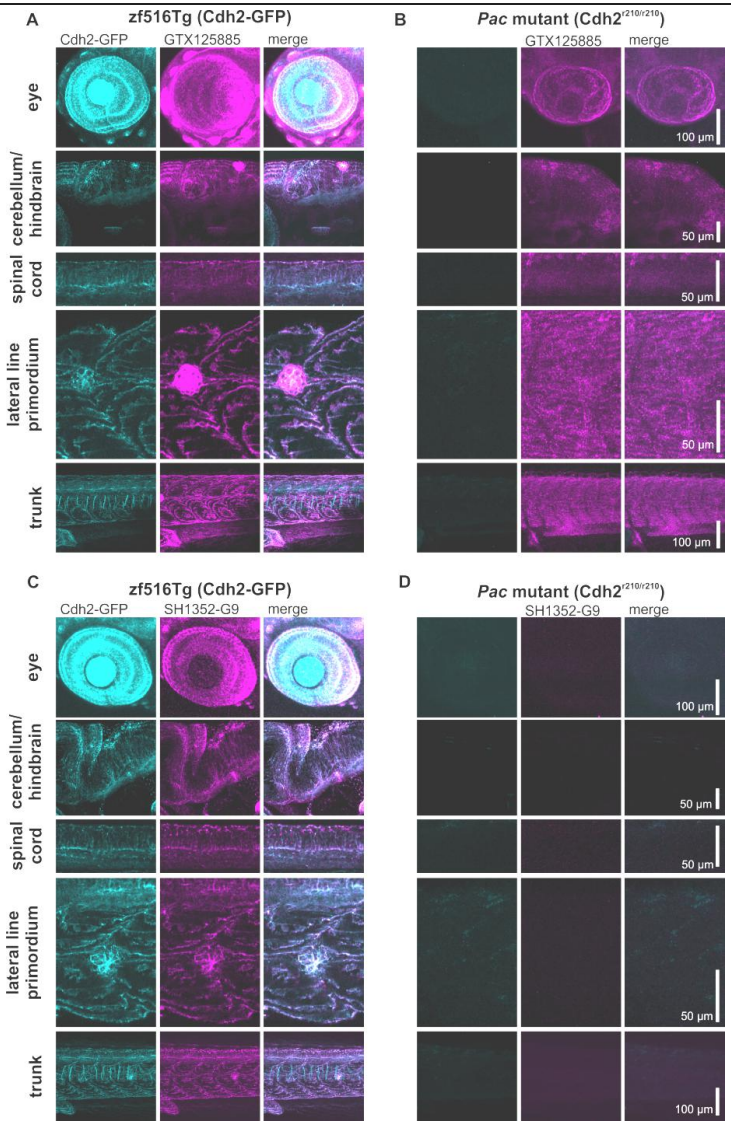

Fig. 8: GTX125885 Ab and SH1352-G9 mAb whole mount staining details .
Confocal images show zf516 Tg (Cdh2-GFP) and Pac mutant larvae stained as described in Fig. 7.

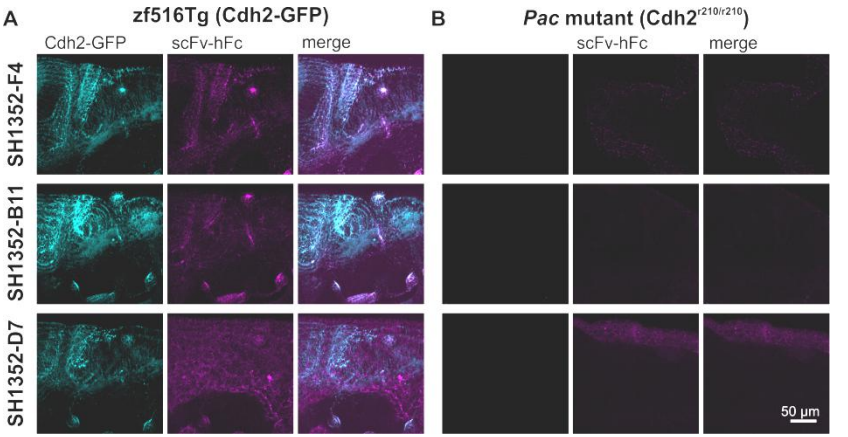

Fig. 9: RecAbs specificity assessment in whole mount IHC.

A) SH1352-B11, -D7, and -F4 scFv-hFc's binding comparison on zebrafish *zf516 Tg* (Cdh2-GFP) and B) homozygous *pac* mutant larvae fixed at 3 dpf. All the scFv-hFc mAbs were tested at the concentration of 10 µg/mL. Cyan = GFP (zCdh2 distribution); Magenta = antibody staining.

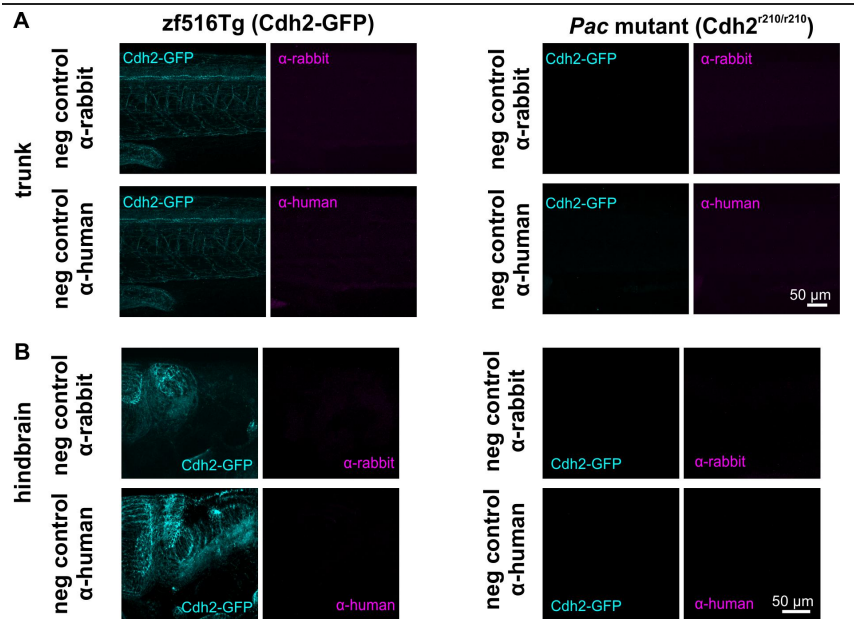

Fig. 10: Whole mount zebrafish IHC secondary antibody controls.
Confocal imaging of 3 dpf larvae A) trunk and B) hindbrain region, after staining with α- human IgG and α-rabbit IgG secondary antibodies respectively APC- or Cy3-conjugated. These controls refer to the results shown in figures 7, 8, and 9. Cyan = GFP (zCdh2 distribution); Magenta = antibody staining.

3.1.7. Some scFv-hFc antibodies bind to human Cdh2 and zCdh2

The ORF encoding human Cdh2-ECD was amplified from HEK293 cells cDNA via PCR and cloned into the pCSE2.6-hIgG-Fc-XP vector for production as mFc-fused antigen. Cloning, production, and purification was performed following the same procedure described for the zCdh2 antigens production (see paragraph 3.1.1.). To assess antibody cross-binding to the extracellular domain of human Cdh2, every antibody was tested in titration ELISA on coated hCdh2-mFc antigen (as previously described, see paragraph 3.1.4.).

An unrelated mFc-fused antigen was used as negative control. Of the antibodies tested, four scFv-hFc recognized the soluble hCdh2-ECD (SH1352-B11, -D7, -E1, F6), of which only two bound the antigen with comparable affinity to the human and zebrafish variants of the Cdh2 (Sh1352-B11, -E1) (Figure 4).

To assess whether the binding of Cadherin2 on cells matches the binding determined in ELISA, HEK293 human cell lines, known to express Cdh2, where used in flow cytometry antibody binding analysis. All the antibodies positive on hCdh2-ECD in ELISA were also positive on cells, with the exception of SH1352-D7. The antibody SH1352-C6 bound to HEK293 cells (Figure 11), while it did not recognized the human Cdh2 in ELISA (Figure 4).

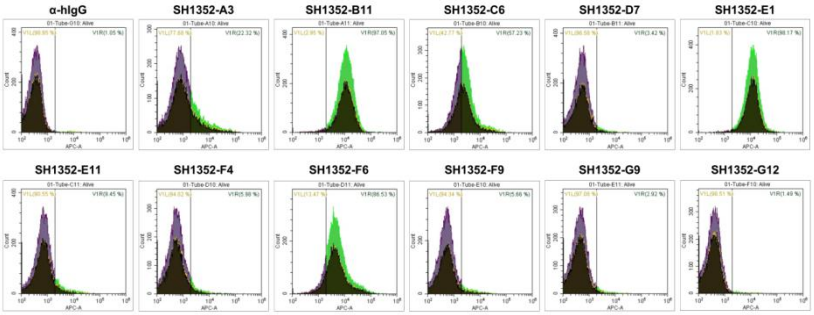

Fig. 11: Evaluation of scFv-hFc Abs binding to HEK293 cells.

Immunofluorescent staining and flow cytometry analysis of human cell lines with α-zCdh2 scFv-hFc antibodies. scFv-hFc mAbs were used at 10 µg/mL.

3.1.8. Epitope mapping of human anti-zCdh2 antibodies

The binding regions recognized by the different scFv-hFc antibodies were assessed via ELISA on zCdh2-ECD fragments. As zCdh2-ECD1-2-hFc was the antigen used for antibody selection, the

fragments designed for epitope analysis were all representing a region of zCdh2 included within the first two extracellular domains of the antigen target: zCdh2-ECD1-mFc (aa 148-254), zCdh2-ECD2-mFc (aa 255-369), zCdh2-148-207-mFc, zCdh2-195-273-mFc, zCdh2-263-324-mFc or zCdh2-315-369-mFc (Figure 2). SH1352-A3 recognized domain 2 (ECD2), while all the remaining antibodies bound to domain 1 (ECD1). Binding analysis using smaller fragments derived from zCdh2-ECD1 and -ECD2 allowed us to further narrow down the epitope containing regions recognized by 6 of the 11 antibodies (Table 3.5).

Table 3.5: scFv-hFc mAbs binding to zCdh2 single domains and domain fragments.

Antibody clone	zCdh2-ECD (aa 148-702)	zCdh2-ECD1 (aa 148-254)	zCdh2-ECD2 (aa 255-369)	zCdh2-CD-148-207	zCdh2-ECD-195-273	CTR-aa	Minimal epitope region bound in ELISA
SH1352-A3	**100 %**	0.68 %	**105.30 %**	0.71 %	**115.30 %**	3.98 %	**aa 255-273**
SH1352-B11	**100 %**	**99.54 %**	2.19 %	0.69 %	**96.12 %**	4.47 %	**aa 195-273**
SH1352-C6	**100 %**	**101.28 %**	2.57 %	**97.06 %**	0.98 %	3.11 %	**aa 148-207**
SH1352-D7	**100 %**	**105.45 %**	2.33 %	0.62 %	0.89 %	2.47 %	**zCdh2-ECD1**
SH1352-E1	**100 %**	**103.00 %**	2.36 %	0.71 %	**93.37 %**	2.51 %	**aa 195-273**
SH1352-E11	**100 %**	**112.00 %**	3.02 %	1.23 %	**106.22 %**	2.42 %	**aa 195-273**
SH1352-F4	**100 %**	**112.01 %**	2.18 %	0.61 %	0.58 %	1.92 %	**zCdh2-ECD1**
SH1352-F6	**100 %**	**103.48 %**	2.02 %	0.68 %	**4.29 %**	2.19 %	**aa 195-273**
SH1352-F9	**100 %**	**101.64 %**	2.01 %	0.67 %	0.67 %	2.47 %	**zCdh2-ECD1**
SH1352-G9	**100 %**	**99.50 %**	2.03 %	0.53 %	0.56 %	1.96 %	**zCdh2-ECD1**
SH1352-G12	**100 %**	**130.19 %**	2.45 %	0.55 %	0.51 %	2.45 %	**zCdh2-ECD1**

To determine the bound epitope more exactly, the four antibody-clones specific in flow cytometry on primary zebrafish cells (SH1352-B11, -D7, -F4, -G9), as well as the unspecific SH1352-C6, were analyzed with single amino acid side chain resolution by PepSpot membrane binding assay (peptide length: 15 aa; peptide overlap: 11 aa). Only SH1352-B11 and SH1352-C6 reacted with the PepSpot membrane (Figure 12), indicating a linear continuous peptide epitope structure. The two epitopes were visualized on a zCdh2-ECD1 model structure (Figure 13) generated with SWISS-MODEL (Arnold et al., 2006; Guex et al., 2009; Kiefer et al., 2009; Biasini et al., 2014) exploiting the high (80.4 %) sequence similarity to the mouse zCdh2-ECD1, the crystal structure of which is known (PDB: 3Q2W) (Harrison et al., 2011).

To analyze why only some antibodies reacted with the zCdh2 peptide, the binding of the five scFv-hFc's to denatured protein was analyzed in western blot after SDS-PAGE of total cell lysate of HEK293 cells overexpressing zCdh2-ECD-mFc. All tested antibodies recognized the target prepared in reducing conditions (Figure 14). At the tested antibody concentration, SH1352-B11 and -C6 seemed to bind better to the target in this assay, and allowed to detect a higher molecular mass band presumably representing the glycosylated form of the protein. SH1352-C6 detected additional proteins than zCdh2, which is in line with the flow cytometry data which show the tendency of this antibody towards broader reactivity.

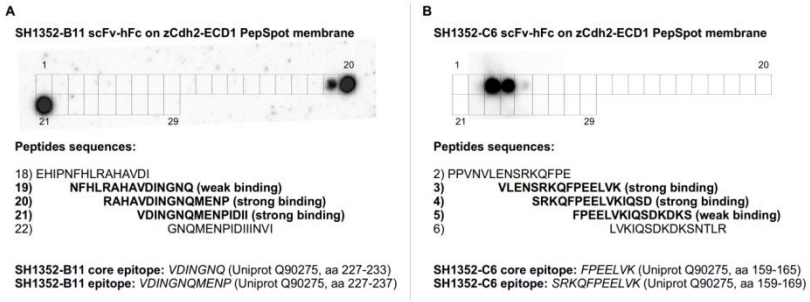

Fig. 12: SH1352-B11 and -C6 mAbs epitope mapping.

Epitope determination of the SH1352-B11 and SH1352-C6 mAbs on PepSpot membranes covering the entire zCdh2-ECD1 domain in 29 spots of 15aa peptides with 11 residues overlap.

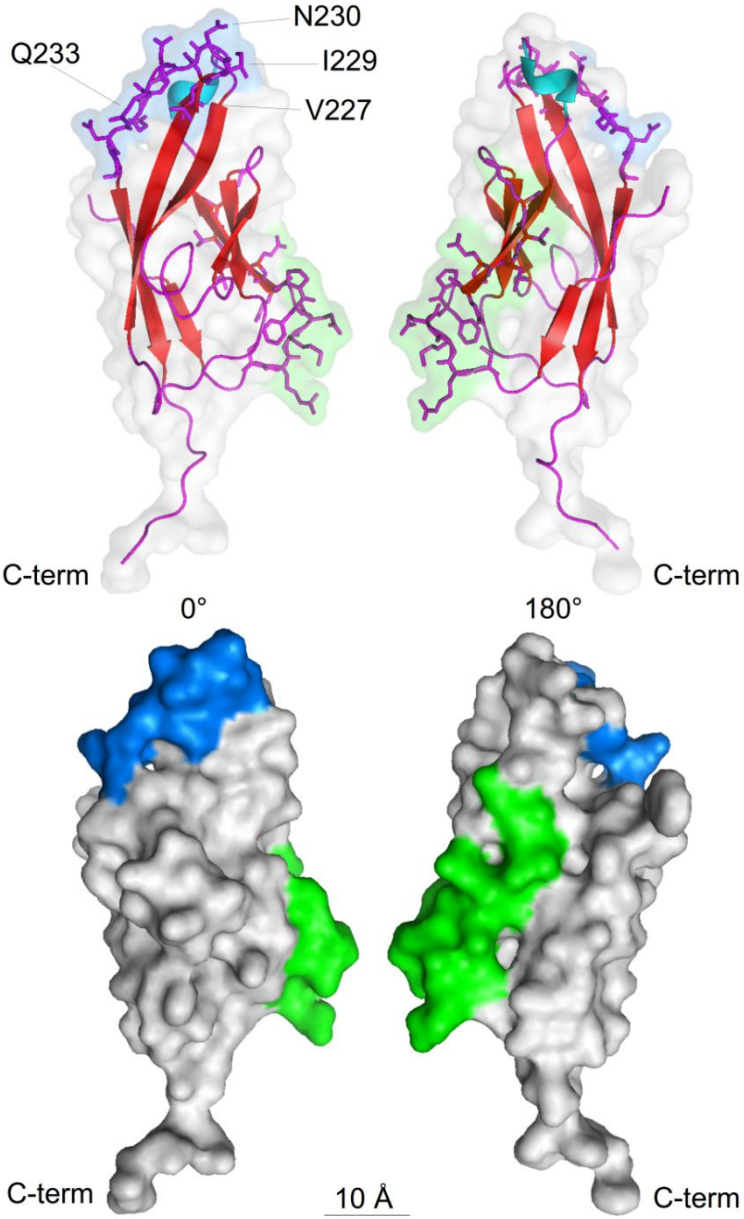
N230
Q233
I229
V227
C-term
C-term
0°
180°
C-term
10 Å
C-term

Fig. 13: SH1352-B11 and -C6 epitopes on zCdh2 model structure.

zCdh2-ECD1 model structure was obtained by homology modelling based on the mouse Cdh2 crystal structure 3Q2W, and represented using PyMol. SH1352-B11 and SH1352-C6 mAbs epitopes are indicated respectively in blue or green. Upper panels: α-helix in cyan, ß-sheets in red, and loops in magenta. Side chains are shown uniquely for the epitope regions and the related solvent accessible surface respectively in blue or green. Lower panels: solvent accessible surface. Of all the SH1352-B11 epitope residues, 1 belongs to a ß-sheet and 10 to a loop, while for SH1352-C6 6 belongs to a ß-sheet and 4 to a loop. The estimated epitope area is of 1,658.301 Å2 and 2,087.116 Å2 respectively for SH1352-B11 and SH1352-C6. zCdh2-ECD1 total area is estimated in around 7,721.633 Å2. Numbering of the amino acids responsible for lateral association of the cadherin dimers on the cell surface is based on the homologous mouse Cdh2 positions.

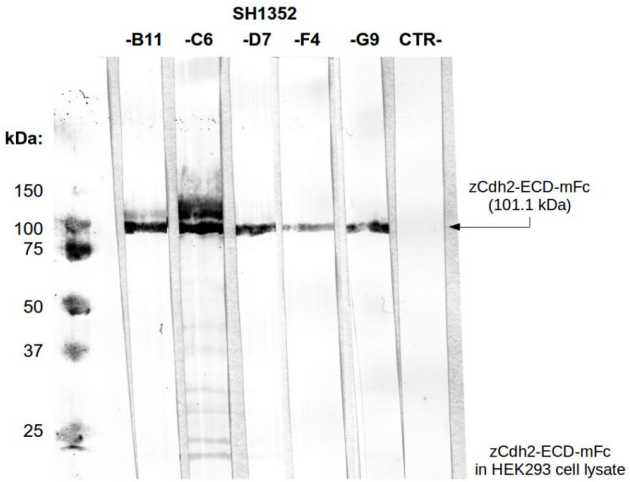

Fig. 14: Assessment of mAbs binding to zCdh2 in western blot.

scFv-hFc mAb to zCdh2 binding to immunoblots of total cell lysate of HEK293 cells expressing zCdh2-ECD-mFc (separated by SDS-PAGE under reducing conditions).

3.2. ER intrabody mediated knockdown *in vitro*

3.2.1. ER intrabody mediated retention works in zebrafish cells

Despite the expression of KDEL receptors in zebrafish has been described (Thisse et al., 2001), an ER intrabody retention in zebrafish has not been demonstrated so far. For this purpose, the knockdown activity of a previously well validated ER intrabody to mouse p75 (Zhang et al., 2012) was tested in zebrafish PAC2 cells after transient co-transfection with an expression vector containing its mouse antigen target fused to YFP. As mouse p75 extracellular domain shows at most 43.5 % amino acid similarity with its zebrafish hortologue (GQ983383.1), the risk of cross-binding is considered to be excluded. The unrelated ER intrabody α-phOx-KDEL binding to the small molecule phenoxazolone, which is not present in living cells, was used as negative control. Surface levels of transfected p75 were determined in flow cytometry 24 hours post transfection (hpt) in the presence of either α-p75 (SH325-G7-KDEL) or α-phOx ER intrabodies (Figure 15).

In the p75-YFP - α-phOx-KDEL sample, every cell expressing the antigen target fused to YFP (YFP-positive cells) could be stained on the surface with the use of a second α-p75 antibody (APC-positive cells) binding to an epitope not overlapping with that of the intrabody. On the contrary, in the presence of the ER intrabody specific to mouse p75, a cell population became evidently characterized by the expression of the target (YFP-positive), but its absence from the cells surface. This demonstrated for the first time an ER intrabody mediated knockdown in zebrafish.

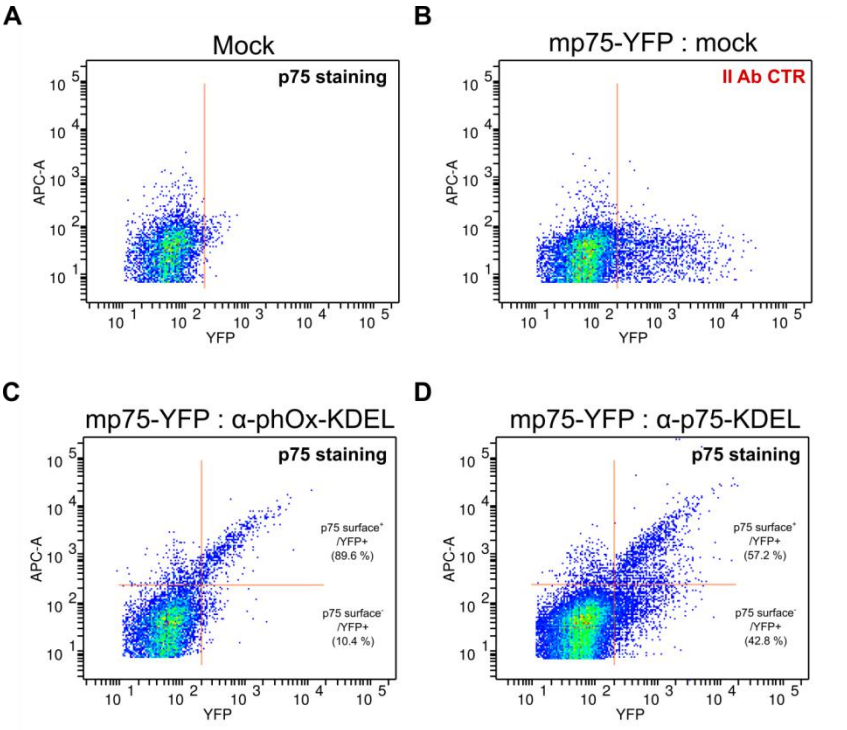

Fig. 15: ER intrabody knockdown of mouse p75 in PAC2 cells.

Mouse p75 immunofluorescent surface staining and flow cytometry analysis of zebrafish PAC2 cells transfected respectively with A) Mock vector, C) mouse p75-YFP + α-phOx-KDEL ER intrabody, D) mouse p75-YFP + α-p75-KDEL ER intrabody. As negative control of the immunostaining, mouse p75-YFP transfected cells have been stained with fluorescently coupled secondary antibody only (B). y-axis: antibody staining (APC-channel), x-axis YFP signal from mouse p75-YFP fusion antigen.

3.2.2. ScFv-hFc antibodies bind endogenous Cadherin 2 in PAC2 cells

The embryonic fibroblast zebrafish cell line PAC2 was analyzed for its usefulness for the characterization of the ER intrabodies binding to zCdh2. First, potential zCdh2 expression on the PAC2 cell surface had to be verified. To obtain further information on the binding profile of the scFv-hFc antibodies to zCdh2, not only the ones found to be specific in FACS of primary cells and whole mounts before, but all the available antibodies where tested in flow cytometry for binding to PAC2 cells. At least 5,000 cells were included in the histograms shown in figure 16. All antibodies shown before to be specific to zCdh2 (Sh1352-B11, -D7, -F4, and -G9) by flow cytometry on primary cells positively stained PAC2 cells. SH1352-C6 and -F6 also bound to the surface exposed antigen target, despite showing a distinct binding profile. SH1352-F6 shows, on PAC2 cells, a binding profile analogue to the one of the antibodies specific on primary cells. The antibodies SH1352-A3, -E1, -E11, -F9 and -G12 were confirmed to bind not at all or only weakly, similar to what has previously been seen with primary zebrafish cells (Figure 5).

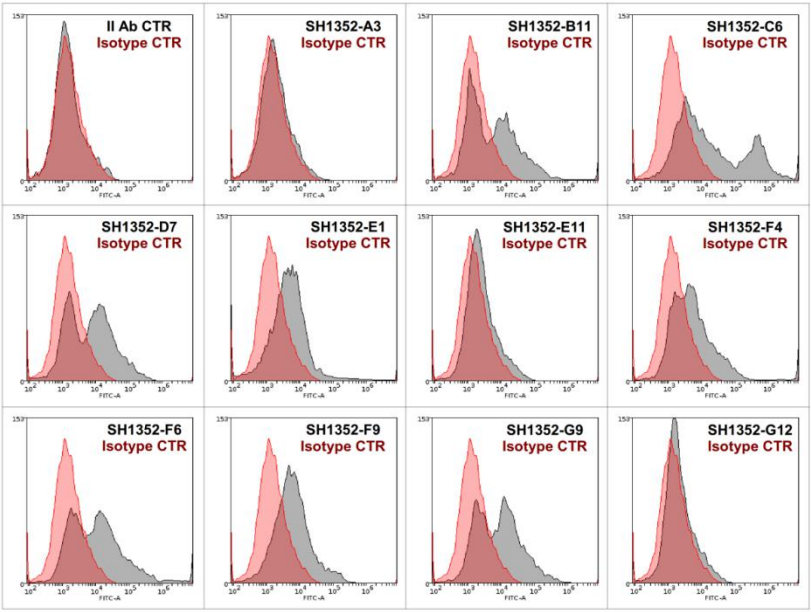

Fig. 16: Evaluation of scFv-hFc Abs binding to zCdh2 on PAC2 cells.
Immunofluorescent staining and flow cytometry analysis of zCdh2 on the surface of zebrafish PAC2 cells with α-zCdh2 scFv-hFc antibodies. scFv-hFc mAbs were used at 10 µg/mL.

3.2.3. Development of an intrabody knockdown/reporter vector for zebrafish

To generate ER intrabody vectors, first all of the cDNA encoding the scFvs against zCdh2 were extended by adding DNA encoding an N-terminal signal peptide (SP) and two C-terminal detection tags (HA-tag, Myc-tag) plus a KDEL retention peptide. These ER intrabody expression cassettes (SP-scFv-HA tag-Myc tag-KDEL) were inserted onto the right arm of the ER intrabody bidirectional knockdown vector (Figure 17 A). On the left arm the fluorescent reporter gene tagRFP-T

was inserted for the direct detection of the expression in living cells and *in vivo*. Extensive studies were performed to select the right enhancer-promoter combination for the planned vector capable to drive bidirectional ubiquitous expression in mammalian cells as well as *in vivo* in zebrafish. Combinations of different core enhancer sequences (SV40, mouse CMV, human CMV, xenopus EF1-α), in fusion with the super core promoter 2 (SCP2) (Juven-Gershon et al., 2006), were used to express simultaneously two fluorescent reporter genes: mClover and tagRFP-T. TagRFP-T has been cloned into the left arm of the construct, while mClover into the right arm, always preceded by a zebrafish optimized Kozak sequence (Grzegorski et al., 2014). To avoid the methylation based silencing effects that accumulate over several generations of transgenic zebrafish, we used CpG-free enhancer and promoter sequences. Every expression cassette was cloned into a minimal Tol2 transposon vector (Kawakami, 2007). The minimal Tol2 sequences allowed for the transposase mediated stable integration into the zebrafish genome of our reporter cassette. Carriers expressing mClover and tagRFP-T in different tissues were raised to adulthood (P0 generation). P0 offspring showing the most widespread transgene expression was also raised to the adulthood (F1 generation). The different expression systems have been studied in HEK cells after transient transfection and *in vivo* in zebrafish embryos after injection of the plasmid into one cell stage embryos (data not shown). Highest expression levels of the two fluorescent reporters, bidirectionality equilibrium, and reporter expression profile *in vivo*, have been selected as criteria to determine the quality of each construct. The vector GiR085-1, carrying the expression cassette tagRFP-T-SCP2-xEF1α-mCMV- spacer-mCMV-xEF1α-SCP2-mClover (Figure 17 B), drove the highest bidirectional expression levels and showed the best transfection rates in HEK293 cells (Figure 17 C), or

zebrafish primary cells (Figure 17 D-E). This vector also stood out by allowing for a high diversity of tissues to express the two reporters in the transient expression zebrafish model (Figure 17 F), an indication of expression ubiquity.

The expression cassette from the bidirectional vector GiR085-1 was therefore selected to generate the ER intrabody bidirectional knockdown vector (Figure 17 A).

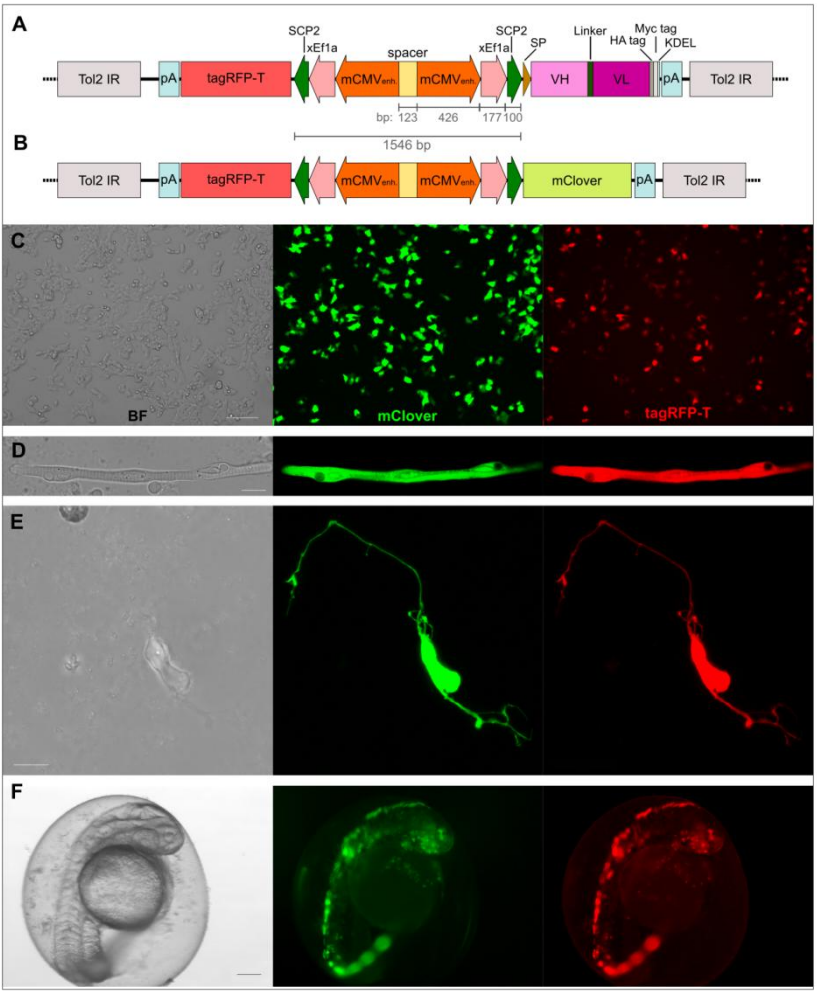

Fig. 17: GiR085-1 reporter expression system and ER intrabody expression cassette.

A) Schematic view of the ER intrabody bidirectional expression cassette. B) Schematic view of the bidirectional fluorescent reporter expression cassette of the vector GiR085-1.

B) The gene expression driven by the construct has been assessed after transfection in HEK293 cells (C), zebrafish primary cells (D-E), and *in vivo* zebrafish after injection (F). D-E) Confocal imaging acquisition by Sassen W.A. Scale bars: 150 µm. IR, inverted repeats; pA, poly-A tail; SCP2, Super Core Promoter 2; xEF1a, *Xenopus laevis* Elongation factor 1-alpha enhancer; mCMVenh., murine Cytomegalovirus enhancer.

3.2.4. Knockdown of zebrafish Cdh2 in PAC2 cells

To confirm whether expression of ER intrabodies against zCdh2 can result in the depletion of endogenous antigen from the surface of fish cells, PAC2 cells where transfected with expression vectors encoding for different ER intrabodies anti-zCdh2. The zCdh2 surface levels where analyzed in flow cytometry after 72 h. The unrelated α-phOx ER intrabody was used as negative control. The amount of zCdh2 on the surface of PAC2 cells transfected with α-phOx ER intrabody vectors was set as 100 %. A reduction of zCdh2 surface levels induced by any of the tested ER intrabodies against this antigen was interpreted as knockdown. SH1352-C6, -D7, -F9, -G9, and, -G12 ER intrabodies induced a reduction of the surface levels of zCdh2 (Figure 18).

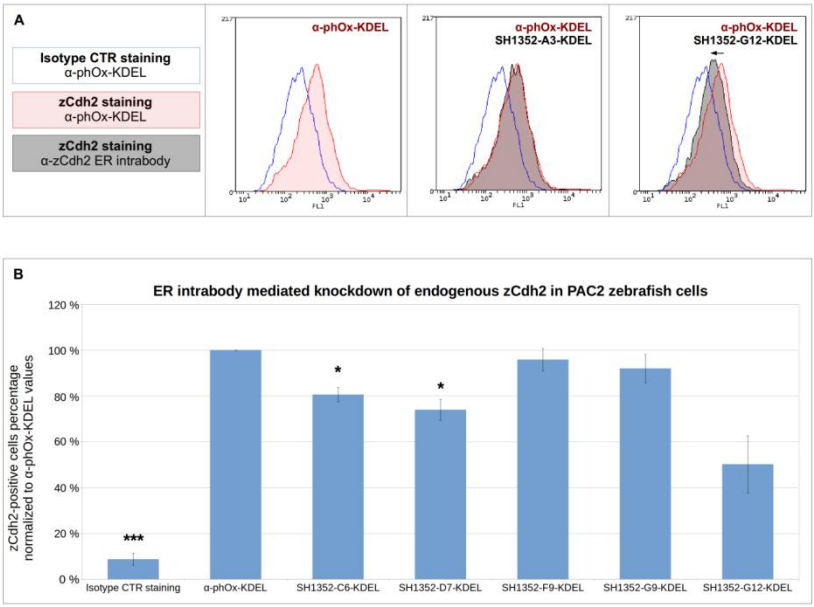

Fig. 18: zCdh2 surface levels quantification after ER intrabody expression in PAC2.

PAC2 cells were electroporated with ER intrabody plasmid DNA. After 72 h from the transfection, immunofluorescent staining and flow cytometry analysis was used to quantify amount of zCdh2 on the cell surface. A) The histograms represent the model used to classify an ER intrabody as positive or negative. SH1352-A3 cells show comparable amounts of cells expressing zCdh2 to the negative CTR- sample (α-phOx-KDEL), and is therefore negative. On the contrary, SH1352-G12 sample show a reduced number of zCdh2 surface-positive cells. B) zCdh2 levels normalized to CTR-. One-way ANOVA, $p < 0.05$, $p < 0.01$, $p < 0.001$.

3.2.5. Zebrafish Cdh2 knockdown in HEK293 cells

To confirm whether ER intrabodies mediated retention of zCdh2 in the ER was resulting in target accumulation inside of the ER lumen, HEK293 cells were co-transfected with both vectors expressing a zCdh2-mClover fusion antigen and ER intrabodies against zCdh2 . This antigen contains the whole zCdh2 extracellular and transmembrane domains, but lacks the cytosolic domain (pCSE2.6-zCdh2-truncated aa 147-738). The cytosolic domain has been replaced by the mClover fluorescent reporter allowing one to measure the absolute cellular levels of zCdh2 (pCSE2.6-zCdh2-ECD-TM-mClover). The mClover emission was acquired at 24 h after the co-transfection with an ER intrabody expressing vector by flow cytometry. Of the five ER intrabodies, which successfully mediated zCdh2 knockdown in PAC2 cells, all except SH1352-F9 determined a reduction of zCdh2-mClover intracellular levels (Figure 19). This reduction is intended as reduction of mClover-positive cells, and/or reduction of the mClover protein levels per cell, which is indicated by the median fluorescent intensity (MFI). The representative histograms of figure 19 A show the transfection efficiency, measured as mClover expression levels, was of approximately 100 % in HEK293. The number of zCdh2-mClover-positive cells per each sample have been normalized to those of cells co-transfected with α-phOx-KDEL negative control expression vector and zCdh2-mClover expression vector.

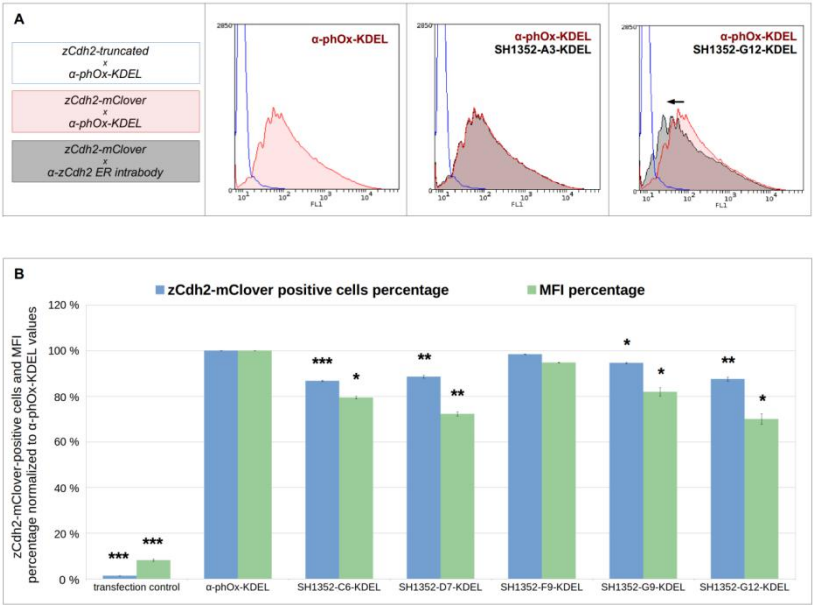

Fig. 19: zCdh2-mClover amount quantification in ER intrabody⁺ HEK293.
HEK293 cells were co-transfected with ER intrabody and zCdh2-mClover plasmid DNA. After 24 h from the transfection, immunofluorescent staining and flow cytometry analysis was used to quantify the absolute intracellular amount of zCdh2-mClover in transfected cells. A) The histograms represent the measure of zCdh2-mClover levels in the presence of the unrelated ER intrabody (α-phOx-KDEL), a negative ER intrabody specific to zCdh2 (SH1352-A3), or a positive ER intrabody to zCdh2 (SH1352-G12). B) zCdh2-mClover levels normalized on those from the α-phOx-KDEL negative control sample. MFI: median fluorescence intensity. One-way ANOVA, $p < 0.05$, $p < 0.01$, $p < 0.001$.

3.3. Transient ER intrabody mediated knockdown of zCdh2 impaired THN migration *in vivo*

After the functionality of the ER intrabody knockdown concept had been established in zebrafish cells, the main remaining question was whether ER intrabodies mediated knockdown of zCdh2 would have work *in vivo* in zebrafish. For proof of principle, intrabody mediated knockdown of Zebrafish Cadherin 2 *in vivo* was analyzed by its capability to interfere with the natural migration of tegmental hindbrain nuclei neurons (THN) and post-migratory primordia formation (Figure 20 A-C). THNs originate from the upper rhombic lip (URL), from *atoh1a*$^+$ neuronal progenitors.

From the same progenitors, but later, originate granule cells (GCs). In Cdh2 mutants, GCs assigned to the formation of the the dorsomedial corpus cerebelli accumulate in an ectopically located and enlarged cluster, which remains in close proximity to the URL. We wanted to verify ER intrabody mediated knockdown of Cdh2 in THNs could result in a phenocopy of the migration phenotype observed in GC cells of Cadherin2 mutant. To assess this, the genes of ER intrabody SH1352-D7-KDEL, or the negative control α-phOx-KDEL, were cloned into a vector mediating their expression, in combination to the fluorescent reporter mKate, under the control of a UAS regulatory element. Injection of these constructs into transgenic *atoh1a:KalTA* embryos (Distel et al., 2010) should provide expression in *atoh1a*$^+$ progenitors, and ultimately in THNs, of the ER intrabodies and the mKate reporter protein. Consequently, the ER intrabody cassettes were cloned into the right arm of a pTol1-5xUAS vector, while mKate fluorescent reporter was cloned into the left arm. The ER intrabody cassette was composed as previously described (Figure 17 A). To mark all the *atoh1a*$^+$ cells, an *atoh1a:KaltTA4* fish line (Distel et al., 2010) was crossed to *Tg(4xUAS:GFP)* carriers and resultant embryos at 1 cell stage were injected with the vector pTol1-5xUAS ER intrabody/mKate.

In SH1352-D7-KDEL ER intrabody/mKate plasmid injected embryos was observed a time dependent increase in the size of the THN neuronal clusters. At 32 hpf and 54 hpf, the area of the THN neuronal cluster pair and their reciprocal distance was measured in mKate and GFP double positive larvae (Figure 20 G). For quantification, the larvae were imaged from a dorsal view in 5 µm z-stacks through the whole developing cerebellum, while the quantification was conducted on maximum z-stacks projections (Figure 20 H-I). The THN cluster area at 32 hpf did not differ substantially in size between larvae injected with α-phOx-KDEL control (3153 ± 1008 µm²) or SH1352-D7-KDEL ER intrabody (3515 µm² ± 1450 µm²). However, at 54 hpf the cluster area of SH1352-D7-KDEL larvae (3374 µm² ± 848 µm² (*N* = 13 embryos)) was found to be 33.78 % wider than in α-phOx-KDEL larvae (2522 µm² ± 787 µm² (*N* = 16 embryos)). Consistent with this result, the distance between the THN clusters was found to be comparable at 32 dpf (11.8 µm ± 9 µm in α-phOx-KDEL larvae and 13.4 µm ± 8.4 µm in SH1352-D7-KDEL larvae), but reduced at 54 hpf in SH1352-D7-KDEL larvae (34.9 µm ± 11.7 µm) compared to the control (53.4 µm ± 13.2 µm). The phenotype created by the expression of ER intrabodies against zCdh2 in THN shows strong analogies to the GCs migration phenotype previously described in Cdh2 mutant zebrafish (Rieger et al., 2009).

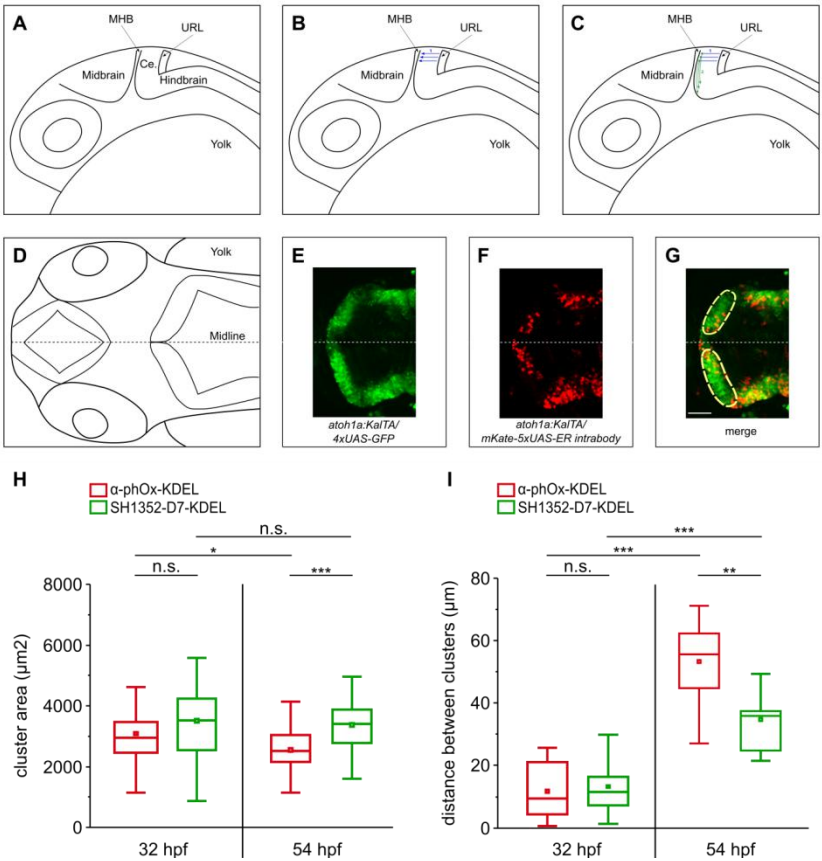

Fig. 20: *In vivo* ER intrabody mediated knockdown of zCdh2 in THNs.

A) Schematic lateral view of developing zebrafish brain. B-C) THN migration schematic representation in lateral view. THN migrate rostrally (blue arrows) from the URL towards the midbrain-hindbrain boundary (MHB), and tangentially (green arrows) along it. D) Schematic dorsal view of developing zebrafish brain. E-G) Confocal images recorded at 54 hpf from *atoh1a:KalTA/4xUAS-GFP* fish injected with pTol1-5xUAS ER intrabody/mKate vector. Images show the maximal projection of multiple 5 µm z-stacks acquired. The interrupted line delimits the area of the THN primordial nuclei. Scale bar: 50 µm. Raw images

courtesy of Daniela Münch. H-I) THN primordia area and their reciprocal distance quantification at 32 hpf and 54 hpf. Both parameters did not significantly vary between SH1352-D7-KDEL and α-phOx-KDEL samples at 32 hpf. On the contrary, at 54 hpf a significant increase of the THN primordia area, and consequent reduction of the distance between the two, were registered in SH1352-D7-KDEL samples compared to the control. Data courtesy of Daniela Münch. One-way ANOVA, $p < 0.05$, $p < 0.01$, $p < 0.001$.

3.4. Generation of an inducible bidirectional expression vector

During the process of generation and validation of an expression system capable of driving widespread transgene expression *in vivo* in zebrafish (see paragraphs: 2.2.1.11 and 3.2.3), we observed some of the tested enhancer/promoter combinations were inducible upon injury (Figure 21). All the tested enhancer/promoters were tested in a bidirectional orientation. TagRFP-T or mClover fluorescent proteins were cloned respectively into the left or the right arm of the construct and used to detect gene expression upregulation upon injury. Increased levels of fluorescent reporter expression after injury could only be found in transgenic larvae carrying the CpG-free mouse CMV enhancer core element : GiR085-1 (tagRFP-T-SCP2-xEF1a-mCMV-spacer-mCMV-xEF1a-SCP2-mClover) or GiR077 (tagRFP-T-SCP2-mCMV-spacer-mCMV-SCP2-mClover). The expression cassette of these constructs are shown respectively in Figure 17 A and 21 A. In figure 21 is shown the fluorescent reporter expression induction in 4 dpf GiR077 larvae at 24 h after spinal cord injury. The induction is circumscribed to the injury site. An analogue construct to those described, is characterized by the presence in tandem of the human CMV enhancer and the xEF1a enhancer to the SCP2. Larvae carrying this construct do not show any fluorescent reporter upregulation upon injury (data not shown).

This finding excludes the xEF1a enhancer or the super core promoter 2 could contribute to confer constructs GiR077 and GiR085-1 the characteristic induction upon injury. Between the two, GiR077 carriers were characterized by very low basal transgene expression in uninjured animals. At 24 hpf, GiR077 F1 transgenic larvae weakly expressed the transgenes in the eye and in the nasal vesicle (Figure 22 B and C), while from day 2 pf expression remained in the lens and the lateral line (Figure 22 D). From day 5, a punctate expression in the intestine appeared additionally (Figure 22 E). With the exception of the lens, the observed expression pattern was previously described as NF-κB specific (Kuri et al., 2017).

Primary cells derived from 3 dpf F1 GiR077 transgenic zebrafish larvae allowed for testing the enhancer response upon stimulation with TNFα, a known activator of the NF-κB pathway. The day after fish dissociation, cells were cultured 8 h in starvation medium (1 % FCS instead of 10 % FCS) and then treated with 30 ng/mL TNFα or left untreated. After 12 h, the mClover-positive cells and relative median fluorescent intensity (MFI) were measured in flow cytometry. TNFα stimulation resulted in a 17.24 % increase of the number of mClover-positive cells.

The overall number of cells which could be activated could be dependent on the expression of either one of the TNF receptors: TNFR1 (TNF receptor type 1) and TNFR2. Hence, more significant is the comparison of the mClover expression levels within positive cells of the TNFα treated over untreated sample, which is indicated by the median fluorescent intensity of the mClover-positive cells ($MFI_{pos.}$) and not of the overall sample ($MFI_{tot.}$). This value was more than 6 times higher in the treated sample, giving a precise indication of the expression upregulation 12 h after TNFα treatment in cells sensitive to this cytokine.

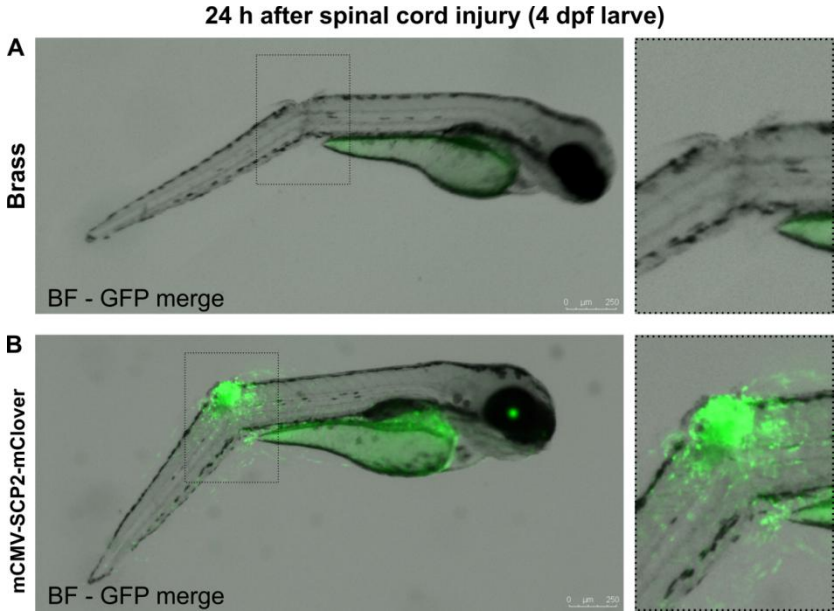

Fig. 21: Spinal cord injury induced expression upregulation in GiR077 transgenic animals.

Image acquisition 24 h after spinal cord injury of 5 dpf brass larvae (A) or GiR077 larvae (B), expressing the tagRFP-T and mClover fluorescent reporters under the control of mCMVenhancer- SCP2promoter elements. Strong reporter expression is observed at the injury site.

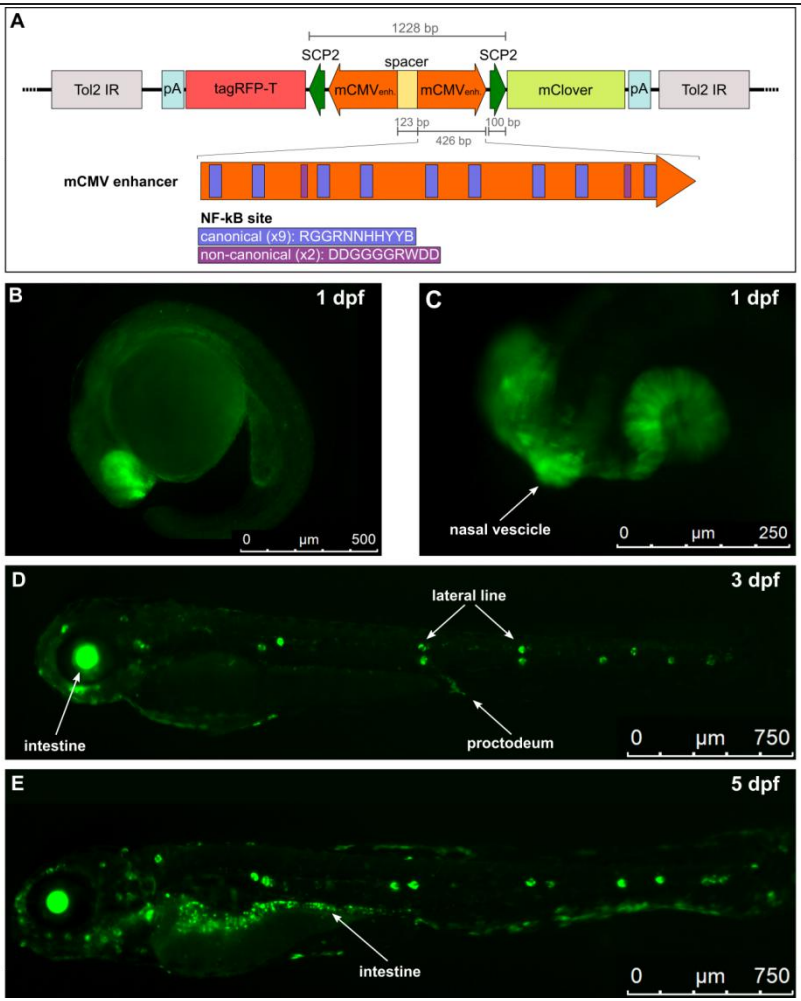

Fig. 22: Mouse CMV enhancer driven reporter expression in vivo.

A) Schematic representation of the CpG-free bidirectional expression cassette flanked by the reporter genes tagRP-T and mClover. Canonical and non-canonical NF-κB sites present in the mouse CMV enhancer sequence are highlighted. Fluorescent mClover signal has been recorded in GiR077 F1 transgenic zebrafish embryos respectively at B-C) 1 dpf, D) 3 dpf, and E) 5 dpf.

At every developmental stage documented mClover expression resembled the typical NF-κB expression profile described in literature for zebrafish, except the additional reporter gene expression in the lens. Dpf, days post fertilization; IR, inverted repeats; pA, poly-A tail; SCP2, Super Core Promoter 2; mCMVenh., murine Cytomegalovirus enhancer.

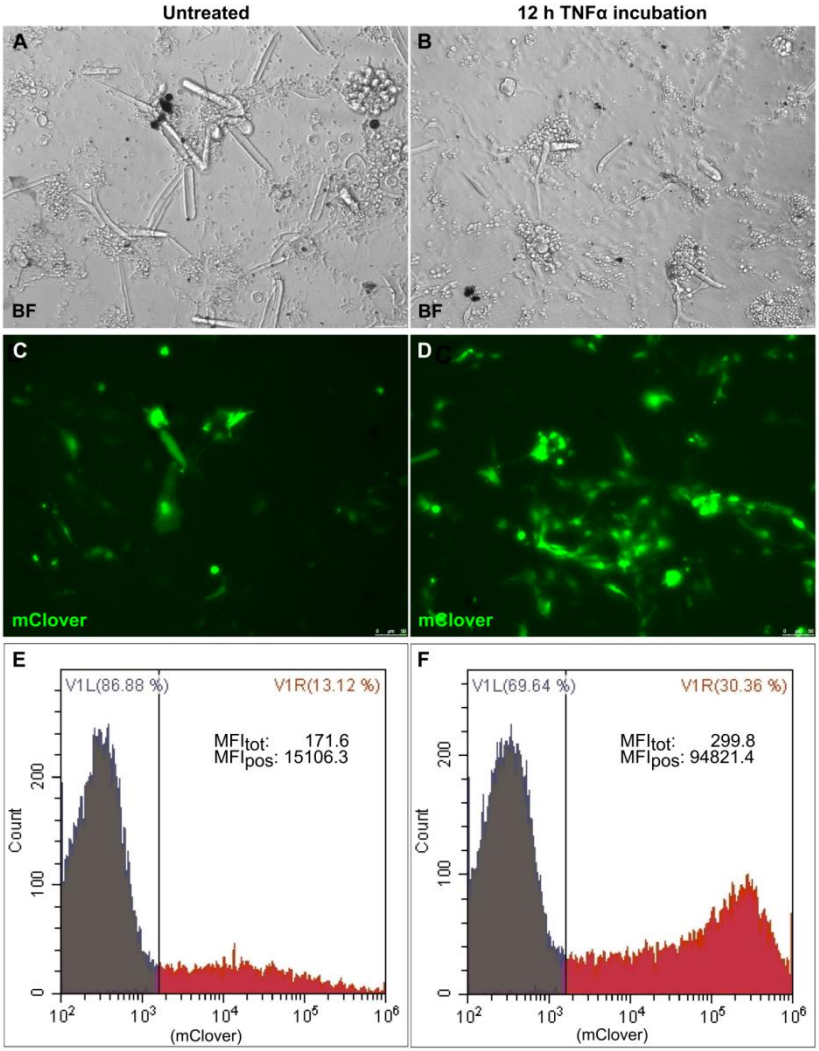

Fig. 23: TNFα induced transgene expression upregulation in GiR077 primary cells.

Primary zebrafish cells obtained from 3 dpf GiR077 transgenic larvae where

cultured in low FCS medium (1 % FCS) for 8 h prior treatment with 30 ng/mL TNFα. Images of control sample and TNFα treated cells A-B) Bright field and C-D) mClover fluorescence acquisition. E-F) Flow cytometry analysis offers the comparison of the mClover-positive cells percentage and mClover expression upregulation within positive cells (MFIpos) for untreated vs TNFα-treated cells.

4. Discussion

4.1. Generation of novel monoclonal antibodies against zCdh2

4.1.1. recAbs improve the detection of Cdh2 during zebrafish development

In this project we generated 11 novel sequence-defined human scFv antibodies against zebrafish Cdh2 via phage display. Four of these antibodies were found to be cross-reactive with the human Cdh2 in ELISA (Figure 4), three of which also bound to Cdh2-positive human cell lines (Figure 11). Before evaluating the efficacy of these scFv's as ER intrabodies, they all underwent a thorough binding profile characterization, with focus on specificity towards the target. Within this process, we have demonstrated that several zebrafish structures identified as Cdh2-positive in at least six different published studies (Tuttle et al., 2014; Xing et al., 2015; Han et al., 2016; Mochizuki et al., 2017; Gays et al., 2017; Powell et al., 2018), which relied on staining with commercially available polyclonal antibodies, may show potentially false positive. These misleading results should be re-evaluated accordingly. Our sequence defined monoclonal antibodies here may serve as better alternatives for Cdh2 detection in whole mounts, FACS, and other assays. Finally, we validated two inexpensive, but extremely reliable approaches for specificity characterization of antibodies against zebrafish endogenously expressed membrane targets or whole protein repertoire after fixation, which are based on the use of antigen null mutants and fluorescent reporter antigen-fusion fish lines.

Zebrafish Cdh2 is member of a large type I transmembrane protein family of adhesion molecules characterized by high structural similarity. The zCdh2 extracellular domain is composed of 5 consecutive Ig-like domains responsible for the formation of cell-cell contacts. Based on InterPro domain classification (ID: IPR007110) (Finn et al., 2017), this

very common protein architecture (Smith and Xue, 1997; Teichmann and Chothia, 2000; Barclay, 2003) can be found in 2503 different zebrafish proteins (ca. 10 % of the zebrafish proteome accordingly to the zebrafish genome project (Howe et al., 2013). The CATH Protein Structure Classification database sequence/structure diversity comparison shows the low degree of sequence/structure diversity among the cadherins compared to other protein families (CATH Superfamily 2.60.40.60). For example, zCdh2 amino acid identity shared with zCdh4-ECD is 68 % for ECD1. This high degree of similarity requires, more than for other targets, a careful process of antibody binding specificity assessment.

We established primary cell flow cytometry to analyze this in detail, allowing to directly compare Wt, zCdh2 null mutants (*pac* mutant), and zCdh2-GFP-RFP (*zf516 Tg*) derived cells. In the latter, the commercial polyclonal antibody GTX125885 stained about 65 % of the cells derived from *zf516 Tg* larvae, while only 29 % of those cells were actually Cdh2 positive, as determined measuring, in parallel to the surface antibody staining, also the GFP fluoresce from Cdh2-GFP-positive samples (Figure 6). More than half of the cells stained by the current "gold standard" antibody did not express Cdh2 at all. This huge false positive signal was corroborated by the observation that approximately 45 % of the *pac* mutant cells were positive - in a fish line where antigen expression is absent (Lele et al., 2002).

In whole mount IHC on 3 days old *zf516 Tg* larvae (Figures 7 and 8), GTX125885 partially recapitulated the zCdh2-GFP expression profile, but additionally stained several zCdh2-GFP-negative tissues. Indeed, along the whole fish body, and markedly in the eyes, of homozygous *pac* mutant larvae, a substantial antibody staining could be observed. Most strikingly, despite its high off-targeting binding, GTX125885 only weakly stained the spinal cord, a tissue where Cdh2-GFP is highly expressed

(Figure 7). Recombinant human MAbs SH1352-G9 and −B11 specifically recognized zCdh2 in flow cytometry on the surface of living primary cells (Figure 5-6), as well as recapitulated precisely the zCdh2-GFP expression pattern profile in whole mount IHC (Figure 7-9). Intriguingly, SH1352-D7 mAb was found to be more suitable in flow cytometry than in whole mount immunostaining and vice versa for SH1352−F4 mAbs. This aspect spotlights the absolute necessity of defining antibody specificity profiles in different assays separately, and add a further element to the notion antibody specificity is not an absolute and immutable property, rather an aspect to contextualize in respect of sample size and preparation, antibody format, and concentration (Uhlen et al., 2016). In this respect, the use of whole mount IHC or whole larvae derived primary cells can be considered preferable to the same tests conducted on a single tissue slice or a single cell line. The highly specific monoclonal antibodies that we generated for flow cytometry may in the future also allow for sorting zCdh2-positive cells for further multiple analysis, e.g. of their transcriptome (Namikawa et al., under minor revision) or proteome, but also for the generation of type-specific cell lines. A small percentage of GFP-positive cells from *zf516 Tg* larvae could not be stained by either polyclonal antibody GTX125885 or our highly specific scFv-hFc antibodies SH1352-B11, -D7, -F4 and -G9 in flow cytometry, or IHC assays. This finding should not surprise as emission in the GFP channel is attributed to the expression of Cdh2-GFP-RFP, but also to eCFP expression in the lens of *zf516 Tg* fish, as shown in the whole mount imaging (Figure 7-8). These cells are zCdh2-negative and can not be stained therefore by the antibody. During the generation of the *zf516 Tg* transgenic line, *crybb1:ECFP* was introduced into the genome to allow for the screening of transgenic progeny earlier than Cdh2 expression occurs in the developing embryos (Revenu et al., 2014; Jiang et al., 1996).

Despite the almost negligible emission of the eCFP in the GFP channel when excited by a 488 nm laser, crybb1 (crystallin Beta B1), as other crystallins in the lens, is present at extremely high concentration, overall estimated to 300–900 mg/mL (Han and Schey, 2006; Zhao et al., 2011). Hence eCFP expression should be similarly high when driven by the crybb1 promoter. Of all the fluorescent proteins with emission maximum in cyan color, ECFP is also known to have a bimodal excitation and emission spectrum, which enhances this phenomenon (Greb 2012; Technical notes by Zeiss). Another explanation may be found in the incubation time (24 h) of the cells after dissociation (which cleaves the Cdh2 on the cell surface). Incubation time is required to allow for the reconstitution of the antigen on the cell membrane. In some cells more than 24 h may be required to display Cdh2-GFP-RFP on the cell surface, while in the same cell some protein may already be folded in the endoplasmic reticulum and therefore already be fluorescent.

4.1.2. Epitope analysis

The novel antibodies generated by phage display provided significantly diverse reactivity patterns, suggesting that they bind different epitope structures. Of the five scFv-Fc mAbs (SH1352-B11, -C6, -D7, -F4, and -G9) tested for binding in the Spot membrane assay (Vernet et al., 2015), only two mAbs (-B11 and −C6) could be mapped on synthetic peptide (Figure 12). In Western blot all these mAbs bound the zCdh2-ECD-mFc antigen prepared under reducing conditions (Figure 14). On the other hand, SH1352-B11 and -C6 were the only antibodies, of the tested 5, capable of binding zCdh2-ECD1 fragments in ELISA (Table 3.5). This suggests that SH1352-D7, -F4, and -G9 mAbs may recognize partially conformational epitopes, which are disrupted by domain breakdown, but may be preserved in western blot analysis as a result of partial refolding or incomplete SDS denaturation. It underlines again the need to always

link statements on antigen specificity to the respective particular assays. The epitope region of those antibodies which did not react on zCdh2-ECD1 PepSpot membrane may be identified using alternative approaches which do not intrinsically prevent protein folding (Fühner et al., in press).

The two epitopes amenable to Spot analysis mapped to a structural homology model of zCdh2-ECD. This model was generated starting from the available crystal structure of the mouse Cdh2 (3Q2W), based on the high sequence similarity of its ECD to the one of zebrafish Cdh2 (75.4 % amino acid similarity for the whole ECD; 80.4 % within ECD1). Sequence similarity of the epitope (VDINGNQMENP, Uniprot Q90275 aa 227-237) of mAb SH1352-B11, which is cross-reactive to human Cdh2, was tested by *in silico* analysis using the non-redundant protein sequence databases/Protein blast. Hits having E-value < 1 were: human Cdh2 (VDINGNQVENP) and zebrafish Cdh4 (VDINGNQMEPP). We found that SH1352-B11 recognizes the human Cdh2, but not the zCdh4. Hence, we can speculate that the amino acidic substitution N236P disrupts the antibody-antigen interaction, while M234V does not - may be since the proline changes the peptide backbone angle while M>V only changes a side chain. Interestingly, the residues V227, I229, N230, and Q233 included in the epitope of SH1352-B11 are also described to be involved in the formation of the cis interface of association between two Cdh2 monomers, necessary for the lateral cadherins association on the cell surface (Harrison et al., 2011). In this process, the Cdh2-ECD1 of a monomer interacts with the Cdh2-ECD2 of a second monomer. This type of interaction is highly specific and, beside Cdh2-Cdh2 homophilic interaction, it can only mediate Cdh2-Cdh4 heterophilic interaction, but not Cdh2-Cdh1 one (Shan et al., 2000; Vendome et al., 2014). This aspect further contributes to delineate the peculiarity of this epitope. As the disruption of the cis interface in mouse Cdh2 mutant cells

(V227D/V320D) compromises the formation of adherens junctions (Bunse et al., 2013), SH1352-B11 binding may exert a similar effect, an effect which may be evaluated in the future. Nevertheless, these findings promise that SH1352-B11 may encode for Cdh2-function interfering antibody. Sequence similarity studies for the SH1352-C6 epitope region (Uniprot: Q90275: aa159-169; SRKQFPEELVK) showed the existence of several zebrafish proteins sharing high (E-value < 1) sequence similarity to it. This result may explain the tendency of this antibody towards some unspecific binding.

On the contrary, the same region of the human Cadherin2 was found to be highly dissimilar (E-value = 50), in accordance with the experimental evidence that SH1352-C6 did not bind hCdh2-ECD-mF in ELISA.

Using ELISA on individual zCdh2-ECD domains it was found that ten of the eleven antibodies generated against recombinant zCdh2 recognize the first ECD of the protein. Potentially, they may all interfere with the "strand-swap" formation of trans interaction between two opposing cadherins molecules (Bunse et al., 2013), encouraging to study a possible application of the new mAbs for functional studies in the future.

4.1.3. Future antibody specificity standards and specificity assessment

At present, the availability of antibodies specific against zebrafish proteins is limited despite the established value of the zebrafish model organism for multiple research purposes. Two of the main strengths of this model are its external fertilization and development, as well as its transparency, which together allow for *in vivo* imaging at cellular resolution of the intact developing embryo. Developmental studies often include protein expression pattern analysis, primary cell sorting, and transcriptome analysis studies (Namikawa, et al., under minor revision). These techniques rely on highly specific antibodies suitable for different

experimental setups. While generation of phage-display derived sequence defined monoclonal antibodies today is robust, fast, and affordable (Schofield et al., 2007; Mersmann et al., 2010; Colwill et al., 2011) the process of validation is the most time-consuming step for research for antibodies from all sources, and not only requires knowledge of the antibody generation process, but also, and most importantly, of the antigen to be detected. This aspect, together with the reduced market for research antibodies to zebrafish proteins, contributes to explain the restricted availability of antibodies against non-mammalian targets. Most of the available antibodies against zebrafish proteins are antibodies generated against mammalian antigens that cross-react with their zebrafish homologous proteins. This concept is well explained by the founder of CiteAb DrChalmers in an interview on the topic (Helsby 2017). Accordingly to CiteAb, a devastating 94.2 % of the mammalian - zebrafish cross-reactive antibodies are polyclonal (4,698 of 4,77 primary antibodies), with their intrinsic risk of exhibiting unwanted reactivities, an issue which involves many antibodies in use (Taussig et al., 2018; Goodman 2018; Bradbury and Plückthun 2015; Berglund et al., 2008; Dove, 2017). A systematic comparison of over 5.000 polyclonal and monoclonal research antibodies from 51 different origins showed that not even 50 % of these antibodies recognized the assigned antigen at all (Berglund et al., 2008). Further, the difficulty to identify identical batches or clones of commercial antibodies - and if successful, to obtain an identical aliquot, negatively affects our capability to reproduce antibody based studies. This not only prevents reproduction of useful studies but in many cases makes it impossible to retrospectively analyze whether a discovery based on antibody staining was the result of specific or unspecific signal - a problem which cannot be underestimated (Berglund et al., 2008). In this framework, the use of monoclonal hybridoma antibodies over

polyclonal preparations can not be considered as the most effective solution for multiple reasons.

First, almost half of published mAb-producing hybridoma cell lines generated so far for research purposes can be assumed to be lost today, partly due to the expense of storage in liquid nitrogen (Alan Sawyer, personal communication). Second, hybridoma derived antibodies can not be further considered unequivocally monoclonal. In an extensive effort, Bradbury and collaborators (Bradbury et al., 2018) sequenced 187 monoclonal hybridomas from a worldwide consortium of different laboratories proving that over than 50 % of these hybridoma cell lines expressed RNA chains encoding for more than one antibody. One third was even shown to secrete more than one IgG, resulting in the production of an oligospecific mixture of antibodies, thus impairing specificity and affinity. The only antibodies which automatically can be considered as monoclonal are sequence defined mAbs generated with recombinant technologies, like phage display. These antibodies can be documented by their sequence, providing infinite reproducibility of studies where they had been used even if the original clone was lost, since it can always be reconstituted from the electronically stored or printed amino acid sequence. While polyclonal antibodies and mAbs from hybridoma supernatants should not be systematically categorized as unspecific, we must be aware that they certainly require more care than sequence defined reagents when assessing their specificity. Unfortunately, if the risk of unwanted cross-reactivities is well known, this is not adequately kept in consideration when testing and validating the available research products (Goodman 2018). Here, the zebrafish model offers ample solution to do so, as a broad collection of knockout lines generated with ZFN, TALEN or CRISPR/Cas9 mutagenesis, and many mutants derived from genetic screens, are available for accurate comparisons with the wild type animals.

In this work, we demonstrated that the advantages of the zebrafish model could be integrated into a pipeline for antibody specificity assessment that is relatively low-cost. It can be assumed that scale up would be possible thanks to readily available automated devices like HTP automated flow cytometry analyzers and automated fish sorters and imagers (Guo et al., 2017). As the portfolio of antibodies to zebrafish proteins has yet to be expanded, it would be highly beneficial to adopt similar exhaustive specificity assessment in the future to improve the quality of future antibody-based studies. Consequently, we hope this work helps to raise the awareness of many scientists who unwittingly ignore the current limits of antibodies based studies reproducibility and reliability. Also, it has to be hoped that antibody providers will reexamine their current standards for specificity assessment and update their antibody generation pipelines to more appropriate current recombinant technologies. In alternative, the zebrafish community in collaboration with a laboratory specialized in the *in vitro* generation of antibodies, could promote an initiative for the generation and characterization of antibodies against the most relevant antigenic targets in the field. Antibody validation, accordingly to the high specificity standards presented in this work, would take place in several independent laboratories specialized in working with designated antigen targets. As result of this community effort, antibody sequences could be made publicly available on the The Zebrafish Information Network (ZFIN) for the all community to use.

4.2. ER Intrabody mediated knockdown in zebrafish

4.2.1. The zebrafish ER retention mechanism supports ER intrabodies

In 1990 Hardwick, Semenza, and colleagues described (Semenza et al., 1990; Hardwick et al., 1990) that the KDEL receptors ERD1 and ERD2 are necessary for the sorting of ER luminal proteins in yeast. Reduction of ERD2 expression leads to the secretion of HDEL (analogue of KDEL in yeast) tagged proteins, while upregulation of ERD2 expression increases HDEL-proteins retention. At that time it was already known that this mechanism is typical of mammalian cells as well (Munro et al, 1987), and that it involves the transit of the KDEL tagged proteins to the cis-Golgi and from this compartment the retrieval to the ER lumen (Pelham, 1988). This retention mechanism can be found even in plants, and can be therefore considered a highly conserved feature of all eukaryotic cells. Intriguingly, the KDEL retention has been shown also in unicellular organisms missing golgi-like organelles as *Giardia lamblia* (Zamponi et al., 2017).

Not too surprisingly, zebrafish is no exception. Three genes encoding KDEL receptors are found in the zebrafish genome kdelr2a, kdelr2b, and kdelr3 (Thisse et al., 2001), where both kdelr2 genes are homologous of mammal ERD2. Studies on the three human KDEL receptors proved their different specificity towards different variants of the KDEL retention signal. Based on the Prosite motif for ER localization [KRHQSA]-[DENQ]-E-L and newly discovered ER localization peptides (Raykhel et al., 2007), exist at least 59 different peptides which mediate good ER protein retention. The most effective KDEL mediated retention will depend on the absolute, as well as relative, expression level of the three KDEL receptors, and their respective specificity.

Despite the KDEL based retention mechanism is proven to exist in zebrafish, the ER intrabody knockdown was so far only proven to work in

human, mouse, rat and plant cells, and had yet to be confirmed to work in the zebrafish model. The ER intrabody against mouse and rat p75 SH325-G7 (Zhang et al., 2012) was chosen for this validation in zebrafish PAC2 cells. The use of an ER intrabody binding to a mouse protein required the co-expression of the antigen target fused to a florescent reporter together with SH325-G7-KDEL or of the negative control ER intrabody α-phOx-KDEL. Contrarily to the negative control sample (Figure 15 C), the presence of mp75-YFP positive cells which did not express the antigen on the cell surface (APC-negative) in the SH325-G7-KDEL sample (Figure 15 D), clearly proved the efficacy of this ER intrabody in mediating mp75 knockdown.

This experiment did not only proved for the first time that ER intrabody mediated knockdown works in zebrafish cells, but that it also can work in a co-transfection heterologous model with high expression levels of the targeted protein.

4.2.2. Endogenous zCdh2 knockdown by ER intrabodies

The new ER intrabodies SH1352-C6, -D7, F9, and -G9 induced a reduction in the number of zCdh2 positive cells by about 20 %, while -G12 up to ~50 % in cell culture (Figure 18). The other mAbs did not exert any effect. The effective ER intrabody mediated reduction of antigen levels from the cell surface was partially masked by two factors. First, by the limited ER intrabody transfection efficiency, diluting the signal because untransfected cells by definition can not show any knockdown. Average transfection efficiency after electroporation in PAC2 cells was at most ~50 %. Second, the low Cdh2 signals in FACS, resulting from low endogenous expression levels, did not allow a complete separation of the $Cdh2^{+}$ and the $Cdh2^{-}$ cell populations. Interestingly, the apparent affinity of the antibodies (as ranked from titration ELISA results in figure 4) does not correlate with knockdown

efficiency, an observation which has also been previously reported for another antigen (Zhang et al., 2012). Similar to the observations for p75, SH1352-G12 was the antibody with the lowest affinity to the antigen in ELISA, but the most efficient in mediating Cdh2 retention. Epitope accessibility in the ER compartment on a freshly forming protein may be significantly different from the conditions used to characterize the antibodies using fully folded, matured, and purified proteins. Alternatively, it cannot be ruled out that this difference may reflect each ER intrabodies relative expression level and folding efficiency in fish cells. These factors can account for knockdown levels more than antibody affinity, and have to be considered in future studies.

4.2.3. The role of antigen degradation after ER retention

The assays which demonstrated the ER intrabody-mediated reduction of zCdh2 from the cell surface provided indirect evidence for the efficacy of the antigen retention in the ER, but did not elucidate whether the retained antigen is degraded afterwards or accumulates in the ER compartment.

In this study, we assessed this by comparing the absolute antigen levels to the cell surface levels of the antigen using an mClover::zCdh2 fusion protein, which allowed its detection independently from its intracellular localization. Significantly, all of the ER intrabodies that mediated a reduction of surface zCdh2 on PAC2 cells also provided a reduction of the endogenous zCdh2 levels, indicating zCdh2-mClover protein degradation in ER intrabody co-transfected HEK293 cells (Figure 19). Cdh2-mClover degradation, indicated by disappearance from the ER lumen, has also been described before for ER intrabodies against VCAM-1 (Strebe et al., 2009). In our experiment the antigen was overexpressed and its levels can be considered to have been significantly higher than the endogenous levels found in PAC2 cells. In

this context, ER intrabodies mediating antigen knockdown are more likely to reduce the number of antigen molecules per cell (Median fluorescent intensity, MFI, reduction), rather than the number of antigen-positive cells. Indeed, when comparing the two measurements, it can be noticed that every sample which showed a reduction in the number of zCdh2-mClover-positive cells also showed an even higher reduction in the MFI which indicates the number of zCdh2-mClover molecules per cell. These results are also in line with other studies which showed the absence of antigen accumulation and UPR activation in ER intrabody expressing cells (Zhang et al., 2012).

The proof of retained antigen degradation is a key feature for the successful use of the ER intrabody technology, since without it, damage induced by accumulation of ER intrabody-bound protein into the ER compartment may lead to false positive phenotypes. It seems to be necessary, however, to confirm this aspect for every different antigen, the naive degradation pathways of which may differ significantly.

4.3. ER intrabody knockdown in zebrafish *in vivo*

4.3.1. THN migration depends on Cdh2 activity

The atonal bHLH transcription factor 1a, more commonly Atoh1a, is a zebrafish transcription factor with proneural activity (Ben-Arie et al., 1997). Its temporal expression is not limited to the developing brain as *atoh1a* expression persists in the adult cerebellum, labeling neuronal progenitors. Neuronal progenitors expressing Atoh1a give rise to multiple neuronal populations including cerebellar granule cells and output neurons, as well as tegmental hindbrain nuclei neuron (THN) (Volkmann et al., 2008 and 2010; Chaplin et al., 2010; Kani et al., 2010). Between 24 hpf and 48 hpf, newly arisen THN migrate from the URL, first rostrally towards the midbrain hindbrain boundary (MHB) and then

ventrally along the MHB (Figure 20 A-C) (Köster and Fraser, 2001; Machold and Fishell, 2005; Wang et al., 2005; Wilson and Wingate, 2006). These cells cross the cerebellar primordium and terminate in the tegmental hindbrain where they form neuronal clusters (Volkmann et al., 2010; Theisen et al., 2018). These clusters will develop into different hindbrain nuclei, including the secondary gustatory/viscerosensory nucleus, the nucleus isthmi, and the superior reticular nucleus. These nuclei project to the optic tectum and the hypothalamus with a potential influence on autonomous function, gustatory and visual system, as described for their equivalent mammalian brain structures, the parabrachial, parabigeminal, and laterodorsal-pedunculopontine tegmental hindbrain nuclei (Volkmann et al., 2010; Wulliman et al., 2011). First, THN and subsequently granule cells (GCs) originate from the URL *atoh1a*$^{+}$ neuronal progenitors. The integrity of migratory processes of GCs has already been shown to depend strictly on Cdh2 activity in zebrafish (Rieger et al., 2009), as well as in mouse (Kerjan et al., 2005), while less is known in regard of the role of Cdh2 in THN migration and tegmental nuclei formation.

ER intrabodies against Cdh2 (SH1352-D7-KDEL) or the negative control α-phOx-KDEL have been expressed in *atoh1a*$^{+}$ THN (Figure 20 E-G) and their effect on neuronal cluster formation studied at 32 hpf and 54 hpf (Figure 20 H-I). At the latest time point the cluster area of SH1352-D7-KDEL larvae was in average 33.78 % wider than in control larvae, while the distance between the clusters reduced by 34.64 %. On the contrary, no significant difference was found at 32 hpf between the two samples. This indication is in accordance with studies which underline that ER intrabody knockdown efficacy is a process whit a strict time dependency (Zhang et al., 2012; Marschall et al., 2014).

Also, ER intrabody plasmid was injected into zebrafish embryos, which implies only several hours after the first ER intrabody molecules were

produced and actively mediating the knockdown of zCdh2. Furthermore, the protein expression after DNA injection is mosaic, so that not all the *atoh1a*$^{+}$ progenitors were actually ER intrabody positive. These aspects consent to hypothesize the generation of stable zebrafish lines expressing the ER intrabody in all the *atoh1a*$^{+}$ cells starting from the first moment after spawning may induce a more pronounced phenotype.

Another limiting factor having a direct impact on the process is the antigen turnover and recycling time, which obviously can differ a lot between different cell surface proteins.

In conclusion, the presence of a significant phenotype at 54 hpf, but not yet at 32 hpf, may reflect the lag time necessary for intrabody production plus the depletion of Cdh2 and the generation of a quantifiable effect on overall cell behavior. It may be wise to generate stable ER intrabody lines and allow for even longer times before phenotype assessment in future studies.

Rieger and colleagues (Rieger et al., 2009) showed Cdh2 cell-cell interaction is necessary to maintain the polarity of GCs and their chain-like orientation during the migration of URL-derived GC progenitors. Particularly the GCs which form the dorsomedial corpus cerebelli in wild type animal, in Cdh2 mutants remain in close proximity to the URL and accumulate in an enlarged ectopically located cluster. The increased area of the THN tegmental nuclei primordia observed upon ER intrabody mediated Cdh2 depletion and their reduced distance from the origin of migration (URL) are in accordance with these previous data on Cdh2 mutant granule cells. It remains to be unveiled if the downregulation of Cdh2 affects migration in the two different cell types by the same molecular mechanism.

The *atoh1a*$^{+}$ THN progenitors (Distel et al., 2010), as well as progenitors of GCs (Rieger et al., 2009; Kani et al., 2010; Volkmann et al., 2008), migrate radially from the URL towards the MHB at first, then tangentially

along the MHB later to finally terminate respectively in the tegmentum or later in the cerebellum (CCe/Va). Cdh2 role during GCs migration consists in coordinating cell-cell contacts and cell polarity via the remodeling of adherens junctions (Rieger et al., 2009). Despite THN and GCs originate from the URL and share part of the migratory route, Cdh2 role in migration may differ between the two cell types. Future studies will be needed to characterize the molecular mechanisms of migrating THN. The use of stronger promoters can increase ER intrabody levels and thereby knockdown efficiency. Different ER localization motifs should also be tested to assess which one has the best ER retaining potential in zebrafish. At least 24 possible variants have been listed as the Prosite motif [KRHQSA]-[DENQ]-E-L (Hulo et al., 2006). Recent studies in human cells showed specificity and affinity level of different KDEL-like variants towards the KDEL receptor 1, 2, or 3 can vary profoundly (Raykhel et al., 2007).

While classic gene knockout approaches completely and irreversibly deplete zCdh2 expression, our approach allows to limit the downregulation of this adhesion molecule in a specific cell type. This may become crucial for the understanding of brain development, as in the Cdh2 mutant fish the whole brain tissue architecture becomes compromised, limiting the capability to differentiate between direct and indirect effects of the knockout on a specific cell type.

4.4. Ubiquitous enhancer/promoter generation and characterization

Currently, the best ubiquitous-like promoter available for zebrafish is the *ubiquitin* promoter (Mosimann et al., 2011), which with its 3.5 Kb in length it is not suitable for the use in bidirectional expression systems. In this work we tested different core enhancers combinations in tandem with the SCP2 screening for ubiquitous and bidirectional expression *in*

vivo in zebrafish. The use of viral enhancers with or without the addition of the *Xenopus laevis*-derived elongation factor 1a enhancer (xEF1a) did not succeed, confirming the known difficulties in the field for the generation of such type of expression system.

4.5. TNFα inducible enhancer/promoter generation and characterization

Zebrafish is gaining popularity as a model for studying the etiology of CNS associated human diseases. Neurodegenerative diseases are often characterized by abnormal cell stimulation via NF-κB activatory cytokines (Verma et al., 2004). Hence, NF-κB responsive genetic elements constitute valuable tools to study the etiology of these diseases.

The cytomegalovirus (CMV) major immediate-early enhancer/promoter is known to respond to common Toll-Like-Receptors (TLRs) agonists such as TNF-alpha (Ramanathan et al., 2006; Koskinen et al., 1999; DeMeritt et al., 2004). In these viruses, gene expression depends strictly on the host transcriptional machinery (Kozak and Roizman, 1974). The use of enhancer/promoter sequences recognized by host transcription factors which are induced during the infection, constitute an evolutionary advantage for the virus (Kropp et al., 2014; Kropp et al., 2015). On the other side, we can benefit from the use of these disease-activated enhancers to drive transgene expression regulated in time and space. During a screening campaign for the identification of virus-derived enhancers capable of driving ubiquitous expression *in vivo* in zebrafish, we found the mCMV CpG-free enhancer element can be induced upon injury *in vivo* (Figure 21) or upon TNFα stimulation in cell culture (Figure 23). Two CpG-free mCMV elements fused to SCP2 elements were cloned back to back to drive bidirectional expression. The expression

profile of the transgenes under the control of this bidirectional expression system in zebrafish (Figure 22 B) resembles the expression profile typical of NF-κB (Kuri et al., 2017).

The reporter system we generated stands out for two aspects we found meritorious of attention. First, the need of generating a methylation-insensitive expression cassette, as the effect of DNA methylation-dependent gene silencing is well described (Meissner 2010) and particularly in respect of transgene expression in zebrafish (Pang et al., 2015). Second, the need of increasing the number of NF-κB binding sites for a highly sensitive reporter expression induction. Indeed, the intensity of the response to proinflammatory cytokines correlates to the number of kB sequences in the enhancer/promoter sequence (Matsuda et al., 2007). Our bidirectional expression cassette is predicted to contain 22 NF-κB binding sites (Figure 22 A). This number of NF-κB binding sites is almost 3 times the number of NF-κB binding sites present in the currently available zebrafish NF-κB reporter vector (Kuri et al., 2017). Despite this improvement, the bidirectional enhancer/promoter length is only 1.2 kb.

This reporter line may be used in several zebrafish inflammation or tissue regeneration models. Additionally to its role as reporter, this enhancer/promoter system can be used for therapeutic approaches, as already proposed (Chtarto et al., 2013), or preferably combined to the ER intrabody knockdown technology to study the role of certain surface or secreted molecules specifically during the processes of tissue regeneration or host infection. Using purely CpG-free expression systems we indirectly contributed to expand the portfolio of enhancer/promoter combinations suitable for non-viral gene therapies approaches, already in clinical trials for the treatment of cystic fibrosis (Alton et al., 2015).

These vector needs to be CpG-free as the presence of even only one CG in bacteria derived plasmid DNA was proven to induce inflammatory responses in mammal lungs proportionally to the number of CGs in the sequence and the pDNA amount (Lindberg et al., 2015).

In the future, the broad availability of different tissue-specific zebrafish enhancers and inducible expression systems will allow for the generation of ER intrabody fish lines where protein knockdown can be finely regulated at spatial and temporal level. This approach would facilitate to use zebrafish to model human diseases which are associated to particular protein activity dysregulation in specific tissues and developmental stages.

5. Conclusions and Outlook

After the recent successful demonstration of ER mediated intrabody knockdown in living transgenic mice (Marschall et al., 2014), this study demonstrated that the same protein-level knockdown technology can also be employed in the important zebrafish model. In this model, only cytosolic genes were knocked down at the protein level so far (Gross et al., 2016), but not yet those expressed through the secretory pathway. While the proof of principle clearly demonstrated compatibility with the zebrafish physiology, it became evident that vector design for ubiquitous gene expression *in vivo* zebrafish - necessary to phenocopy null mutant phenotypes - is not trivial in this context and will need more attention in future applications. However, this question can be systematically assessed experimentally given the ease of zebrafish genetic manipulation and available transgenic lines, thus promising to bypass the *in vivo* mouse transgenic system for ER intrabodies in speed and versatility in the near future. Further, the lack of immortalized, fast proliferating zebrafish cell lines, more easy to cultivate and transfect, constituted a practical limitation to the screen of ER intrabodies. These restrictions were substantially overcome by methodological improvements achieved in this study on the way, like progress in electroporation of zebrafish cells (Sassen et al., 2017; Russo et al., 2018, JoVE) or FACS protocols using primary cells (Russo et al., 2018, N Biotechnol.), which will further facilitate these as well as general studies of zebrafish. Overall this work contributed to enrich the portfolio of protein-based methods for studying the gene function in zebrafish, a model that lack alternatives to the well consolidated DNA and RNA based knockout and knockdown techniques.

6. Summary

In this study we present the generation of 11 novel sequence-defined human scFv antibodies against zebrafish Cdh2 via phage display. We further describe the process of antibody validation for highly specific protein identification in different assays and for targeted protein knockdown *in vitro* and *in vivo* in zebrafish.

Zebrafish is gaining popularity for being better suited than mice for studying *in vivo*, in real time, and on larger sample numbers the correlation between complex behavior and physiological activity at single cell level in the presence of specific stimuli (Vladimirov et al., 2018). Also thanks to its ease of genetic manipulation (Sassen and Köster 2015), zebrafish has been already convincingly used to model human diseases for fast HTP drug screenings (Griffin et al., 2017). Nevertheless, in contrast to the constantly growing availability, in quantity and quality, of tools and techniques for zebrafish *in vivo* studies and genetic engineering, the zebrafish community is still limited by the lack of well characterized antibodies against zebrafish proteins for reliable protein localization studies and antibody-based methods for protein knockdown. Aim of this work was to provide a case study that shows how to obviate or compensate, at least in part, for these limitations. We generated via phage display 11 novel sequence-defined human scFv antibodies against zebrafish Cdh2. Three of these antibodies were found to be cross-reactive with the human Cdh2 in ELISA and flow cytometry on human cell lines. A thorough binding profile characterization unveiled that two of the generated antibodies were highly specific in both whole mount immunostaining, as well as in flow cytometry on primary cells derived from 3 dpf larvae. In parallel, these extensive specificity assessment proved that the only available commercial antibody against zCdh2 identified as zCdh2^{+} cells that do not express the antigenic target at all. This finding put under the spotlight

at least six different published studies where this commercial antibody was used to mark *zcdh2*-expressing tissues (Tuttle et al., 2014; Xing et al., 2015; Han et al., 2016; Mochizuki et al., 2017; Gays et al., 2017; Powell et al., 2018). Our sequence defined monoclonal antibodies here may serve as better alternatives for Cdh2 detection in whole mounts, FACS, and other assays. Indirectly, we validated two inexpensive, but very robust approaches to characterize antibody specificity.

In a second phase of the project, we used the antibodies generated against zCdh2 as tools for protein knockdown *in vitro* and *in vivo*. Antibodies in the scFv format where genetically fused to the KDEL peptide sequence DNA and expressed in living cells, or *in vivo* in zebrafish, to mediate zCdh2 ER-retention and consequently its functional knockdown. When expressed *in vivo* in *atoh1a*$^{+}$ progenitors, one of these ER intrabodies was shown to interfere with THN nuclei primordia formation. A phenotype similar to the one already described for granule cells originating from the same neuronal progenitors in zCdh2 defective mutants (Rieger et al., 2009). This constituted the first successful attempt to utilize the ER intrabody technology in zebrafish. This knockdown approach, together with the use of cytosolic stable antibodies/antibody-like molecules for protein activity interference (Gross et al., 2016), constitute a significant expansion of the available zebrafish tools for gene function studies and for modeling human diseases in this organism model. Acting at protein level, these knockdown approaches allow for better protein isoform discrimination and also constitute a valuable alternative in gene function studies where RNA and DNA based knock-down/-out methods generated controversial results (Kok et al., 2015; Stojic et al., 2018). Overall, we proved that protein based approaches can have a beneficial impact on the zebrafish community, provided that the process of generation of these tools is subjected to a extensive and thoughtful characterization processes.

7. Bibliography

1. Ablain J, Zon LI. Of fish and men: Using zebrafish to fight human diseases. *Trends Cell Biol*. 2013;23(12):584-586. doi:10.1016/j.tcb.2013.09.009.
2. Alton EWFW, Armstrong DK, Ashby D, et al., Repeated nebulisation of non-viral CFTR gene therapy in patients with cystic fibrosis: A randomised, double-blind, placebo-controlled, phase 2b trial. *Lancet Respir Med*. 2015;3(9):684-691. doi:10.1016/S2213-2600(15)00245-3.
3. Amsterdam A, Burgess S, Golling G, et al., A large-scale insertional mutagenesis screen in zebrafish. *Genes Dev*. 1999;13(20):2713-2724.
4. Amsterdam A, Nissen RM, Sun Z, Swindell EC, Farrington S, Hopkins N. *Identification of 315 Genes Essential for Early Zebrafish Development*.; 2004.
5. Amsterdam A, Sadler KC, Lai K, et al., Many Ribosomal Protein Genes Are Cancer Genes in Zebrafish. Derek Stemple, ed. *PLoS Biol*. 2004;2(5):e139. doi:10.1371/journal.pbio.0020139.
6. Amstutz P, Binz HK, Parizek P, et al., Intracellular kinase inhibitors selected from combinatorial libraries of designed ankyrin repeat proteins. *J Biol Chem*. 2005;280(26):24715-24722. doi:10.1074/jbc.M501746200.
7. Anderson JL, Mulligan TS, Shen M-C, et al., mRNA processing in mutant zebrafish lines generated by chemical and CRISPR-mediated mutagenesis produces unexpected transcripts that escape nonsense-mediated decay. Mullins MC, ed. *PLOS Genet*. 2017;13(11):e1007105. doi:10.1371/journal.pgen.1007105.
8. Anelli V, Villefranc JA, Chhangawala S, et al., Oncogenic BRAF disrupts thyroid morphogenesis and function via twist expression. *Elife*. 2017;6. doi:10.7554/eLife.20728.
9. Antinucci P, Hindges R. A crystal-clear zebrafish for in vivo imaging. *Sci Rep*. 2016;6(1):29490. doi:10.1038/srep29490.

10. Arnold K, Bordoli L, Kopp J, Schwede T. The SWISS-MODEL workspace: a web-based environment for protein structure homology modelling. *Bioinformatics*. 2006;22(2):195-201. doi:10.1093/bioinformatics/bti770.

11. Au SH, Storey BD, Moore JC, et al., Clusters of circulating tumor cells traverse capillary-sized vessels. *Proc Natl Acad Sci*. 2016;113(18):4947-4952. doi:10.1073/pnas.1524448113.

12. Bagatto B, Francl J, Liu B, Liu Q. Cadherin2 (N-cadherin) plays an essential role in zebrafish cardiovascular development. *BMC Dev Biol*. 2006;6:23. doi:10.1186/1471-213X-6-23.

13. Baraban SC, Dinday MT, Hortopan GA. Drug screening in Scn1a zebrafish mutant identifies clemizole as a potential Dravet syndrome treatment. *Nat Commun*. 2013;4(1):2410. doi:10.1038/ncomms3410.

14. Barclay AN. Membrane proteins with immunoglobulin-like domains—a master superfamily of interaction molecules. *Semin Immunol*. 2003;15(4):215-223. doi:10.1016/S1044-5323(03)00047-2.

15. Baxendale S, Van Eeden F, Wilkinson R. The Power of Zebrafish in Personalised Medicine. *Adv Exp Med Biol*. 2017. doi:10.1007/978-3-319-60733-7_10.

16. Bedell VM, Westcot SE, Ekker SC. Lessons from morpholino-based screening in zebrafish. *Brief Funct Genomics*. 2011;10(4):181-188. doi:10.1093/bfgp/elr021.

17. Bedell VM, Wang Y, Campbell JM, et al., In vivo genome editing using a high-efficiency TALEN system. *Nature*. 2012;491(7422):114-118. doi:10.1038/nature11537.

18. Beer LA, Tatge H, Schneider C, et al., The binary toxin CDT of Clostridium difficile as a tool for intracellular delivery of bacterial glucosyltransferase domains. *Toxins*. 2018;10(6), 225. doi:10.3390/toxins10060225.

19. Ben-Arie N, Bellen HJ, Armstrong DL, et al., Math1 is essential for genesis of cerebellar granule neurons. *Nature*. 1997;390(6656):169-172. doi:10.1038/36579.

20. Berger J, Currie PD. Zebrafish models flex their muscles to shed light on muscular dystrophies. *Dis Model Mech*. 2012;5(6):726-732. doi:10.1242/dmm.010082.

21. Berglund L, Björling E, Oksvold P, et al., A genecentric Human Protein Atlas for expression profiles based on antibodies. *Mol Cell Proteomics*. 2008;7(August 2005):2019-2027. doi:10.1074/mcp.R800013-MCP200.

22. Biasini M, Bienert S, Waterhouse A, et al., SWISS-MODEL: modelling protein tertiary and quaternary structure using evolutionary information. *Nucleic Acids Res*. 2014;42(Web Server issue):W252-8. doi:10.1093/nar/gku340.

23. Biocca S, Pierandrei-Amaldi P, Campioni N, Cattaneo A. Intracellular immunization with cytosolic recombinant antibodies. *Biotechnology (N Y)*. 1994;12(4):396-399.

24. Biocca S, Ruberti F, Tafani M, Pierandrei-Amaldi P, Cattaneo A. Redox state of single chain Fv fragments targeted to the endoplasmic reticulum, cytosol and mitochondria. *Biotechnology (N Y)*. 1995;13(10):1110-1115.

25. Boer EF, Jette CA, Stewart RA. Neural Crest Migration and Survival Are Susceptible to Morpholino-Induced Artifacts. Riley BB, ed. *PLoS One*. 2016;11(12):e0167278. doi:10.1371/journal.pone.0167278.

26. Bradbury A, Pluckthun A. Reproducibility: Standardize antibodies used in research. *Nature*. 2015;518(7537):27-29. doi:10.1038/518027a.

27. Bradbury ARM, Sidhu S, Dübel S, McCafferty J. Beyond natural antibodies: the power of in vitro display technologies. *Nat Biotechnol*. 2011;29(3):245-254. doi:10.1038/nbt.1791.

28. Bradbury ARM, Trinklein ND, Thie H, et al., When monoclonal antibodies are not monospecific: Hybridomas frequently express additional functional variable regions. *MAbs*. 2018;10(4):539-546. doi:10.1080/19420862.2018.1445456.

29. Breitling F, Dübel S, Seehaus T, Klewinghaus I, Little M. A surface expression vector for antibody screening. *Gene*. 1991;104(2):147-153.

30. Bridge AJ, Pebernard S, Ducraux A, Nicoulaz A-L, Iggo R. Induction of an interferon response by RNAi vectors in mammalian cells. *Nat Genet*. 2003;34(3):263-264. doi:10.1038/ng1173.

31. Bunse S, Garg S, Junek S, et al., Role of N-cadherin cis and trans interfaces in the dynamics of adherens junctions in living cells. *PLoS One*. 2013;8(12):1-16. doi:10.1371/journal.pone.0081517.

32. Cattaneo A, Biocca S. The selection of intracellular antibodies. *Trends Biotechnol*. 1999;17(3):115-121.

33. Ceol CJ, Houvras Y, Jane-Valbuena J, et al., The histone methyltransferase SETDB1 is recurrently amplified in melanoma and accelerates its onset. *Nature*. 2011;471(7339):513-518. doi:10.1038/nature09806.

34. Chan SW, Bye JM, Jackson P, Allain JP. Human recombinant antibodies specific for hepatitis C virus core and envelope E2 peptides from an immune phage display library. *J Gen Virol*. 1996;77(10):2531-2539. doi:10.1099/0022-1317-77-10-2531.

35. Chaplin N, Tendeng C, Wingate RJT. Absence of an external germinal layer in zebrafish and shark reveals a distinct, anamniote ground plan of cerebellum development. *J Neurosci*. 2010;30(8):3048-3057. doi:10.1523/JNEUROSCI.6201-09.2010.

36. Chen R, Shi L, Hakenberg J, et al., Analysis of 589,306 genomes identifies individuals resilient to severe Mendelian childhood diseases. *Nat Biotechnol*. 2016;34(5):531-538. doi:10.1038/nbt.3514.

37. Chtarto A, Bockstael O, Gebara E, et al., An Adeno-Associated Virus-Based Intracellular Sensor of Pathological Nuclear Factor-κB Activation for Disease-Inducible Gene Transfer. Rota R, ed. *PLoS One*. 2013;8(1):e53156. doi:10.1371/journal.pone.0053156.

38. Colwill K, Persson H, Jarvik NE, et al., A roadmap to generate renewable protein binders to the human proteome. *Nat Methods*. 2011;8(7):551-558. doi:10.1038/nmeth.1607.

39. Cutler C, Multani P, Robbins D, et al., Prostaglandin-modulated umbilical cord blood hematopoietic stem cell transplantation. *Blood*. 2013;122(17):3074-3081. doi:10.1182/blood-2013-05-503177.

40. de Wildt RMT, Mundy CR, Gorick BD, Tomlinson IM. Antibody arrays for high-throughput screening of antibody–antigen interactions. *Nat Biotechnol*. 2000;18(9):989-994. doi:10.1038/79494.

41. DeMeritt IB, Milford LE, Yurochko AD. Activation of the NF-kappaB pathway in human cytomegalovirus-infected cells is necessary for efficient transactivation of the major immediate-early promoter. *J Virol*. 2004;78(9):4498-4507. doi:10.1128/JVI.78.9.4498-4507.2004.

42. Dickerson JE, Zhu A, Robertson DL, Hentges KE. Defining the Role of Essential Genes in Human Disease. Ouzounis CA, ed. *PLoS One*. 2011;6(11):e27368. doi:10.1371/journal.pone.0027368.

43. Dietzl G, Chen D, Schnorrer F, et al., A genome-wide transgenic RNAi library for conditional gene inactivation in Drosophila. *Nature*. 2007;448(7150):151-156. doi:10.1038/nature05954.

44. Distel M, Hocking JC, Volkmann K, Köster RW. The centrosome neither persistently leads migration nor determines the site of axonogenesis in migrating neurons in vivo. *J Cell Biol*. 2010;191(4):875-890. doi:10.1083/jcb.201004154.

45. Dong J, Thompson AA, Fan Y, et al., A Single-Domain Llama Antibody Potently Inhibits the Enzymatic Activity of Botulinum Neurotoxin by Binding to the Non-Catalytic α-Exosite Binding Region. *J Mol Biol*. 2010;397(4):1106-1118. doi:10.1016/J.JMB.2010.01.070.

46. Donoso G, Herzog V, Schmitz A. Misfolded BiP is degraded by a proteasome-independent endoplasmic-reticulum-associated degradation pathway. *Biochem J*. 2005;387(Pt 3):897-903. doi:10.1042/BJ20041312.

47. Dove A. Technology Feature | Agreeable antibodies: Antibody validation challenges and solutions. *Science (80-)*. 2017;357(6356):1165-1167. doi:10.1126/science.357.6356.1165.

48. Doyon Y, McCammon JM, Miller JC, et al., Heritable targeted gene disruption in zebrafish using designed zinc-finger nucleases. *Nat Biotechnol*. 2008;26(6):702-708. doi:10.1038/nbt1409.

49. Echeverri CJ, Beachy PA, Baum B, et al., Minimizing the risk of reporting false positives in large-scale RNAi screens. *Nat Methods*. 2006;3(10):777-779. doi:10.1038/nmeth1006-777.

50. El-Brolosy MA, Stainier DYR. Genetic compensation: A phenomenon in search of mechanisms. Moens C, ed. *PLOS Genet*. 2017;13(7):e1006780. doi:10.1371/journal.pgen.1006780.

51. Eve AMJ, Place ES, Smith JC. Comparison of Zebrafish tmem88a mutant and morpholino knockdown phenotypes. Gibert Y, ed. *PLoS One*. 2017;12(2):e0172227. doi:10.1371/journal.pone.0172227.

52. Feige MJ, Hendershot LM, Buchner J. How antibodies fold. *Trends Biochem Sci*. 2010;35(4):189-198. doi:10.1016/J.TIBS.2009.11.005.

53. Ferreira-Cornwell MC, Luo Y, Narula N, Lenox JM, Lieberman M, Radice GL. Remodeling the intercalated disc leads to cardiomyopathy in mice misexpressing cadherins in the heart. *J Cell Sci*. 2002;115(Pt 8):1623-1634.

54. Finn RD, Attwood TK, Babbitt PC, et al., InterPro in 2017-beyond protein family and domain annotations. *Nucleic Acids Res*. 2017;45(D1):D190-D199. doi:10.1093/nar/gkw1107.

55. Foote J, Raman A, Song H, et al., A relation between the principal axes of inertia and ligand binding. *Proc Natl Acad Sci U S A*. 2000;97(3):978-983. doi:10.1073/pnas.97.3.978.

56. Frenzel A, Kügler J, Helmsing S, et al., Designing Human Antibodies by Phage Display. *Transfus Med Hemother*. 2017;44(5):312-318. doi:10.1159/000479633.

57. Froude JW, Pelat T, Miethe S, et al., Generation and characterization of protective antibodies to Marburg virus. *MAbs*. 2017;9(4):696-703. doi:10.1080/19420862.2017.1299848.

58. Fühner, V., Heine, P.A., Zilkens, K., Meier, D., Roth, K.D.R., Moreira, G.M.S.G., Hust, M. and Russo G. Epitope Mapping via Phage Display from single gene libraries. Human Monoclonal Antibodies, Ed: M. Steinitz. In: *Methods in Molecular Biology* (in press).

59. Gaiano N, Amsterdam A, Kawakami K, Allende M, Becker T, Hopkins N. Insertional mutagenesis and rapid cloning of essential genes in zebrafish. *Nature*. 1996;383(6603):829-832. doi:10.1038/383829a0.

60. Gänzler-Odenthal SI, Redies C. Blocking N-cadherin function disrupts the epithelial structure of differentiating neural tissue in the embryonic chicken brain. *J Neurosci*. 1998;18(14):5415-5425.

61. Gays D, Hess C, Camporeale A, et al., An exclusive cellular and molecular network governs intestinal smooth muscle cell differentiation in vertebrates. *Development*. 2017;(January):dev.133926. doi:10.1242/dev.133926.

62. Gerety SS, Wilkinson DG. Morpholino artifacts provide pitfalls and reveal a novel role for pro-apoptotic genes in hindbrain boundary development. *Dev Biol*. 2011;350(2):279-289. doi:10.1016/j.ydbio.2010.11.030.

63. Glanville J, Zhai W, Berka J, et al., Precise determination of the diversity of a combinatorial antibody library gives insight into the human immunoglobulin repertoire. *Proc Natl Acad Sci U S A*. 2009;106(48):20216-20221. doi:10.1073/pnas.0909775106.

64. Golling G, Amsterdam A, Sun Z, et al., Insertional mutagenesis in zebrafish rapidly identifies genes essential for early vertebrate development. *Nat Genet*. 2002;31(2):135-140. doi:10.1038/ng896.

65. Goodman SL. The antibody horror show: an introductory guide for the perplexed. *N Biotechnol*. 2018;45:9-13. doi:10.1016/J.NBT.2018.01.006.

66. Gray AC, Sidhu SS, Chandrasekera PC, Hendriksen CFM, Borrebaeck CAK. Animal-based antibodies: Obsolete. *Science*. 2016;353(6298):452-453. doi:10.1126/science.aag3305.

67. Greb C. Fluorescent Proteins – Introduction and Photo Spectral Characteristics. April 2012. https://www.leica-microsystems.com/science-lab/fluorescent-proteins-introduction-and-photo-spectral-characteristics/.

68. Griffin A, Hamling KR, Hong S, Anvar M, Lee LP, Baraban SC. Preclinical Animal Models for Dravet Syndrome: Seizure Phenotypes, Comorbidities and Drug Screening. *Front Pharmacol*. 2018;9:573. doi:10.3389/fphar.2018.00573.

69. Griffin A, Hamling KR, Knupp K, Hong SG, Lee LP, Baraban SC. Clemizole and modulators of serotonin signalling suppress seizures in Dravet syndrome. *Brain*. 2017;140(3):669-683. doi:10.1093/brain/aww342.

70. Gross GG, Straub C, Perez-Sanchez J, et al., An E3-ligase-based method for ablating inhibitory synapses. *Nat Methods*. 2016;13(8):673-678. doi:10.1038/nmeth.3894.

71. Grzegorski SJ, Chiari EF, Robbins A, Kish PE, Kahana A. Natural variability of Kozak sequences correlates with function in a zebrafish model. *PLoS One*. 2014;9(9):e108475. doi:10.1371/journal.pone.0108475.

72. Guex N, Peitsch MC, Schwede T. Automated comparative protein structure modeling with SWISS-MODEL and Swiss-PdbViewer: a historical perspective. *Electrophoresis*. 2009;30 Suppl 1(S1):S162-73. doi:10.1002/elps.200900140.

73. Guglielmi L, Denis V, Vezzio-Vié N, et al., Selection for intrabody solubility in mammalian cells using GFP fusions. *Protein Eng Des Sel*. 2011;24(12):873-881. doi:10.1093/protein/gzr049.

74. Gumbiner BM. Regulation of cadherin-mediated adhesion in morphogenesis. *Nat Rev Mol Cell Biol*. 2005;6(8):622-634. doi:10.1038/nrm1699.

75. Guo Y, Veneman WJ, Spaink HP, Verbeek FJ. Three-dimensional reconstruction and measurements of zebrafish larvae from high-throughput axial-view in vivo imaging. *Biomed Opt Express*. 2017;8(5):2611. doi:10.1364/BOE.8.002611.

76. Haffter P, Granato M, Brand M, et al., The identification of genes with unique and essential functions in the development of the zebrafish, Danio rerio. *Development*. 1996;123(1).

77. Haffter P, Odenthal J, Mullins MC, et al., Mutations affecting pigmentation and shape of the adult zebrafish. *Dev Genes Evol*. 1996;206(4):260-276. doi:10.1007/s004270050051.

78. Han J, Schey KL. MALDI tissue imaging of ocular lens α-crystallin. *Investig Ophthalmol Vis Sci*. 2006;47(7):2990-2996. doi:10.1167/iovs.05-1529.

79. Han P, Bloomekatz J, Ren J, et al., Coordinating cardiomyocyte interactions to direct ventricular chamber morphogenesis. *Nature*. 2016;534(7609):700-704. doi:10.1038/nature18310.

80. Hardwick KG, Lewis MJ, Semenza J, Dean N, Pelham HR. ERD1, a yeast gene required for the retention of luminal endoplasmic reticulum proteins, affects glycoprotein processing in the Golgi apparatus. *EMBO J*. 1990;9(3):623-630. doi:10.1002/j.1460-2075.1990.tb08154.x.

81. Harrison OJ, Jin X, Hong S, et al., The Extracellular Architecture of Adherens Junctions Revealed by Crystal Structures of Type I Cadherins. *Structure*. 2011;19(2):244-256. doi:10.1016/j.str.2010.11.016.

82. Hatta K, Takeichi M. Expression of N-cadherin adhesion molecules associated with early morphogenetic events in chick development. *Nature*. 1986;320(6061):447-449. doi:10.1038/320447a0.

83. Hay M, Thomas DW, Craighead JL, Economides C, Rosenthal J. Clinical development success rates for investigational drugs. *Nat Biotech*. 2014;32(1):40-51. doi:10.1038/nbt.2786

84. Hirohashi S. Inactivation of the E-cadherin-mediated cell adhesion system in human cancers. *Am J Pathol*. 1998;153(2):333-339. doi:10.1016/S0002-9440(10)65575-7.

85. Hoet RM, Cohen EH, Kent RB, et al., Generation of high-affinity human antibodies by combining donor-derived and synthetic

complementarity-determining-region diversity. *Nat Biotechnol*. 2005;23(3):344-348. doi:10.1038/nbt1067.

86. Howe K, Clark MD, Torroja CF, et al., The zebrafish reference genome sequence and its relationship to the human genome. *Nature*. 2013;496(7446):498-503. doi:10.1038/nature12111.

87. Hsu MY, Wheelock MJ, Johnson KR, Herlyn M. Shifts in cadherin profiles between human normal melanocytes and melanomas. *J Investig dermatology Symp Proc*. 1996;1(2):188-194.

88. Hulo N, Bairoch A, Bulliard V, et al., The PROSITE database. *Nucleic Acids Res*. 2006;34(90001):D227-D230. doi:10.1093/nar/gkj063.

89. Hust M, Meyer T, Voedisch B, et al., A human scFv antibody generation pipeline for proteome research. *J Biotechnol*. 2011;152(4):159-170. doi:10.1016/J.JBIOTEC.2010.09.945.

90. Huston JS, Levinson D, Mudgett-Hunter M, et al., Protein engineering of antibody binding sites: recovery of specific activity in an anti-digoxin single-chain Fv analogue produced in Escherichia coli. *Proc Natl Acad Sci U S A*. 1988;85(16):5879-5883. doi:10.1073/PNAS.85.16.5879.

91. Hwang WY, Fu Y, Reyon D, et al., Efficient genome editing in zebrafish using a CRISPR-Cas system. *Nat Biotechnol*. 2013;31(3):227-229. doi:10.1038/nbt.2501.

92. Islam S, Carey TE, Wolf GT, Wheelock MJ, Johnson KR. Expression of N-cadherin by human squamous carcinoma cells induces a scattered fibroblastic phenotype with disrupted cell-cell adhesion. *J Cell Biol*. 1996;135(6):1643-1654. doi:10.1083/jcb.135.6.1643.

93. Jackson AL, Bartz SR, Schelter J, et al., Expression profiling reveals off-target gene regulation by RNAi. *Nat Biotechnol*. 2003;21(6):635-637. doi:10.1038/nbt831.

94. Jackson AL, Bartz SR, Schelter J, et al., off-target gene regulation by RNAi. *Nat Biotechnol*. 2003;21(6):635-638.

95. Jackson AL, Linsley PS. Noise amidst the silence: Off-target effects of siRNAs? *Trends Genet*. 2004;20(11):521-524. doi:10.1016/j.tig.2004.08.006.

96. Jagannathan S, Bradley RK. Translational plasticity facilitates the accumulation of nonsense genetic variants in the human population. *Genome Res*. 2016;26(12):1639-1650. doi:10.1101/gr.205070.116.

97. Jiang YJ, Brand M, Heisenberg CP, et al., Mutations affecting neurogenesis and brain morphology in the zebrafish, Danio rerio. *Development*. 1996;123:205-216.

98. Ju B, Chen W, Orr B a, et al., Oncogenic KRAS promotes malignant brain tumors in zebrafish. *Mol Cancer*. 2015;14(1):1-11. doi:10.1186/s12943-015-0288-2.

99. Juven-Gershon T, Cheng S, Kadonaga JT. Rational design of a super core promoter that enhances gene expression. *Nat Methods*. 2006;3(11):917-922. doi:10.1038/nmeth937.

100. Kani S, Bae YK, Shimizu T, et al., Proneural gene-linked neurogenesis in zebrafish cerebellum. *Dev Biol*. 2010;343(1-2):1-17. doi:10.1016/j.ydbio.2010.03.024.

101. Kawakami K. Tol2: a versatile gene transfer vector in vertebrates. *Genome Biol*. 2007;8 Suppl 1(Suppl 1):S7. doi:10.1186/gb-2007-8-s1-s7.

102. Kawauchi T, Sekine K, Shikanai M, et al., Rab GTPases-Dependent Endocytic Pathways Regulate Neuronal Migration and Maturation through N-Cadherin Trafficking. *Neuron*. 2010;67:588-602. doi:10.1016/j.neuron.2010.07.007.

103. Kerjan G, Dolan J, Haumaitre C, et al., The transmembrane semaphorin Sema6A controls cerebellar granule cell migration. *Nat Neurosci*. 2005;8(11):1516-1524. doi:10.1038/nn1555.

104. Kettleborough RNW, Busch-Nentwich EM, Harvey SA, et al., A systematic genome-wide analysis of zebrafish protein-coding gene function. *Nature*. 2013;496(7446):494-497. doi:10.1038/nature11992.

105. Kiefer F, Arnold K, Kunzli M, Bordoli L, Schwede T. The SWISS-MODEL Repository and associated resources. *Nucleic Acids Res*. 2009;37(Database):D387-D392. doi:10.1093/nar/gkn750.

106. King FDS and RW. Vigilance and Validation: Keys to Success in RNAi Screening. *ACS Chem Biol*. 2011;5(2):163-176.

107. Kittler R, Pelletier L, Ma C, et al., RNA interference rescue by bacterial artificial chromosome transgenesis in mammalian tissue culture cells. *Proc Natl Acad Sci U S A*. 2005;102(7):2396-2401. doi:10.1073/pnas.0409861102.

108. Kohl A, Amstutz P, Parizek P, et al., Allosteric inhibition of aminoglycoside phosphotransferase by a designed ankyrin repeat protein. *Structure*. 2005;13(8):1131-1141. doi:10.1016/j.str.2005.04.020.

109. Kok FO, Shin M, Ni C-W, et al., Reverse genetic screening reveals poor correlation between morpholino-induced and mutant phenotypes in zebrafish. *Dev Cell*. 2015;32(1):97-108. doi:10.1016/j.devcel.2014.11.018.

110. Kontermann RE. Intrabodies as therapeutic agents. *Methods*. 2004;34(2):163-170. doi:10.1016/j.ymeth.2004.04.002.

111. Koskinen PK, Kallio EA, Tikkanen JM, Sihvola RK, Häyry PJ, Lemström KB. Cytomegalovirus infection and cardiac allograft vasculopathy. *Transpl Infect Dis*. 1999;1(2):115-126.

112. Köster RW, Fraser SE. Direct imaging of in vivo neuronal migration in the developing cerebellum. *Curr Biol*. 2001;11(23):1858-1863. doi:10.1016/S0960-9822(01)00585-1.

113. Kostetskii I, Moore R, Kemler R, Radice GL. Differential adhesion leads to segregation and exclusion of N-cadherin-deficient cells in chimeric embryos. *Dev Biol*. 2001;234(1):72-79. doi:10.1006/dbio.2001.0250.

114. Kozak M, Roizman B. Regulation of herpesvirus macromolecular synthesis: nuclear retention of nontranslated viral RNA sequences. *Proc Natl Acad Sci U S A*. 1974;71(11):4322-4326. doi:10.1073/PNAS.71.11.4322.

115. Kropp KA, Angulo A, Ghazal P. Viral Enhancer Mimicry of Host Innate-Immune Promoters. Rall GF, ed. *PLoS Pathog*. 2014;10(2):e1003804. doi:10.1371/journal.ppat.1003804.

116. Kropp KA, Hsieh WY, Isern E, et al., A Temporal Gate for Viral Enhancers to Co-opt Toll-Like-Receptor Transcriptional Activation Pathways upon Acute Infection. Sun R, ed. *PLOS Pathog*. 2015;11(4):e1004737. doi:10.1371/journal.ppat.1004737.

117. Kügler J, Wilke S, Meier D, et al., Generation and analysis of the improved human HAL9/10 antibody phage display libraries. *BMC Biotechnol*. 2015;15(1):10. doi:10.1186/s12896-015-0125-0.

118. Kuhlmann L, Cummins E, Samudio I, Kislinger T. Cell-surface proteomics for the identification of novel therapeutic targets in cancer. *Expert Rev Proteomics*. 2018;15(3):259-275. doi:10.1080/14789450.2018.1429924.

119. Kulkarni MM, Booker M, Silver SJ, et al., Evidence of off-target effects associated with long dsRNAs in Drosophila melanogaster cell-based assays. *Nat Methods*. 2006;3(10):833-838. doi:10.1038/nmeth935.

120. Kuri P, Ellwanger K, Kufer TA, Leptin M, Bajoghli B. A high-sensitivity bi-directional reporter to monitor NF-κB activity in cell culture and zebrafish in real time. *J Cell Sci*. 2017;130(3):648-657. doi:10.1242/jcs.196485.

121. Langer CCH, Ejsmont RK, Schönbauer C, Schnorrer F, Tomancak P. In vivo RNAi rescue in Drosophila melanogaster with genomic transgenes from Drosophila pseudoobscura. *PLoS One*. 2010;5(1):e8928. doi:10.1371/journal.pone.0008928.

122. Lele Z, Folchert A, Concha M, et al., Parachute/N-Cadherin Is Required for Morphogenesis and Maintained Integrity of the Zebrafish Neural Tube. *Development*. 2002;129(14):3281-3294. http://dev.biologists.org/content/129/14/3281.figures-only.

123. Li G, Herlyn M. Dynamics of intercellular communication during melanoma development. *Mol Med Today*. 2000;6(4):163-169. doi:10.1016/S1357-4310(00)01692-0.

124. Li M, Zhao L, Page-McCaw PS, Chen W. Zebrafish Genome Engineering Using the CRISPR-Cas9 System. *Trends Genet*. 2016;32(12):815-827. doi:10.1016/j.tig.2016.10.005.

125. Li T, Huang S, Jiang WZ, et al., TAL nucleases (TALNs): hybrid proteins composed of TAL effectors and FokI DNA-cleavage domain. *Nucleic Acids Res*. 2011;39(1):359-372. doi:10.1093/nar/gkq704.

126. Lindberg MF, Le Gall T, Carmoy N, et al., Efficient in vivo transfection and safety profile of a CpG-free and codon optimized luciferase plasmid using a cationic lipophosphoramidate in a multiple intravenous administration procedure. *Biomaterials*. 2015;59:1-11. doi:10.1016/j.biomaterials.2015.04.024.

127. Liu S, Leach SD. Zebrafish Models for Cancer. *Annu Rev Pathol Mech Dis*. 2011;6(1):71-93. doi:10.1146/annurev-pathol-011110-130330.

128. Luccardini C, Hennekinne L, Viou L, et al., N-Cadherin Sustains Motility and Polarity of Future Cortical Interneurons during Tangential Migration. *J Neurosci*. 2013;33(46):18149-18160. doi:10.1523/JNEUROSCI.0593-13.2013.

129. Luo Y, Ferreira-Cornwell M, Baldwin H, et al., Rescuing the N-cadherin knockout by cardiac-specific expression of N- or E-cadherin. *Development*. 2001;128(4):459-469.

130. M W. *The Zebrafish Book. A Guide for The Laboratory Use of Zebrafish (Danio Rerio)*. 4th ed. University of Oregon Press, Eugene, OR; 2000.

131. Ma Y, Creanga A, Lum L, Beachy PA. Prevalence of off-target effects in Drosophila RNA interference screens. *Nature*. 2006;443(7109):359-363. doi:10.1038/nature05179.

132. Machold R, Fishell G. Math1 Is Expressed in Temporally Discrete Pools of Cerebellar Rhombic-Lip Neural Progenitors. *Neuron*. 2005;48(1):17-24. doi:10.1016/j.neuron.2005.08.028.

133. MacRae CA, Peterson RT. Zebrafish as tools for drug discovery. *Nat Publ Gr*. 2015;14. doi:10.1038/nrd4627.

134. Majoul I, Straub M, Hell SW, Duden R, Soeling H-D. KDEL-Cargo Regulates Interactions between Proteins Involved in COPI Vesicle Traffic: Measurements in Living Cells Using FRET. *Dev Cell*. 2001;1(1):139-153. doi:10.1016/S1534-5807(01)00004-1.

135. Marques IJ, Weiss FU, Vlecken DH, et al., Metastatic behaviour of primary human tumours in a zebrafish xenotransplantation model. *BMC Cancer*. 2009;9:1-14. doi:10.1186/1471-2407-9-128.

136. Marschall ALJ, Dübel S. Antibodies inside of a cell can change its outside: Can intrabodies provide a new therapeutic paradigm? *Comput Struct Biotechnol J*. 2016;14:304-308. doi:10.1016/j.csbj.2016.07.003.

137. Marschall AL, Single FN, Schlarmann K, et al., Functional knock down of VCAM1 in mice mediated by endoplasmatic reticulum retained intrabodies. *MAbs*. 2014;6(6):1394-1401. doi:10.4161/mabs.34377.

138. Matsuda M, Tsukiyama T, Bohgaki M, Nonomura K, Hatakeyama S. Establishment of a newly improved detection system for NF-κB activity. *Immunol Lett*. 2007;109(2):175-181. doi:10.1016/j.imlet.2007.02.007.

139. Matt Helsby. Which antibodies for zebrafish are the most used? | CiteAb Blog. CiteAb. https://blog.citeab.com/which-antibodies-for-zebrafish-are-the-most-used/. Published 2017.

140. Meissner A. Epigenetic modifications in pluripotent and differentiated cells. *Nat Biotechnol*. 2010;28(10):1079-1088. doi:10.1038/nbt.1684.

141. Meng X, Noyes MB, Zhu LJ, Lawson ND, Wolfe SA. Targeted gene inactivation in zebrafish using engineered zinc-finger nucleases. *Nat Biotechnol*. 2008;26(6):695-701. doi:10.1038/nbt1398.

142. Mercatali L, La Manna F, Groenewoud A, et al., Development of a Patient-Derived Xenograft (PDX) of Breast Cancer Bone Metastasis in a Zebrafish Model. *Int J Mol Sci*. 2016;17(8):1375. doi:10.3390/ijms17081375.

143. Mersmann M, Meier D, Mersmann J, et al., Towards proteome scale antibody selections using phage display. *N Biotechnol*. 2010;27(2):118-128. doi:10.1016/j.nbt.2009.10.007.

144. Meusser B, Hirsch C, Jarosch E, Sommer T. ERAD: the long road to destruction. *Nat Cell Biol*. 2005;7(8):766-772. doi:10.1038/ncb0805-766.

145. Miethe S, Rasetti-Escargueil C, Avril A, et al., Development of human-like scFv-Fc neutralizing botulinum neurotoxin E. *PLoS One*. 2015;10(10):1-20. doi:10.1371/journal.pone.0139905.

146. Miyatani S, Shimamura K, Hatta M, et al., Neural cadherin: role in selective cell-cell adhesion. *Science*. 1989; 245(4918):631-5

147. Mochizuki T, Luo Y-J, Tsai H-F, Hagiwara A, Masai I. Cell division and cadherin-mediated adhesion regulate lens epithelial cell movement in zebrafish. *Development*. 2017;144(4):708-719. doi:10.1242/dev.138909.

148. Mollova S, Retter I, Hust M, Dübel S, Müller W. Analysis of Single Chain Antibody Sequences Using the VBASE2 Fab Analysis Tool. In: *Antibody Engineering*. Berlin, Heidelberg: Springer Berlin Heidelberg; 2010:3-10. doi:10.1007/978-3-642-01147-4_1.

149. Moore JC, Langenau DM. Allograft Cancer Cell Transplantation in Zebrafish. In: *Advances in Experimental Medicine and Biology*. Vol 916. ; 2016:265-287. doi:10.1007/978-3-319-30654-4_12.

150. Mosimann C, Kaufman CK, Li P, Pugach EK, Tamplin OJ, Zon LI. Ubiquitous transgene expression and Cre-based recombination driven by the ubiquitin promoter in zebrafish. *Development*. 2011;138(1):169-177. doi:10.1242/dev.059345.

151. Munro S, Pelham HRB. *A C-Terminal Signal Prevents Secretion of Luminal ER Proteins*. Vol 48.; 1987.

152. Namikawa K, Dorigo A, Zagrebelsky M, Russo G, Kirmann T, Fahr W, Dübel S, Korte M and Köster RW. Modeling neurodegenerative Spinocerebellar Ataxia type 13 in zebrafish using a Purkinje neuron specific tunable co-expression system. *J Neurosci*. (Under minor revision)

153. Narasimhan VM, Hunt KA, Mason D, et al., Health and population effects of rare gene knockouts in adult humans with related parents. *Science*. 2016;352(6284):474-477. doi:10.1126/science.aac8624.

154. Nasevicius A, Ekker SC. Effective targeted gene 'knockdown' in zebrafish. *Nat Genet*. 2000;26(2):216-220. doi:10.1038/79951.

155. Nguyen AT, Koh V, Spitsbergen JM, Gong Z. Development of a conditional liver tumor model by mifepristone-inducible Cre recombination to control oncogenic kras V12 expression in transgenic zebrafish. *Sci Rep*. 2016;6(1):19559. doi:10.1038/srep19559.

156. Nieman MT, Prudoff RS, Johnson KR, Wheelock MJ. N-cadherin promotes motility in human breast cancer cells regardless of their E-cadherin expression. *J Cell Biol*. 1999;147(3):631-644. doi:10.1083/jcb.147.3.631.

157. Novodvorsky P, Watson O, Gray C, et al., klf2ash317 Mutant Zebrafish Do Not Recapitulate Morpholino-Induced Vascular and Haematopoietic Phenotypes. Ramchandran R, ed. *PLoS One*. 2015;10(10):e0141611. doi:10.1371/journal.pone.0141611.

158. Nusslein-Volhard C. The zebrafish issue of Development. *Development*. 2012;139(22):4099-4103. doi:10.1242/dev.085217.

159. Pang SC, Wang HP, Zhu ZY, Sun YH. Transcriptional Activity and DNA Methylation Dynamics of the Gal4/UAS System in Zebrafish. *Mar Biotechnol*. 2015;17(5):593-603. doi:10.1007/s10126-015-9641-0.

160. Patton EE, Widlund HR, Kutok JL, et al., BRAF Mutations Are Sufficient to Promote Nevi Formation and Cooperate with p53 in the Genesis of Melanoma. *Curr Biol*. 2005;15:249-254. doi:10.1016/j.

161. Pebernard S, Iggo RD. Determinants of interferon-stimulated gene induction by RNAi vectors. *Differentiation*. 2004;72(2-3):103-111. doi:10.1111/j.1432-0436.2004.07202001.x.

162. Pelham HR. Evidence that luminal ER proteins are sorted from secreted proteins in a post-ER compartment. *EMBO J*. 1988;7(4):913-918.

163. Pelham HRB. *The Dynamic Organisation of the Secretory Pathway*. Vol 21:413-419; 1996.

164. Perl AK, Wilgenbus P, Dahl U, Semb H, Christofori G. A causal role for E-cadherin in the transition from adenoma to carcinoma. *Nature*. 1998;392(6672):190-193. doi:10.1038/32433.

165. Persengiev SP, Zhu X, Green MR. Nonspecific, concentration-dependent stimulation and repression of mammalian gene expression by small interfering RNAs (siRNAs). *RNA*. 2004;10(1):12-18.

166. Phelps M, Chen E. Zebrafish Rhabdomyosarcoma. In: *Advances in Experimental Medicine and Biology*. Vol 916. ; 2016:371-389. doi:10.1007/978-3-319-30654-4_16.

167. Philibert P, Stoessel A, Wang W, et al., A focused antibody library for selecting scFvs expressed at high levels in the cytoplasm. *BMC Biotechnol*. 2007;7(1):81. doi:10.1186/1472-6750-7-81.

168. Pickart MA, Klee EW, Nielsen AL, et al., Genome-wide reverse genetics framework to identify novel functions of the vertebrate secretome. *PLoS One*. 2006;1(1). doi:10.1371/journal.pone.0000104.

169. Place ES, Smith JC. Zebrafish atoh8 mutants do not recapitulate morpholino phenotypes. Riley BB, ed. *PLoS One*. 2017;12(2):e0171143. doi:10.1371/journal.pone.0171143.

170. Postlethwait JH, Johnson SL, Midson CN, et al., A genetic linkage map for the zebrafish. *Science*. 1994;264(5159):699-703. doi:10.1126/SCIENCE.8171321.

171. Powell D, Lou M, Barros Becker F, Huttenlocher A. Cxcr1 mediates recruitment of neutrophils and supports proliferation of tumor-initiating astrocytes in vivo. *Sci Rep*. 2018;8(1):13285. doi:10.1038/s41598-018-31675-0.

172. Radice GL, Rayburn H, Matsunami H, Knudsen KA, Takeichi M, Hynes RO. Developmental defects in mouse embryos lacking N-cadherin. *Dev Biol*. 1997;181(1):64-78. doi:10.1006/dbio.1996.8443.

173. Ramanathan M, Haskó G, Leibovich SJ. Analysis of Signal Transduction Pathways in Macrophages Using Expression Vectors with CMV Promoters: A Cautionary Tale. *Inflammation*. 2006;29(2-3):94-102. doi:10.1007/s10753-006-9005-z.

174. Ramirez CL, Foley JE, Wright DA, et al., Unexpected failure rates for modular assembly of engineered zinc fingers. *Nat Methods*. 2008;5(5):374-375. doi:10.1038/nmeth0508-374.

175. Raykhel I, Alanen H, Salo K, et al., A molecular specificity code for the three mammalian KDEL receptors. *J Cell Biol*. 2007;179(6):1193-1204. doi:10.1083/jcb.200705180.

176. Redies C, Engelhart K, Takeichi M. Differential expression of N- and R-cadherin in functional neuronal systems and other structures of the developing chicken brain. *J Comp Neurol*. 1993;333(3):398-416. doi:10.1002/cne.903330307.

177. Redies C, Takeichi M. Expression of N-cadherin mRNA during development of the mouse brain. *Dev Dyn*. 1993;197(1):26-39. doi:10.1002/aja.1001970104.

178. Redies C. Cadherins in the central nervous system. *Prog Neurobiol*. 2000;61(6):611-648. doi:10.1016/S0301-0082(99)00070-2.

179. Rennekamp AJ, Peterson RT. 15 years of zebrafish chemical screening. *Curr Opin Chem Biol*. 2015;24:58-70. doi:10.1016/j.cbpa.2014.10.025.

180. Revenu C, Streichan S, Dona E, Lecaudey V, Hufnagel L, Gilmour D. Quantitative cell polarity imaging defines leader-to-follower transitions

during collective migration and the key role of microtubule-dependent adherens junction formation. *Development*. 2014;141(6):1282-1291. doi:10.1242/dev.101675.

181. Rieger S, Senghaas N, Walch A, Köster RW. Cadherin-2 controls directional chain migration of cerebellar granule neurons. *PLoS Biol*. 2009;7(11):1000240. doi:10.1371/journal.pbio.1000240.

182. Robu ME, Larson JD, Nasevicius A, et al., p53 Activation by Knockdown Technologies. *PLoS Genet*. 2007;3(5):e78. doi:10.1371/journal.pgen.0030078.

183. Roche - Manufacturing. https://www.roche.com/research_and_development/drawn_to_science/zebrafish.htm.

184. Rondot S, Koch J, Breitling F, Dübel S. A helper phage to improve single-chain antibody presentation in phage display. *Nat Biotechnol*. 2001;19(1):75-78. doi:10.1038/83567.

185. Rossi A, Kontarakis Z, Gerri C, et al., Genetic compensation induced by deleterious mutations but not gene knockdowns. *Nature*. 2015;524(7564):230-233. doi:10.1038/nature14580.

186. Rousseau BA, Hou Z, Gramelspacher MJ, Zhang Y. Programmable RNA Cleavage and Recognition by a Natural CRISPR-Cas9 System from Neisseria meningitidis. *Mol Cell*. 2018;69(5):906-914.e4. doi:10.1016/j.molcel.2018.01.025.

187. Russo G, Lehne F, Pose Méndez SM, Dübel S, Köster RW, Sassen WA. Culture and Transfection of Zebrafish Primary Cells. *J Vis Exp*. 2018;(138):1-9. doi:10.3791/57872.

188. Russo G, Meier D, Helmsing S, et al., Parallelized Antibody Selection in Microtiter Plates. Phage display, Ed: Lim, T.S. And Hust, M. In: *Methods in Molecular Biology* 2018; 1701:273-284. doi:10.1007/978-1-4939-7447-4_14.

189. Russo G, Theisen U, Fahr W, et al., Sequence defined antibodies improve the detection of cadherin 2 (N-cadherin) during zebrafish development. *N Biotechnol*. 2018;45:98-112. doi:10.1016/j.nbt.2017.12.008.

190. Saerens D, Pellis M, Loris R, et al., Identification of a Universal VHH Framework to Graft Non-canonical Antigen-binding Loops of Camel Single-domain Antibodies. *J Mol Biol*. 2005;352(3):597-607. doi:10.1016/j.jmb.2005.07.038.

191. Sander JD, Dahlborg EJ, Goodwin MJ, et al., Selection-free zinc-finger-nuclease engineering by context-dependent assembly (CoDA). *Nat Methods*. 2011;8(1):67-69. doi:10.1038/nmeth.1542.

192. Sassen A, Köster RW. A molecular toolbox for genetic manipulation of zebrafish. *Adv Genomics Genet*. 2015;5:151-163. doi:10.2147/AGG.S57585.

193. Sassen WA, Lehne F, Russo G, Wargenau S, Dübel S, Köster RW. Embryonic zebrafish primary cell culture for transfection and live cellular and subcellular imaging. *Dev Biol*. 2017;430(1):18-31. doi:10.1016/j.ydbio.2017.07.014.

194. Scheel a a, Pelham HR. Purification and characterization of the human KDEL receptor. *Biochemistry*. 1996;35(31):10203-10209. doi:10.1021/bi960807x.

195. Schmitz A, Schneider A, Kummer MP, Herzog V. Endoplasmic Reticulum-Localized Amyloid beta-Peptide is Degraded in the Cytosol by Two Distinct Degradation Pathways. *Traffic*. 2004;5(2):89-101. doi:10.1111/j.1600-0854.2004.00159.x.

196. Schneider CA, Rasband WS, Eliceiri KW. NIH Image to ImageJ: 25 years of image analysis. *Nat Methods*. 2012;9(7):671-675.

197. Schofield DJ, Pope AR, Clementel V, et al., Application of phage display to high throughput antibody generation and characterization. *Genome Biol*. 2007;8(11):R254. doi:10.1186/gb-2007-8-11-r254.

198. Semenza JC, Hardwick KG, Dean N, Pelham HRB. ERD2, a yeast gene required for the receptor-mediated retrieval of luminal ER proteins from the secretory pathway. *Cell*. 1990;61(7):1349-1357. doi:10.1177/1534650105280330.

199. Seo MJ, Jeong KJ, Leysath CE, Ellington AD, Iverson BL, Georgiou G. Engineering antibody fragments to fold in the absence of disulfide bonds. *Protein Sci*. 2009;18(2):259-267. doi:10.1002/pro.31.

200. Seok H, Lee H, Jang E-S, Chi SW. Evaluation and control of miRNA-like off-target repression for RNA interference. *Cell Mol Life Sci*. 2018;75(5):797-814. doi:10.1007/s00018-017-2656-0.

201. Shan WS, Tanaka H, Phillips GR, et al., Functional cis-heterodimers of N- and R-cadherins. *J Cell Biol*. 2000;148(3):579-590. doi:10.1083/JCB.148.3.579.

202. Shikanai M, Nakajima K, Kawauchi T. N-cadherin regulates radial glial fiber-dependent migration of cortical locomoting neurons. *Commun Integr Biol*. 2011;4(3):326-330. doi:10.4161/cib.4.3.14886.

203. Sidhu SS. Antibodies for all: The case for genome-wide affinity reagents. *FEBS Lett*. 2012;586(17):2778-2779. doi:10.1016/j.febslet.2012.05.044.

204. Sledz CA, Holko M, de Veer MJ, Silverman RH, Williams BRG. Activation of the interferon system by short-interfering RNAs. *Nat Cell Biol*. 2003;5(9):834-839. doi:10.1038/ncb1038.

205. Smith DK, Xue H. Sequence profiles of immunoglobulin and immunoglobulin-like domains. *J Mol Biol*. 1997;274(4):530-545. doi:10.1006/jmbi.1997.1432.

206. Soltes G, Hust M, Ng KKY, et al., On the influence of vector design on antibody phage display. *J Biotechnol*. 2007;127(4):626-637. doi:10.1016/j.jbiotec.2006.08.015.

207. Stojic L, Lun ATL, Mangei J, et al., Specificity of RNAi, LNA and CRISPRi as loss-of-function methods in transcriptional analysis. *Nucleic Acids Res*. 2018;46(12):5950-5966. doi:10.1093/nar/gky437.

208. Strebe N, Guse a., Schüngel M, et al., Functional knockdown of VCAM-1 at the posttranslational level with ER retained antibodies. *J Immunol Methods*. 2009;341(1-2):30-40. doi:10.1016/j.jim.2008.10.012.

209. Streisinger G, Walker C, Dower N, Knauber D, Singer F. Production of clones of homozygous diploid zebra fish (Brachydanio rerio). *Nature*. 1981;291(5813):293-296.

210. Sulem P, Helgason H, Oddson A, et al., Identification of a large set of rare complete human knockouts. *Nat Genet*. 2015;47(5):448-452. doi:10.1038/ng.3243.

211. Suyama K, Shapiro I, Guttman M, Hazan RB. A signaling pathway leading to metastasis is controlled by N-cadherin and the FGF receptor. *Cancer Cell*. 2002;2(4):301-314. doi:10.1016/S1535-6108(02)00150-2.

212. Suzuki SC, Takeichi M. Cadherins in neuronal morphogenesis and function. *Dev Growth Differ*. 2008;50(SUPPL. 1). doi:10.1111/j.1440-169X.2008.01002.x.

213. Takeichi M. Cadherin cell adhesion receptors as a morphogenetic regulator. *Science*. 1991;251(5000):1451-1455.

214. Taniguchi H, Kawauchi D, Nishida K, Murakami F. Classic cadherins regulate tangential migration of precerebellar neurons in the caudal hindbrain. *Development*. 2006;133(10):1923-1931. doi:10.1242/dev.02354.

215. Taussig MJ, Fonseca C, Trimmer JS. Antibody validation: a view from the mountains. *N Biotechnol*. 2018;45:1-8. doi:10.1016/J.NBT.2018.08.002.

216. Teichmann SA, Chothia C. Immunoglobulin superfamily proteins in Caenorhabditis elegans. *J Mol Biol*. 2000;296(5):1367-1383. doi:10.1006/jmbi.1999.3497.

217. Tepass U, Truong K, Godt D, Ikura M, Peifer M. Cadherins in embryonic and neural morphogenesis. *Nat Rev Mol Cell Biol*. 2000;1(2):91-100. doi:10.1038/35040042.

218. Theisen U, Hennig C, Ring T, Schnabel R, Köster RW. *Neurotransmitter-Mediated Activity Spatially Controls Neuronal Migration in the Zebrafish Cerebellum*. Vol 16.; 2018. doi:10.1371/journal.pbio.2002226.

219. Thisse, B., Pflumio, S., Fürthauer, M., Loppin, B., Heyer, V., Degrave, A., Woehl, R., Lux, A., Steffan, T., Charbonnier, X.Q. and Thisse C. Expression of the zebrafish genome during embryogenesis (NIH R01 RR15402). ZFIN Direct Data Submission. (http://zfin.org). 2001.

220. Tiller T, Schuster I, Deppe D, et al., A fully synthetic human Fab antibody library based on fixed VH/VL framework pairings with favorable biophysical properties. *MAbs*. 2013;5(3):445-470. doi:10.4161/mabs.24218.

221. Tremblay JM, Kuo C-L, Abeijon C, et al., Camelid single domain antibodies (VHHs) as neuronal cell intrabody binding agents and inhibitors of Clostridium botulinum neurotoxin (BoNT) proteases. *Toxicon*. 2010;56(6):990-998. doi:10.1016/J.TOXICON.2010.07.003.

222. Trott M, Weiß S, Antoni S, et al., Functional Characterization of Two scFv-Fc Antibodies from an HIV Controller Selected on Soluble HIV-1 Env Complexes: A Neutralizing V3- and a Trimer-Specific gp41 Antibody. Pöhlmann S, ed. *PLoS One*. 2014;9(5):e97478. doi:10.1371/journal.pone.0097478.

223. Tuttle AM, Hoffman TL, Schilling TF. Rabconnectin-3a Regulates Vesicle Endocytosis and Canonical Wnt Signaling in Zebrafish Neural Crest Migration. *PLoS Biol*. 2014;12(5). doi:10.1371/journal.pbio.1001852.

224. Uhlen M, Bandrowski A, Carr S, et al., A proposal for validation of antibodies. *Nat Methods*. September 2016. doi:10.1038/nmeth.3995.

225. Uhlén M, Fagerberg L, Hallström BM, et al., Tissue-based map of the human proteome. *Science (80-)*. 2015;347(6220). doi:10.1126/science.1260419.

226. van Eeden FJ, Granato M, Schach U, et al., Mutations affecting somite formation and patterning in the zebrafish, Danio rerio. *Development*. 1996;123(1).

227. Vendome J, Felsovalyi K, Song H, et al., Structural and energetic determinants of adhesive binding specificity in type I cadherins. *Proc Natl Acad Sci*. 2014;111(40):E4175-E4184. doi:10.1073/pnas.1416737111.

228. Verma IM. Nuclear factor (NF)-κB proteins: therapeutic targets. *Ann Rheum Dis*. 2004;63(suppl 2):ii57-ii61. doi:10.1136/ARD.2004.028266.

229. Vernet T, Choulier L, Nominé Y, et al., Spot peptide arrays and SPR measurements: throughput and quantification in antibody selectivity studies. *J Mol Recognit*. 2015;28(10):635-644. doi:10.1002/jmr.2477.

230. Vieira J, Messing J. [1] Production of single-stranded plasmid DNA. In: *Methods in Enzymology*. Vol 153. Academic Press; 1987:3-11. doi:10.1016/0076-6879(87)53044-0.

231. Visintin M, Settanni G, Maritan A, Graziosi S, Marks JD, Cattaneo A. The intracellular antibody capture technology (IACT): towards a consensus sequence for intracellular antibodies. *J Mol Biol*. 2002;317(1):73-83. doi:10.1006/jmbi.2002.5392.

232. Vladimirov N, Wang C, Höckendorf B, Pujala A, Tanimoto M, Mu Y, Yang CT, Wittenbach JD, Freeman J, Preibisch S, Koyama M, Keller PJ & Ahrens MB. Brain-wide circuit interrogation at the cellular level guided by online analysis of neuronal function. *Nat Methods*. 2018; 15 (12): 1117–1125.

233. Volkmann K, Chen Y-Y, Harris MP, Wullimann MF, Köster RW. The zebrafish cerebellar upper rhombic lip generates tegmental hindbrain nuclei by long-distance migration in an evolutionary conserved manner. *J Comp Neurol*. 2010;518(14):NA-NA. doi:10.1002/cne.22364.

234. Volkmann K, Rieger S, Babaryka A, Köster RW. The zebrafish cerebellar rhombic lip is spatially patterned in producing granule cell populations of

different functional compartments. *Dev Biol*. 2008;313(1):167-180. doi:10.1016/j.ydbio.2007.10.024.

235. Walker C, Streisinger G. Induction of Mutations by gamma-Rays in Pregonial Germ Cells of Zebrafish Embryos. *Genetics*. 1983;103(1):125-136.

236. Wang W, Svanberg E, Delbro D, Lundholm K. NOS isoenzyme content in brain nuclei as related to food intake in experimental cancer cachexia. *Mol Brain Res*. 2005;134(2):205-214. doi:10.1016/j.molbrainres.2004.10.038.

237. Welker AM, Jaros BD, Puduvalli VK, Imitola J, Kaur B, Beattie CE. Standardized orthotopic xenografts in zebrafish reveal glioma cell-line-specific characteristics and tumor cell heterogeneity. *Dis Model Mech*. 2016;9(2):199-210. doi:10.1242/dmm.022921.

238. White RM, Sessa A, Burke C, et al., Transparent Adult Zebrafish as a Tool for In Vivo Transplantation Analysis. *Cell Stem Cell*. 2008;2(2):183-189. doi:10.1016/j.stem.2007.11.002.

239. Wiley DS, Redfield SE, Zon LI. Chemical screening in zebrafish for novel biological and therapeutic discovery. *Methods Cell Biol*. 2017;138:651-679. doi:10.1016/bs.mcb.2016.10.004.

240. Wilson LJ, Wingate RJT. Temporal identity transition in the avian cerebellar rhombic lip. *Dev Biol*. 2006;297(2):508-521. doi:10.1016/j.ydbio.2006.05.028.

241. Wörn A, Plückthun A. Stability engineering of antibody single-chain Fv fragments. *J Mol Biol*. 2001;305(5):989-1010. doi:10.1006/JMBI.2000.4265.

242. Wullimann MF, Mueller T, Distel M, Babaryka A, Grothe B, Köster RW. The long adventurous journey of rhombic lip cells in jawed vertebrates: a comparative developmental analysis. *Front Neuroanat*. 2011;5(April):27. doi:10.3389/fnana.2011.00027.

243. Xing C, Gong B, Xue Y, et al., TGFβ1a regulates zebrafish posterior lateral line formation via Smad5 mediated pathway. *J Mol Cell Biol*. 2015;7(1):48-61. doi:10.1093/jmcb/mjv004.

244. Yagi T, Takeichi M. Cadherin superfamily genes: Functions, genomic organization, and neurologic diversity. *Genes Dev*. 2000;14(10):1169-1180. doi:10.1101/gad.14.10.1169.

245. Zamponi N, Zamponi E, Mayol GF, Lanfredi-Rangel A, Svärd SG, Touz MC. Endoplasmic reticulum is the sorting core facility in the Golgi-lacking protozoan *Giardia lamblia*. *Traffic*. 2017;18(9):604-621. doi:10.1111/tra.12501.

246. Zehner M, Marschall AL, Bos E, et al., The Translocon Protein Sec61 Mediates Antigen Transport from Endosomes in the Cytosol for Cross-Presentation to CD8+ T Cells. *Immunity*. 2015;42(5):850-863. doi:10.1016/j.immuni.2015.04.008.

247. ZEISS. ZEISS Microscopy Online Campus | Jellyfish Fluorescent Proteins. http://zeiss-campus.magnet.fsu.edu/articles/probes/jellyfishfps.html.

248. Zhang B, Xuan C, Ji Y, Zhang W, Wang D. Zebrafish xenotransplantation as a tool for in vivo cancer study. *Fam Cancer*. 2015;14(3):487-493. doi:10.1007/s10689-015-9802-3.

249. Zhang C, Helmsing S, Zagrebelsky M, et al., Suppression of p75 neurotrophin receptor surface expression with intrabodies influences Bcl-xL mRNA expression and neurite outgrowth in PC12 cells. *PLoS One*. 2012;7(1):e30684. doi:10.1371/journal.pone.0030684.

250. Zhao Y, Ju F, Zhao Y, et al., The expression of αA- and βB1-crystallin during normal development and regeneration, and proteomic analysis for the regenerating lens in Xenopus laevis. *Mol Vis*. 2011;17:768-778.

251. Zhu H, Luo L. Diverse Functions of N-Cadherin in Dendritic and Axonal Terminal Arborization of Olfactory Projection Neurons. *Neuron*. 2004; 42:63-75.

Ithaka

As you set out for Ithaka
hope the voyage is a long one,
full of adventure, full of discovery.
Laistrygonians and Cyclops,
angry Poseidon—don't be afraid of them:
you'll never find things like that on your way
as long as you keep your thoughts raised high,
as long as a rare excitement
stirs your spirit and your body.
Laistrygonians and Cyclops,
wild Poseidon—you won't encounter them
unless you bring them along inside your soul,
unless your soul sets them up in front of you.

Hope the voyage is a long one.
May there be many a summer morning when,
with what pleasure, what joy,
you come into harbors seen for the first time;
may you stop at Phoenician trading stations
to buy fine things,
mother of pearl and coral, amber and ebony,
sensual perfume of every kind—
as many sensual perfumes as you can;
and may you visit many Egyptian cities
to gather stores of knowledge from their scholars.

Keep Ithaka always in your mind.
Arriving there is what you are destined for.
But do not hurry the journey at all.
Better if it lasts for years,
so you are old by the time you reach the island,
wealthy with all you have gained on the way,
not expecting Ithaka to make you rich.

Ithaka gave you the marvelous journey.
Without her you would not have set out.
She has nothing left to give you now.

And if you find her poor, Ithaka won't have fooled you.
Wise as you will have become, so full of experience,
you will have understood by then what these Ithakas mean.

Constantine P. Cavafy, 1911
(Translated by Edmund Keeley & Philip Sherrard)

Acknowledgments

In this very moment I realize that a thesis submission has something in common with Ulysses landfall on Ithaka's coast more than with anything else. Like in the poem from C.P. Cavafy, the destination had the merit of serving as pretext to set out for what happened to be a marvelous journey full of adventure, full of discovery. A journey that would not have been possible and enjoyable without the people I am mentioning here, to whom goes all of my appreciation for finally making this experience memorable and unique.

In the first place, I want to express my sincere gratitude to my mentors and thesis examiners Prof. Stefan Dübel and Prof. Reinhard Köster, who gave me the means to undertake this adventure and the support I needed along the way. I will always be thankful for receiving the chance to also test my own ideas and for being spared from the risk of loosing myself into the maze of fascinating projects I was lucky enough to be part of. I received unique opportunities and the time I needed to develop scientifically before the start of a new challenge. This was all exceptional to me.

I want to thank Prof. Michael Hust for taking part in the thesis committee, for giving me the opportunity to supervise the practical courses, and for providing an exemplary model of students management.

Anyone who worked in science knows how much this job can be strenuous and frustrating. When there is someone to believe in you it is much easier to find the motivation during a rough time. Thanks Thomas for being a reference point in science as in life.

My gratitude also goes to Dr. André Frenzel, Dr. Ulrike Theisen, and Dr. Kazuhiko Namikawa for their precious scientific help during these years. Whenever I needed support, you gave it to me without hesitation. Additionally, you nourished that romantic idea I always had in my mind of researchers as people putting always science first, proving that scientific curiosity remains the main driving force in our job.

To Doris Meier goes a very special thanks. When I started you taught me all you new of this job. Later, we worked shoulder to shoulder on a project that was more like the realization of a dream to me. I will never forget those productive and frenzied days.

I also want to thank Saskia Helmsing for the irreplaceable support in the lab, for being always an example of good scientific practice, and for patiently teaching me German words...
Thanks to the students I supervised in the past years. Miriam, Kristian, Max, I have the impression who had to learn the most from the time we spent together in the end that was me.

I thank all of my fellow labmates for sharing the joyful and the difficult moments, for gathering together around a birthday cake or the table of a pub.

In particular, I want to thank Wieland Fahr. I consider our mental understanding a gift. The endless conversations upon politic, and sociology have been the best seasoning of horribly prepared food from the canteen.

Thanks also to Viola Fühner. It was a great time to supervise students together. Likely more for us than for the poor students.. Also thanks to Esther Wenzel, writing our thesis side by side made the task less exhausting and more effective. Thanks to Alessandro Dorigo for the life-saver coffee breaks, which also served to push away the occasional nostalgia for home.

Thanks to Cornelia Oltmann. With infinite patience you made an Italian student survive the impact with the German bureaucratic apparatus. That was not an easy task!

Thanks to Timo Fritsch, for managing our fish facilities and for being always accommodating.

Thanks to all the personnel from the Institute of Biology, Biotechnology and Bioinformatics, as well as from the Zoological institute for the indirect help.

For the many evenings of escapism from difficult reality, thanks to Ramon, Tomaz, Rahul, and the gang of architects. Together we always had fun.

I also want to thank Gigi, for constantly demonstrating that in life, as in science, often it is from the most unconventional way of thinking that you reach the best results.
Thanks Tata's, Fabio, Marco, and all the friends in Italy, or spread around Europe, for pretending that in friendship the distance is not an influential factor.

Thanks to my friends jugglers. Your uncomplicated approach to life is the best therapy to any discomfort.

There is a person who had to experience indirectly almost the same ups and downs this PhD studies put me through, this person is Lotte. I saw you many times making the sacrifice of giving priority to my needs over yours, yet without ever suppressing your personal will and interests. Of these things I loved the first and I admired the second. For this, for the infinite help, and the fun we have together, I wish you will be on my side

in any other adventure is ahead of us. Thanks also to your family for being so encouraging and welcoming.

Tutta la mia famiglia, e soprattutto la mia sorellona, mio padre e Pino, meritano una menzione speciale in questi ringraziamenti. Imbarcarmi in questo viaggio non mi è stato facile, ma non ho mai considerato quanto fosse stato difficile anche per voi. Non me lo avete mai fatto pesare, al contrario, mi avete supportato in ogni momento e con ogni mezzo. Se sono riuscito in questo progetto lo devo a voi più di ogni altro.

Non c'è stata volta che cadendo non mi sia rialzato aggrappandomi al pensiero di lei che non mi avrebbe mai fatto rimanere a terra un solo minuto. Adesso come allora la persona che mi ha dato di più. Dedico questo lavoro a lei che oggi sarebbe stata ancor più felice di me nel vedermi realizzato.